Review Article

Mohammadmahdi Akbari Edgahi, Seyed Morteza Naghib*, Amirhossein Emamian, Hosseinali Ramezanpour, Fatemeh Haghiralsadat, and Davood Tofighi

A practical review over surface modification, nanopatterns, emerging materials, drug delivery systems, and their biophysiochemical properties for dental implants: Recent progresses and advances

https://doi.org/10.1515/ntrev-2022-0037
received September 30, 2021; accepted January 1, 2022

Abstract: In this paper, we reviewed the recent advances in nanoscale modifications and evaluated their potential for dental implant applications. Surfaces at the nanoscale provide remarkable features that can be exploited to enhance biological activities. Herein, titanium and its alloys are considered as the main materials due to their background as Ti-based implants, which have been yielding satisfactory results over long-term periods. At first, we discussed the survivability and the general parameters that have high impacts on implant failure and the necessities of nanoscale modification. Afterward, fabrication techniques that can generate nanostructures on the endosseous implant body are categorized as mechanical, chemical, and physical methods. These techniques are followed by biomimetic nanotopographies (*e.g.*, nanopillars, nanoblades, *etc.*) and their biological mechanisms. Alongside the nanopatterns, the applications of nanoparticles (NPs) including metals, ceramics, polymers, *etc.*, as biofunctional coating or delivery systems are fully explained. Finally, the biophysiochemical impacts of these modifications are discussed as essential parameters for a dental implant to provide satisfactory information for future endeavors.

Keywords: implant, modification, nanostructure, nanoparticles, mechano-bactericidal, drug delivery

1 Introduction

Dental implants are the mainstream solution for lost teeth. They are fabricated to mimic the function of teeth and return the lost confidence to the patients. In the early 1980s, a 5 to 10 year follow-up on the survivability of dental prosthesis indicated an 81 and 91% survival rate in maxilla and mandible, respectively [1]. In this term, the definitions of survival rate and success rate are different. The survival rate represents the sustainability of the dental implants but the success rate also includes the patients' general satisfaction. Therefore, after 40 years, statistics still show complications, especially in patients with diabetes or smoking background, which implies the necessities for the development of dental implants [2–5].

From the beginning of the 21st century, nanoscale modifications have been of great interest [6–8]. Materials at nanoscale display unique properties that can significantly enhance the characteristics of dental implants and further osteogenic responses [9]. These modifications have a key role in controlling essential parameters of an implant. Additionally, remarkable modifications can be obtained by the utilization of different nanoparticles (NPs) or nanopatterns, whereas manifold techniques can

* **Corresponding author: Seyed Morteza Naghib,** Nanotechnology Department, School of Advanced Technologies, Iran University of Science and Technology, P.O. Box 16846-13114, Tehran, Iran, e-mail: naghib@iust.ac.ir
Mohammadmahdi Akbari Edgahi: Nanotechnology Department, School of Advanced Technologies, Iran University of Science and Technology, P.O. Box 16846-13114, Tehran, Iran
Amirhossein Emamian, Hosseinali Ramezanpour: Research and Development Unit, AVITA Dental System, KFP-Dental Company, Tehran, Iran
Fatemeh Haghiralsadat: Department of Advanced Medical Sciences and Technologies, School of Paramedicine, Shahid Sadoughi University of Medical Sciences, Yazd, Iran
Davood Tofighi: Department of Psychology and Biostatistics, Epidemiology, and Research Design Support (BERD), Clinical and Translational Science Center, University of New Mexico, Albuquerque, New Mexico, United States of America

produce microscale surfaces, there is only a limited number of commercial techniques that grant nanoscale structures. These techniques, according to their performing conditions, are categorized as mechanical, chemical, and physical methods [10–18]. Considering the transgingival nature of dental implants, they form three main interfaces with the host's biological system that consists of (i) the subgingival hard tissue interface of the endosseous implant body, (ii) the soft tissue transgingival interface at the implant neck and platform, and (iii) the interface to the oral cavity with its salivary environment at the transgingival and the supragingival region [17].

At the implant interface, where most complications are laid on, researchers have been evaluating the responses of bone to various NPs and nanopatterns [19–22]. Coating the implant surface with nanoscale particles surpassed the restriction of produced residues for some metallic elements (*e.g.*, Cu) or extended their applications. Herein, NPs are classified as (i) metallic-based, (ii) ceramic-based, (iii) polymer-based, (iv) carbon-based, (v) protein-based, and (vi) drug-based [21–33]. Utilization of these NPs may either provide a suitable environment for biological agents or restrict the harmful agents from disturbing the biological system. Respecting these issues, a long-lasting coating with both promotive and restrictive functions is the optimal requirement for dental implants.

Aside from the inherent function of NPs, by engineering their characteristics, especially ceramic- and polymer-based materials, they can be used as delivery systems for a broad range of biomaterial or biomolecules with biogenic or biocidal activities [23]. Drug delivery in implants mainly occurs under degradation, diffusion, or osmosis mechanisms. Hence, the role of solubility in both the material matrix and payload is highlighted. Designing delivery systems create a suitable environment for these biomolecules to release at a controlled rate and maintain their function over a longer period. Therefore, a desirable drug delivery system can aid us to conquer several bone diseases and secure the success of implantation.

In addition to multifunctional coatings, surface nanotopographies are tremendously useful for biomedical applications that offer a broad spectrum of properties like mechano-bactericidal activity, which leads to the formation of multifunctional modifications. This activity was first found in nature by assessing bugs' wings like *Psaltoda claripennis* against Gram-negative bacteria and it was completely related to physical antibacterial mechanisms and not chemical ones [34]. Technically, the mechano-bactericidal function of the surface belongs to the physical geometries of the nanopatterns that increase the stress beyond the elastic tolerance of the membrane [19]. Therefore, the quantity of biomaterials and subsequent adsorption rate are not involved in the elimination of bacteria, which help the surface to maintain its antibacterial function for longer periods than chemical compounds.

In this review, we cover some uses of nanotechnology for the modification of the endosseous implant body. Modifying an implant does not have a gold standard and every method may display acceptable results. However, utilization of state-or-art procedures provides the opportunity to combat the current challenges and guarantees success with higher satisfaction for patients. In the following sections, we provide pieces of information to fulfill the demands for optimizing dental implants.

2 Nanofabrication techniques

To modify the surface morphology of the implant, diverse techniques can be performed (Table 1). The utilization of these techniques, depending on the procedure and performing conditions, results in different surface characteristics. From a broad range of modification techniques, the following ones are frequently used to develop nanoscale surfaces at the endosseous body and can be commercially applicable. Of these techniques, mechanical methods are the initial stage of processing and they target the roughness and grain size of the surface layer. By including the acid etching (AE) from chemical methods, the average roughness (R_a) of the surface can be predicted. The second stage is the accompaniment of either chemical or physical methods. Chemical methods refer to the use of chemical solutions, while physical methods are considered as the formation of materials under dry conditions.

Bear in mind that despite the potential of producing the same surface (*e.g.*, HAp-coated Ti) by the same or two different techniques, the ultimate result and performance may be different [35,36]. Hence, nanofabrication techniques and their performing conditions should be wisely selected.

2.1 Mechanical methods

Of the initial manufacturing processes of implants, mechanical methods were commonly used until the 1990s. Gradually, by the development of surface morphology at smaller scales, machining, grinding, polishing, and sandblasting (SB) are employed to modify the surface and enhance the general roughnesses, whereas shot peening (SP) and attrition are

used as surface-improving methods to refine the grain size of the top surface.

2.1.1 Machining

Back in the 1990s, machining was an essential step of dental implant treatment and it refers to the lathing, milling, or threading of manufacturing processes. The R_a values obtained by machining on the Ti surface were 300 nm to 1 µm with 2–10 nm thickness of the amorphous TiO_2 layer [37]. This imperfect surface generated by machining can promote cell adhesion and increase osteointegration but it simultaneously prolongs the healing period [38]. Salou *et al.* produced a regular array of TiO_2 nanotubes with a diameter of 37 nm and thickness of 160 nm by machining and it displayed notable enhancements in osteogenesis and osteointegration [39].

2.1.2 Grinding

Grinding involves diverse methods of abrasive activities to treat metallic surfaces. Generally, there are two frequently used procedures by either utilization of a belt machine with the help of a robotic arm or a grinding wheel with coarse particles to abrade the surface. The belt machine is at disadvantage to producing nanoscale surfaces but the grinding wheel with abrasive grade 60 is able to produce R_a values of less than 1 µm [40].

In spite of its simplicity, grinding low thermal conductive metals or alloys like Ti grade-5 could cause issues including thermal damage, surface burn, residual stresses, and grit dislodgement [41]. Therefore, conducting parameters in each procedure should be carefully adjusted. Madarkar *et al.* abraded Ti grade-5 by using ultrasonic vibration-assisted minimum quantity lubrication (UMQL) and conventional MQL (CMQL) to improve the quality of the surface. They reported that the variation of vegetable oil in UMQL led to different hydrophilicity, density, and viscosity as well as a reduction in cutting forces compared to CMQL. However, resulting roughnesses from UMQL were slightly higher than those of CMQL [42].

2.1.3 Polishing

Alike grinding, polishing is a cost-efficient method that follows similar protocols but with the use of fine abrasive particles. Generally, polishing is conducted through multiple processes using coarse abrasive SiC paper with 50 to 220 grit for the initial step and then finer abrasive SiC papers above 600 grit for the next step to obtain a mirror-like surface [40]. In chemical mechanical polishing, the produced R_a values are highly dependent on the slurry. In this case, alumina (Al_2O_3), silica (SiO_2), and diamond slurry are frequently used since they should be chemically inert [43–45]. Ozdemir *et al.* evaluated the influence of pad types to optimize the roughness while forming an oxide layer on the surface. They reported that the lowest roughness, R_a of 350 ± 30 nm, was obtained *via* alumina slurry with 3 wt% hydrogen peroxide (H_2O_2) [44].

2.1.4 Sandblasting (SB)

SB, also known as grit blasting, is a commonly used method to treat the surface and modify the R_a values. Despite machining, surface topography achieved by SB is highly dependent on the particle size [46]. Generally, SB refers to the projection of micro/NPs such as Al_2O_3, silica, titania (TiO_2), and CaP bioceramics through a nozzle onto the surface by compressed air to erode the surface (Figure 1). R_a values of blasted Ti were 300 nm to 3 µm [32]. More importantly, the particles used should be chemically stable and not cause further complications [47]. SB is a more favorable technique due to its capability of controlling surface roughness. This advantage became noteworthy as Jamet *et al.* found that the accumulation of bacteria on a rougher surface is higher than a smoother surface [48]. Schupbash *et al.* analyzed the surface of seven different dental implant manufacturers. They reported that the presence of particles made by SB on implants is different and not all manufacturers control the remaining particles on their implant surfaces [49].

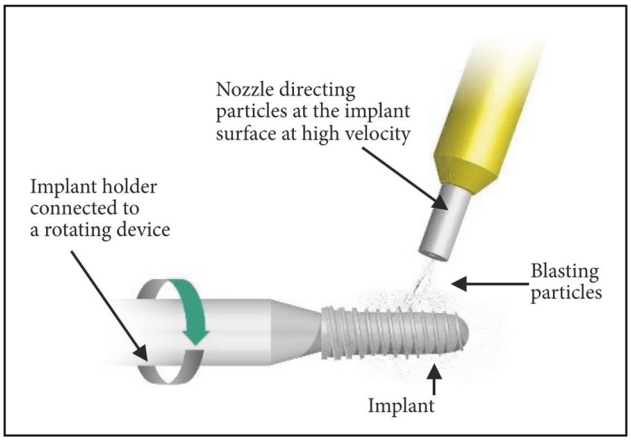

Figure 1: Schematic illustration of the SB process [49]. Copyright 2014, Hindawi.

2.1.5 SP

SP, also known as shot blasting, is a surface-improving method that promotes performance and reduces maintenance of the metallic components with a cost-effective solution. SP is a similar action as SB but with sufficient force strikes to create a plastic deformation. Herein, large metallic or ceramic balls with 0.25–1 mm diameter at 20–150 m/s velocity bombard the surface [50]. Technically, peening is employed to refine the grain structure of the surface by inducing residual compressive stress through a projection of high quality and inert particles to remove unfavorable tensile stresses from the surface [51]. With SP, it is possible to obtain 25–80 nm grains on the surface layer [52]. Deng *et al.* and Ganesh *et al.* studied the physiobiological effect of SP on Ti surfaces. The results displayed that utilization of different particles can fairly or significantly change the roughness, yet it can always increase hardness and fatigue resistance. Also, a treated surface can enhance cell adhesion, differentiation, and viability [51,53].

2.1.6 Attrition

Surface mechanical attrition treatment (SMAT) is a derived version of the SP method with a higher potential to produce a nanocrystalline surface layer. In SMAT, 2–10 mm diameter particles at 5–15 m/s velocity project multidirectionally to the surface, and consequently, create multidirectional severe plastic deformations. Compared to SP, SMAT has higher kinetic energies that lead to the formation of a thicker nanocrystalline surface layer and deeper residual compressive stress [54]. Jamesh *et al.* investigated the effects of SMAT on the CP-Ti surface using 8 mm diameter Al_2O_3 for 900, 1,800, and 2,700 s. They reported that at each time interval, the roughness of the surface increased whereas the level of hydrophilicity decreased. Also, they mentioned that the 900 s projection was not able to form apatite until the 28th day [55].

2.2 Chemical methods

To alter the topography of the implant surface, chemical methods are the best choices. These methods include several techniques that change an inert surface of an implant to a bioactive surface *via* oxidation, deposition, coating, or immobilization. Chemical solutions and their compounding ratios are the vital parts of the chemical surface treatment that can result in different physiobiological responses [56].

Primarily, chemical methods consist of AE, hydrogen peroxide treatment (HPT), alkali treatment (AT), sol–gel, electrochemical treatment, chemical vapor deposition, and biochemical methods, which form a nanolayer on the implant surface. Moreover, these methods are composed of other diverse techniques like esterification, coupling agent, and surface grafting that grant improvement in the biological activity of the surface, but, herein, they are omitted due to the inability to generate nanostructures [10].

2.2.1 AE

AE is used to clean and remove any oxide contamination from the layer and produce a homogenous surface (Figure 2). Chemical acids such as sulfuric acid (H_2SO_4), hydrochloric acid (HCl), hydrofluoric acid (HF), and nitric acid (HNO_3) are commonly used acids to produce the R_a values of 300 nm to 1 μm with approximately 10 nm thickness of the amorphous TiO_2 layer [57]. AE is commercially a popular technique and is usually accompanied by another acid as dual AE or another technique (*e.g.*, pre-SB or double AE) to improve osteoconductivity [58].

Typically, etching an implant surface changes the R_a values that lead to increasing anchorage of fibrin and osteogenic cells [59]. To obtain favorable roughness, diverse parameters including bulk material, material phases, surface structure, surface impurities, acid, temperature, and soaking time must be taken into account. Variola *et al.* reported that a nanopit network with different diameters ranging from 20 to 100 nm can be fabricated *via* a

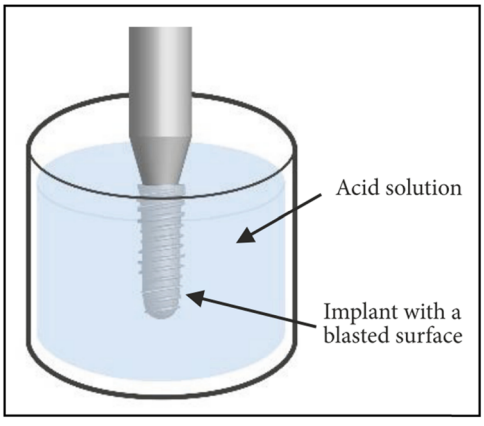

Figure 2: Schematic illustration of the AE process [49]. Copyright 2014, Hindawi.

combination of strong acids or bases and oxidants on CP-Ti [60]. Lamolle *et al.* etched Ti implants with HF acid and reported that by controlling the aforementioned parameters and solution contents, it is possible to fabricate micro- and nanoscale topography to increase biocompatibility and provide a suitable substrate for cell growth [61].

2.2.2 HPT

HPT is a technique to enhance the bioactivity of Ti implants by the formation of a gel-like anatase layer on the implant. Anatase permits the bone-like apatite to deposit after the immersion in simulated body fluid (SBF) [62]. The altered surface escalates the osteoblast-like cells and subsequently accelerates osteointegration [63]. Wang *et al.* fabricated an amorphous layer of TiO_2 on the CP-Ti sheets by the combination of HPT with AE, followed by thermally treating up to 800°C (Figure 3). They concluded that the optimal solution contents and heating temperature to obtain the highest bioactivity were H_2O_2/0.1 M HCl (1 M X/0.1 M Y)-solution and 400–500°C [35]. Khodaei *et al.* evaluated the addition of F^- or Cl^- to H_2O_2 solution and concluded that the addition of different ions to oxidizing ions can affect the phase morphology and wettability [64].

2.2.3 AT

AT is the use of basic solutions (*e.g.*, NaOH) to form a bioactive nanostructured layer like sodium titanate ($Na_2O_7Ti_3$) on the implant surface [65]. Upon immersion in SBF, sodium ions in the layer are exchanged with H_3O^+ from the adjacent fluid and form Ti–OH groups; these groups interact with Ca^{2+} ions and produce amorphous calcium titanate ($CaTiO_3$), and ultimately, with phosphate polyatomic ions (*e.g.*, HPO_4^{2-}), they form amorphous bone-like apatite on the implant surface. The formation of the apatite layer on the Ti surface provides a favorable substrate for bone marrow cell differentiation [66].

Pattanayak *et al.* found that exposing Ti to the strong acid solutions (pH < 1.1) or strong basic solutions (pH > 13.6) can form bone-like apatite on the surface after immersion in SBF within 3 days. Also, they observed immediate apatite formation after the heat treatment process. Generally, the generation of the apatite layer relates

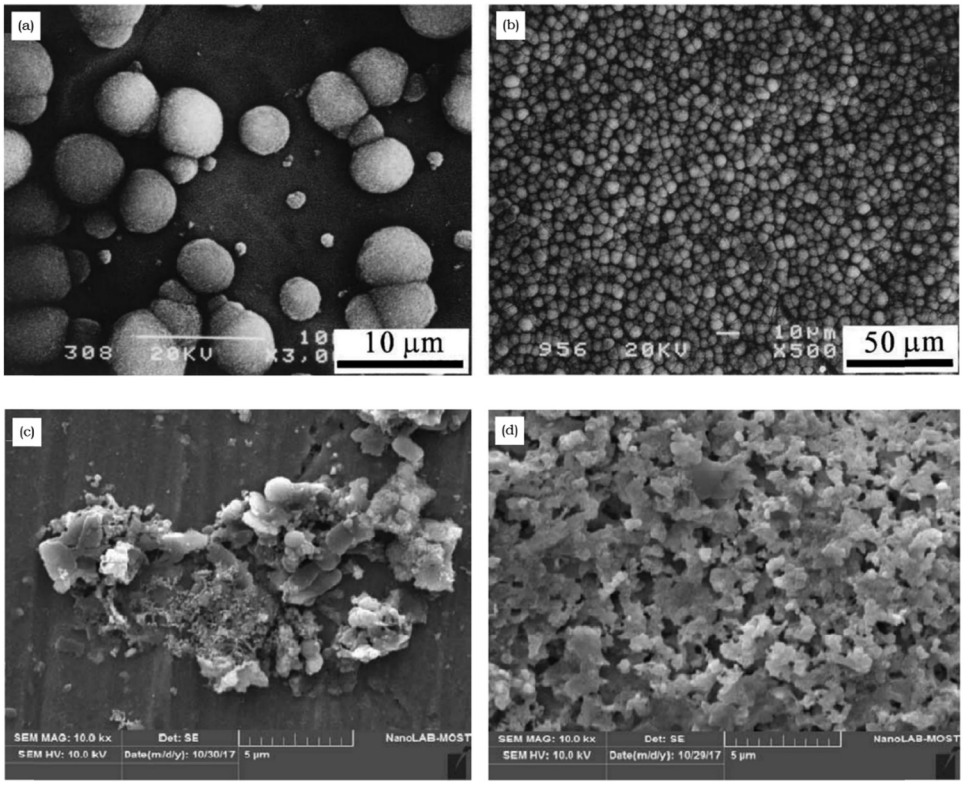

Figure 3: Scanning electron microscopy (SEM) images of hydroxyapatite deposited on the Ti surface (a and b) using HPT and (c and d) sol–gel techniques. The newly formed apatite layer depending on different conditions, pH, temperature, and time led to (a and c) initial and (b and d) complete stages of HAp formation. [35] Copyright 2002, Elsevier; [36] Copyright 2020, Medico-Legal Update.

to the magnitude of the positive or negative surface charge developed on the Ti surface (Figure 4) [67]. Wang *et al.* developed an economical surface treatment *via* a combination of AE and AT techniques to enhance hydrophilicity and osteoconductivity of poly(etheretherketone) (PEEK). They used 98 wt% H_2SO_4 as an AE solution for 5–90 s and 6 wt% NaOH for 20 s. The best enhancement was observed at 30 s etching, which decreased the contact angle (CA) from 78° to 37° [68].

2.2.4 Sol–gel

Sol–gel, also called wet chemical deposition, is a widely used technique to enhance the bioactivity of the implant surface (Figure 5). The sol–gel technique is based on colloidal suspensions in a liquid solution that generates a solid layer by deposition of micro/NPs on a substrate. Simply, it is used to coat a thin film of biomimetic compounds (*e.g.*, CaP compounds) to subsequently increase osteointegration [69].

Of the notable benefits of this technique, it is possible to maintain the activity of biomolecules and deposit more complex compounds (*e.g.*, compounds with the incorporation of drugs) on the implant surface [70]. Moreover, sol–gel has the potential to deposit an extended range of metal oxides such as TiO_2, TiO_2–CaP composite, or silica-based coatings on metallic/nonmetallic surfaces [71]. Esmael *et al.* successfully coated HAp and chitosan NPs on the Ti surface and immersed it in SBF. They reported that utilization of HAp has a synergetic impact on both the bioactivity and new apatite formation (Figure 3) [36].

2.2.5 Electrochemical treatment

Electrochemical treatment mainly refers to the three techniques, namely, anodic oxidation (AO), macro-arc oxidation, and electrophoretic deposition, which are commonly used in dental implant surface treatments.

2.2.5.1 AO

AO, also known as anodization, is a technique to fabricate nanostructured surfaces *via* potentiostatic or galvanostatic anodization by controlling several parameters including electrolyte composition, electric current, anode potential, temperature, and distance between the anode and cathode (Figure 6). Herein, implant as the anode is immersed in a homogenous electrolyte containing strong acids such as phosphoric acid (H_3PO_4), ammonium fluoride (NH_4F), H_2SO_4, HF, or HNO_3 or inhomogeneous electrolytes such as NaCl:NH_4F [73] and $NaHSO_4$:HF:NaF [74] with the passage of a high current density or voltage.

AO enhances the corrosion resistance of metals (*e.g.*, CP-Ti or Ta) by the formation of thick oxide layers. Moreover, the fluoride ions present in the electrolyte results in a nanotubular structure on titania [75]. Fialho *et al.* compared single and double AO on the Ta surface

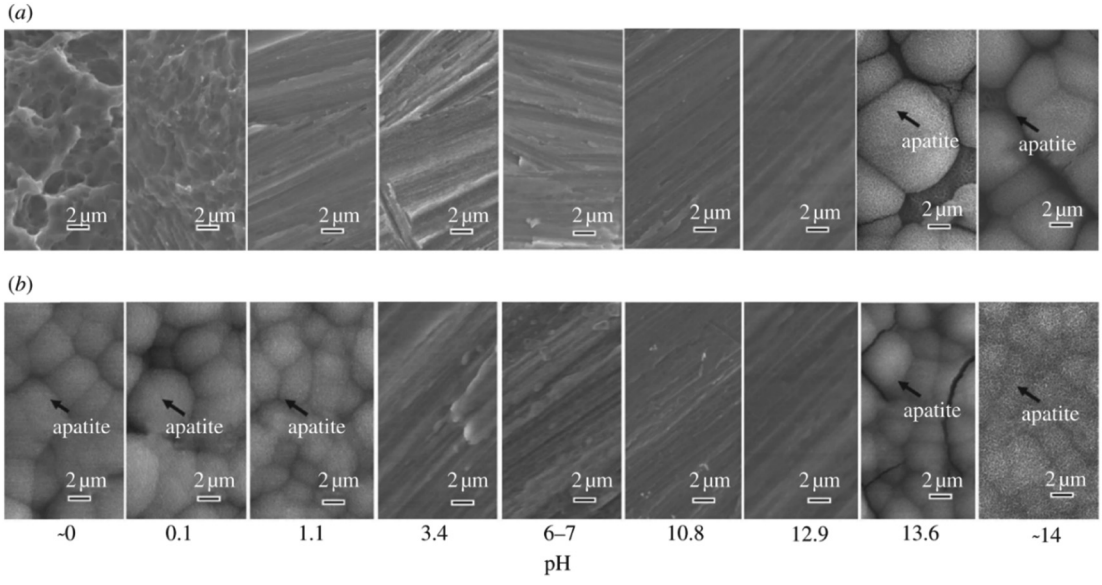

Figure 4: FE-SEM images of the Ti surface exposed to solutions with different pH values and subsequently immersed in SBF for 3 days (a) before and (b) after heat treatment [67]. Copyright 2012, The Royal Society.

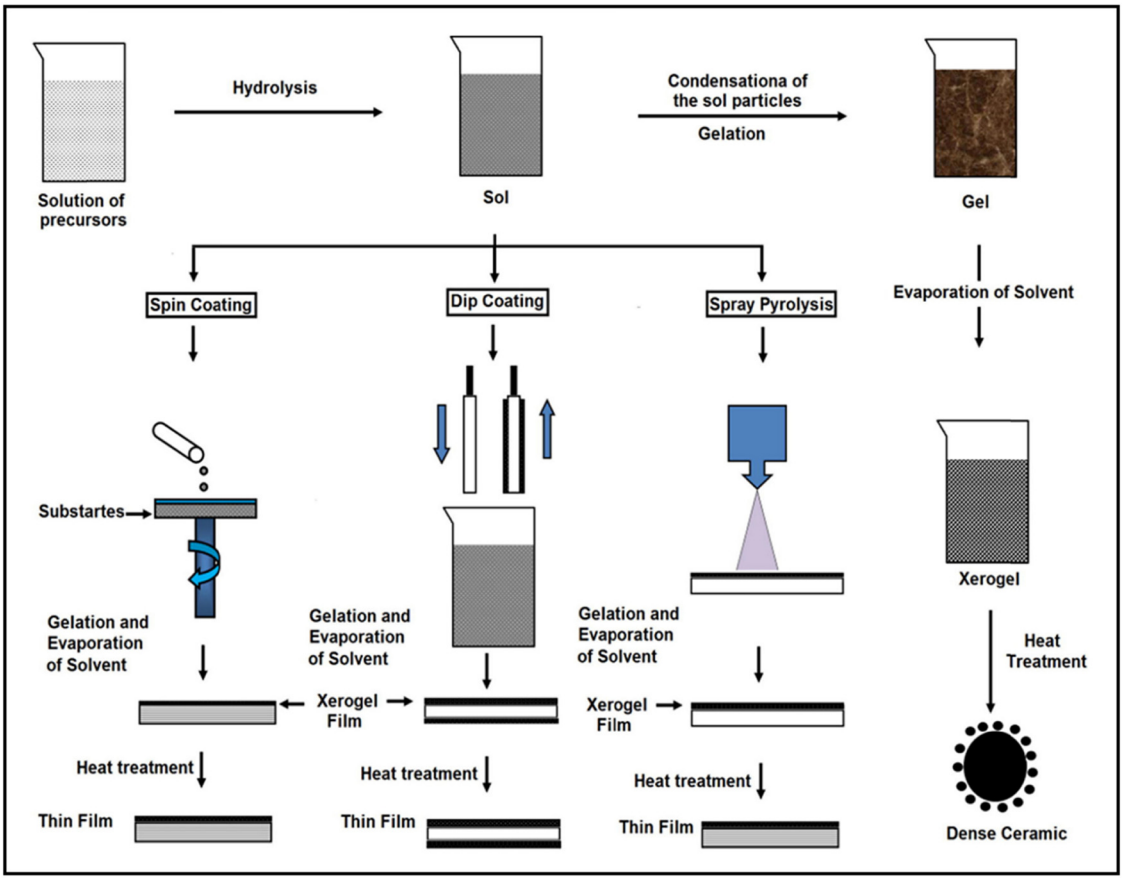

Figure 5: Schematic illustration of the sol–gel techniques [72]. Copyright 2020, Frontiers.

with the incorporation of Ca^{2+}, PO_4^{3-}, and Mg^{2+} ions on the surface; after the first anodization, enhancements in roughness and hydrophilicity were observed but after the second one, they also formed an amorphous tricalcium phosphate (TCP) on the surface [76].

2.2.5.2 Micro-arc oxidation (MAO)

MAO, also called plasma electrolytic oxidation (PEO), is the modified version of the AO technique with the assistance of plasma and high voltage to fabricate oxide protective layers on metallic surfaces like Ti, Ta, Mg, Al, and Zr and their alloys [78]. Alike AO, the implant as the anode and the stainless steel as the cathode are immersed in an electrolyte and a high voltage is applied on the electrolyte that gradually coats an oxide layer on the implant surface [79].

In MAO, the electrolyte composition is the key parameter that defines the final composition, porosity, and thickness of the coated layer. Sedelnikova *et al.* fabricated the Sr–Si–CaP and Ag–CaP incorporated coatings with different ratios of electrolytes and reported that the Ag–CaP coating contained pores and isometric particles of β-TCP uniformly distributed but the Sr–Si–CaP coating had spheroidal elements and open pores on their surfaces [80].

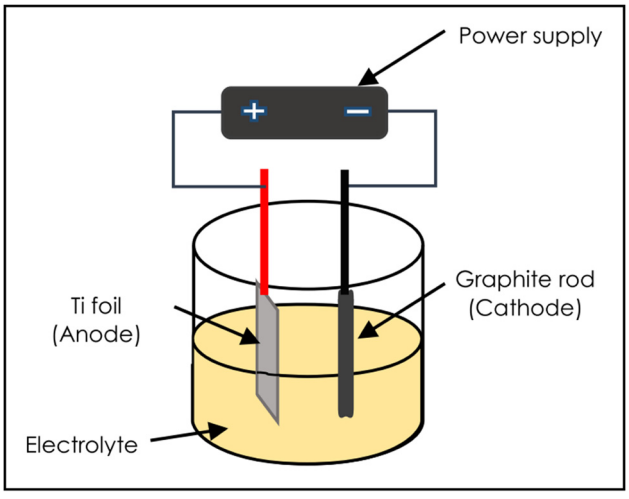

Figure 6: Schematic illustration of the AO process [77]. Copyright 2017, Journal Teknologi.

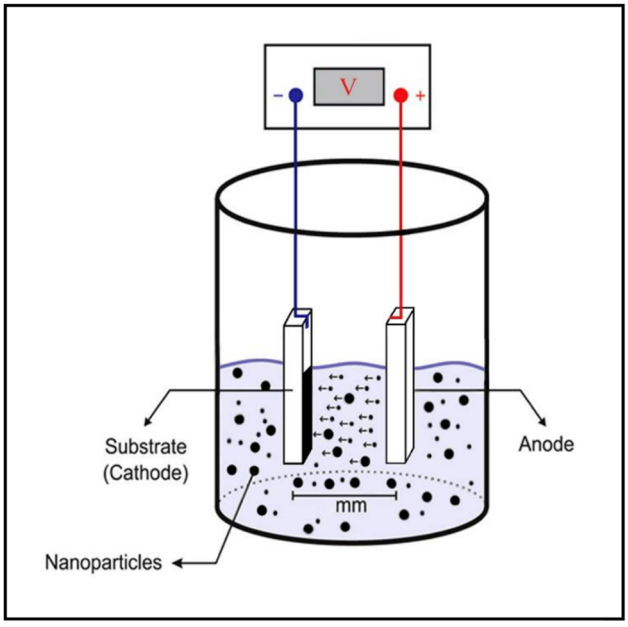

Figure 7: Schematic illustration of the electrophoretic deposition process [84]. Copyright 2015, ACS.

2.2.5.3 Electrophoretic deposition (ED)

ED is a cathode-based electrochemical method. ED refers to the deposition of colloidal particles on the substrate by passing a high voltage in a suspension (Figure 7). This method has the potential to coat HAp NPs with 18 nm thickness on the surface within 30 min [81]. Moreover, the combination of MAO and ED can generate a top layer of phase-pure HAp and an interlayer of anticorrosive TiO_2 [82]. Hashim *et al.* evaluated the syntheses and deposition of TiO_2, ZnO, and Al_2O_3 by rapid breakdown anodization (RBA) and ED. They reported that Ti, TiO_2 and Zn, ZnO particles were able to form bone-like apatite using the RBA technique but Al_2O_3 did not have the potential [83].

2.2.6 Chemical vapor deposition (CVD)

CVD is used to form thin layers on the implant surface by gaseous compounds. CVD involves chemical reactions between gas-phase chemicals and the surface that deposits nonvolatile compounds on the surface (Figure 8). Kania deposited diamond NPs on Ti orthopedic implants and observed notable increases in hardness, toughness, and adhesion [85]. CVD can be performed by many approaches and include atmospheric-pressure CVD (APCVD), low-pressure CVD (LPCVD), plasma-enhanced CVD (PECVD), and laser-enhanced CVD (LECVD). Moreover, a combination of CVD and PVD as a hybrid method was also developed [11].

CVD is capable of metalloceramic coatings by which it is possible to form nanocrystalline metallic bonds at the interlayer and hard-ceramic bond on the surface that subsequently overcomes adhesion problems in ceramic hard coatings on metallic substrates [86]. Chen *et al.* evaluated enhanced fluorine and oxygen mono/dual CVD to produce nanoscale coatings with antibacterial activity on the Ti surface. They found that fluorine deposited surface is able to kill *Staphylococcus aureus* (*S. aureus*) bacteria. Also, the presence of F and O elements has synergetic impacts on antibacterial activity, promotion in cell spreading, improvement in corrosion resistance, and biocompatibility [87].

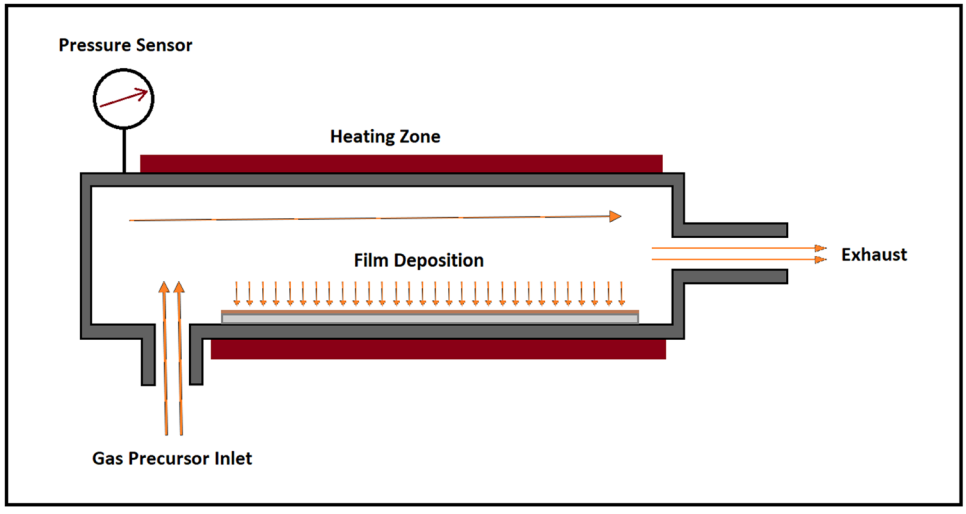

Figure 8: Schematic illustration of a chemical vapor deposition system.

2.2.7 Biochemical methods

To modify the implant surface with superior biological activities, biomolecular cues (BMCs) and antibacterial agents or drugs are the best candidates. The utilization of these large molecules is classified under biochemical methods, which is a subgroup of chemical methods. Hence, sole or incorporation of different biological materials with biomaterials has been seen, like BMCs with osteoinductive effect (*e.g.*, cell adhesive proteins), nano CaP compounds with BMCs or antibacterial drugs, or direct coating of antibacterial agents or drugs. It should be noted that obtaining the aforementioned coatings can also be achieved *via* methods like sol–gel and magnetron sputtering (MS). However, SAMs are technically used to coat nanoscale biochemical molecules on the implant.

2.2.7.1 Self-assembled monolayers (SAMs)

SAMs can spontaneously coat nanoscale biochemical molecules by exposing specific substrates and functional end groups (Figure 9). SAMs are formed by the adsorption and self-assembly of molecules (*e.g.*, alkane phosphate) and biomolecules [*e.g.*, growth factors like bone morphogenetic protein-2 (BMP-2)] at the interface, which may either accelerate or provide different bioactivities [88–90]. Herein, surface roughness has a superior impact on the anchorage of fibroblast cells than wettability [15]. Moreover, surface modification techniques and molecular grafting have a synergetic role to increase the reactiveness between the outward surface and tailored ends of SAM molecules [91].

SAMs have the potential to immobilize biocompatible molecules on the surface (linking function) that helps the ECM components (*e.g.*, laminin [92], fibronectin [93], heparin [94], collagen [95], antibiotics [96], and growth factors [97]) to covalently bound onto the Ti surface. Urface *et al.* self-assembled arginine-glycine-aspartic-cysteine (RGDC) on the gold-coated Ti surface and observed enhancements in cell attachment, spreading, and proliferation [98].

2.3 Physical methods

Physical methods of modification are the transformation of an inert surface to a bioactive one under dry processes. These methods include a variety of single/hybrid procedures which generate a bioactive surface *via* the formation

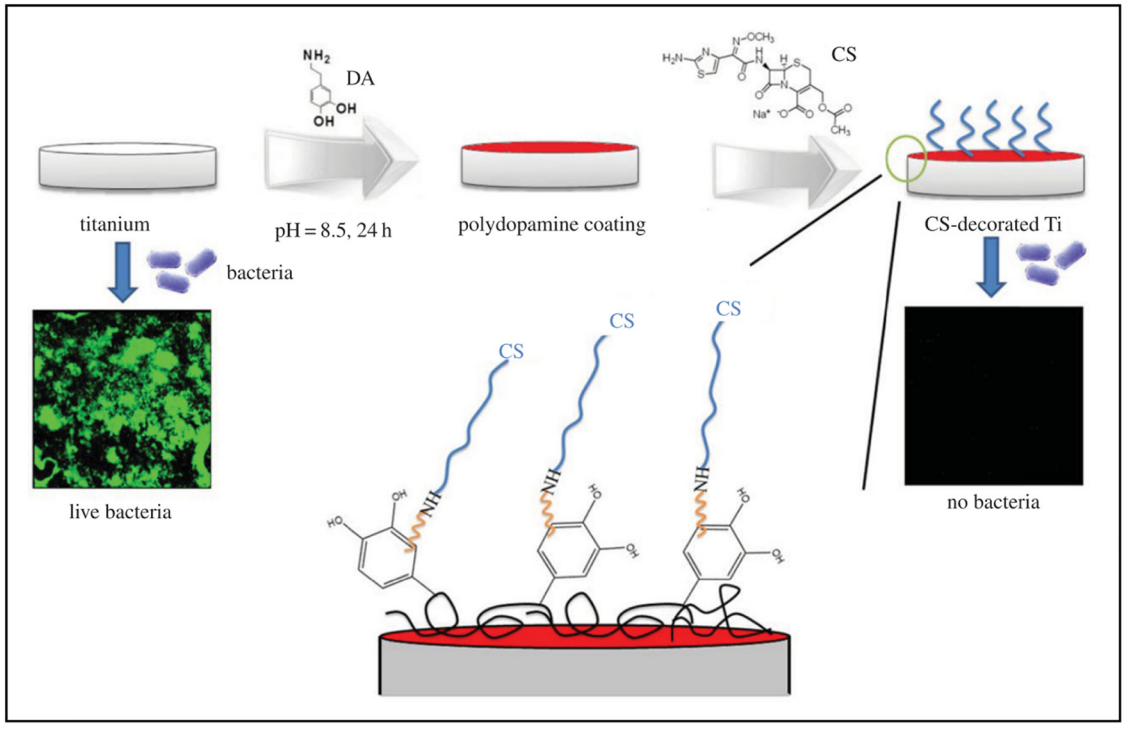

Figure 9: Schematic illustration of the SAM process, preparing, and analyzing antibacterial activity of cefotaxime sodium-decorated Ti by coating polydopamine (PDA). The possible chemical structure, as well as the suggested reaction mechanism, is also shown [96]. Copyright 2014, Journal of the Royal Society Interface.

of layers of material on the surface or decontaminating it. Primarily, physical methods include plasma spray (PS), physical vapor deposition, ion-beam deposition, lithography, and laser treatment.

2.3.1 Plasma spray (PS)

PS is the most widely used technique to coat biomaterials on the implant surface. PS is the process of projection and condensation of high-temperature molten droplets on the surface (Figure 10). The temperature achieved by PS is much higher than similar procedures, which vary its applications of coating an extended group of materials such as Au, Ag, Ti, Zr, as well as other metals, ceramics, and polymers with the thickness of <100 nm [21,66,99]. Wang *et al.* coated Ti surface with Ta after two-step of AO and reported that Ta/TiO_2 nanotubes were fabricated at micro- and nanoscales. Also, numerous enhancements in roughness, wettability, adhesion, differentiation, mineralization, and osteogenesis-related gene were observed [100].

2.3.2 Physical vapor deposition (PVD)

PVD is used to produce metal particles that react with reactive gases to form compounds deposited on the implant surface. Technically, high-energy ions are ejected in a vacuum chamber that changes the surface of the substrate and form thin films (Figure 11).

PVD includes three techniques, namely, evaporation, ion plating, and sputtering. Herein, sputtering, also known as sputtering deposition (SD), and derived techniques of ion plating are the most commonly used methods to deposit nanostructured films on the implant surface. Moreover, the development of SD led to more advanced techniques called ion beam sputtering (IBS) and MS (Figure 12) [101]. Huang *et al.* evaluated the incorporation of antibacterial agents onto the surface of the implant *via* the MS technique. They observed an acceptable bactericidal effect under optimum processing parameters [102].

2.3.3 Ion-beam-assisted deposition (IBAD)

IBAD is the combination of ion implantation and SD. In the IBAD technique, the implant surface is covered with an elemental cloud that is formed by ion bombarded precursors and targeted by highly energetic gas ions (*e.g.*, inert Ar^+ ions or reactive O^{2+} ions) to collide the gaseous ions to substrate ions and decrease the energy of the precursors in the elemental cloud to form a thin layer of material on the surface (Figure 13).

This technique has several potentials including synthesis of the highly pure layer under ultraclean process and notable adhesion between the deposited layer and implant; also the process does not change the bulk properties of the substrate and it can be performed under controlled conditions [105]. The variables such as time, temperature, and amount of the water vapor present are considered as the

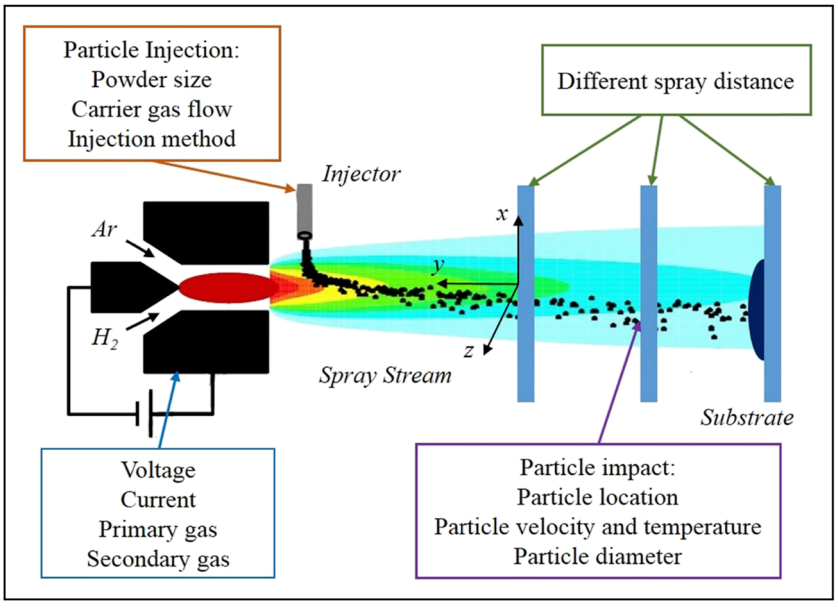

Figure 10: Schematic illustration of the PS process [72]. Copyright 2020, Frontiers.

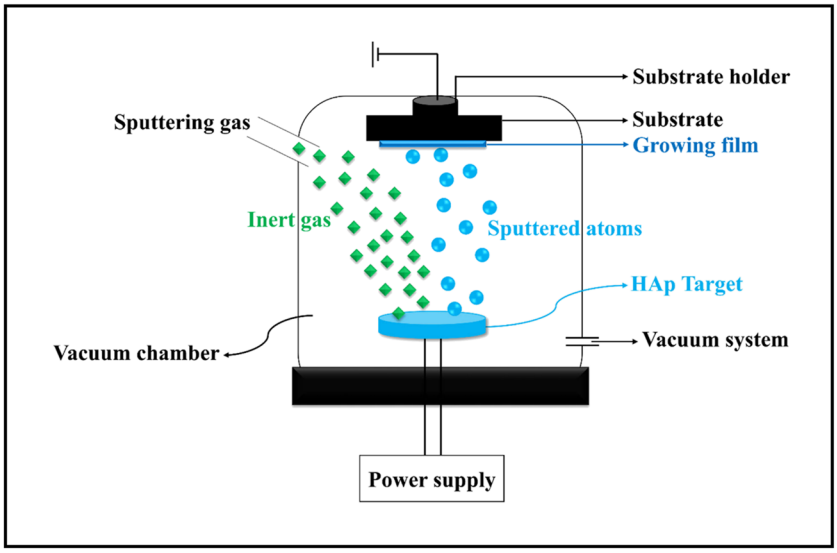

Figure 11: Schematic illustration of the physical vapor deposition process, sputtering, for deposition of target coatings [103]. Copyright 2021, MDPI.

main contributors to favorable crystallinity. Usually, this method is accompanied by heat treatment to change the amorphicity of the deposited layer to a crystalline phase. Miralami *et al.* fabricated ZrO_2 and TiO_2 coatings on the Ti surface. They found that nanostructures generated by IBAD enhanced bone-associated gene expression at initial cell adhesion, proliferation, and differentiation [106].

2.3.4 Lithography

Lithography is a favorable technique in electronic industries and is used to pattern specific models on a rigid substrate. Lithography consists of both top-down and bottom-up procedures to fabricate nanostructures. In top-down procedures, three widely used techniques

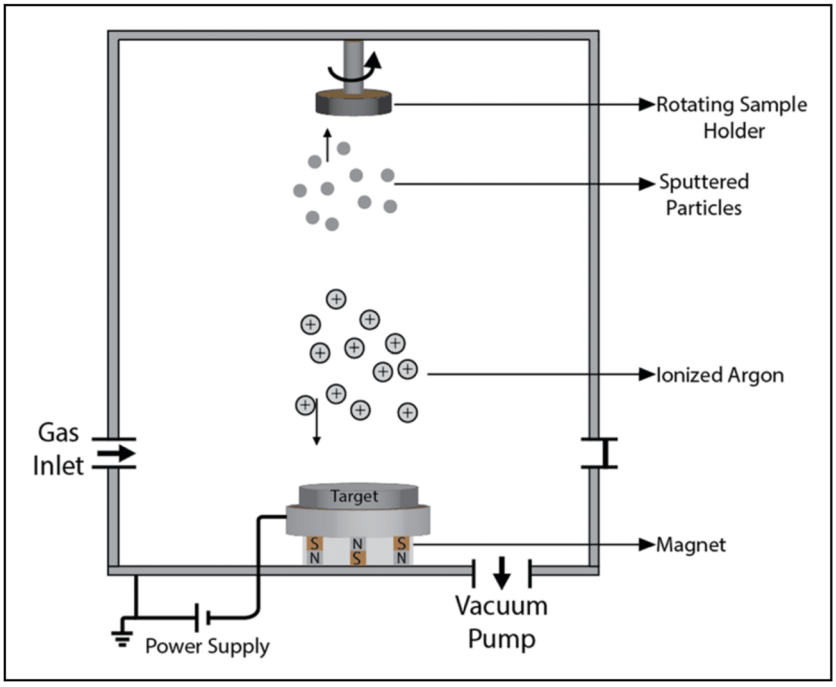

Figure 12: Schematic illustration of the MS process [104]. Copyright 2020, Royal Society of Chemistry.

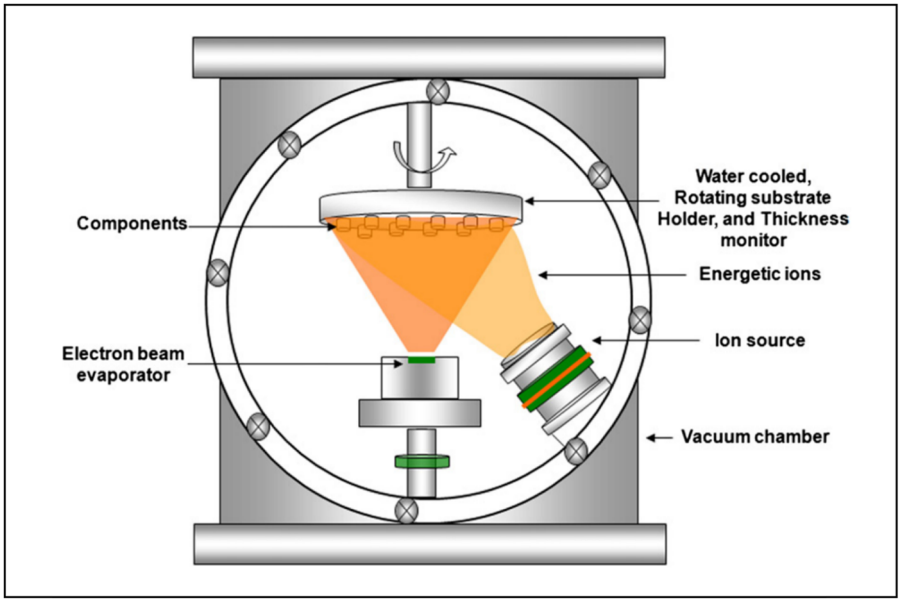

Figure 13: Schematic illustration of the IBAD system and process [105]. Copyright 2011, Elsevier™.

including photolithography, electron beam lithography, and colloidal lithography are used and in bottom-up procedures, techniques like polymer phase separation, colloidal lithography, and block copolymer lithography are well-known [20,107]. The concept of patterning is simple, for example in photolithography, a predefined pattern is fabricated on a mask and locates upon the substrate that has been coated by a photoresist layer (*e.g.*, chromium) and after the exposure of ultraviolet (UV) radiations, the pattern will transfer into the surface and the remaining photoresist layer can be chemically etched (Figure 14) [13]. Generating nanostructures with photolithography smaller than 100 nm is restricted by its diffraction limits [108]. However, electron beam lithography has overcome the limitation and has the potential to fabricate nanostructures down to 5–7 nm [109,110].

2.3.5 Laser treatment

Laser treatment uses high-energy beams to generate 3D structures at the micro/nanoscale. This technique is

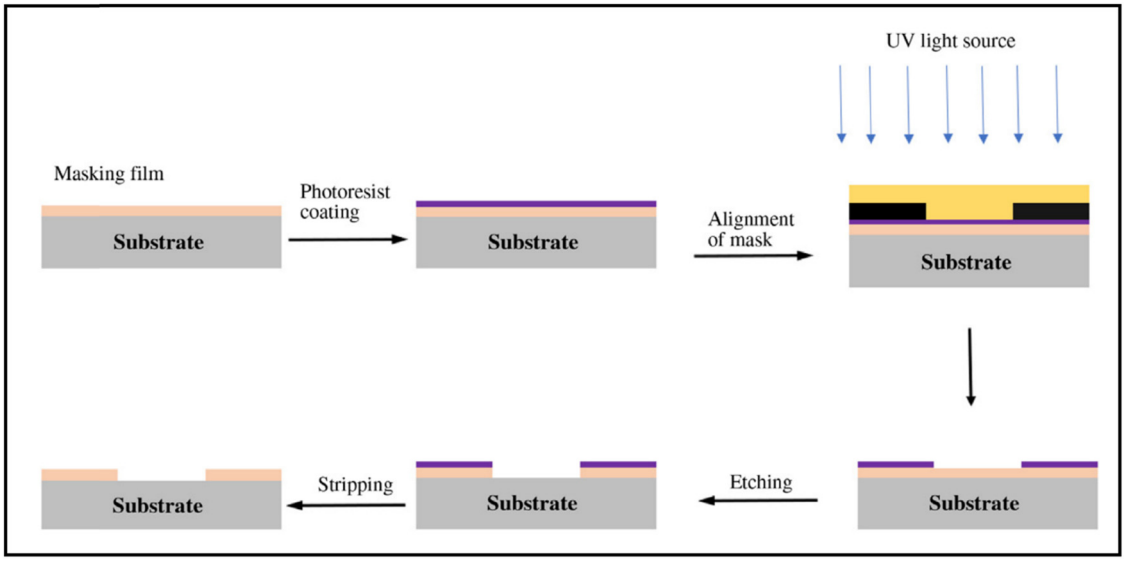

Figure 14: Schematic illustration of photolithography [111]. Copyright 2019, Elsevier™.

capable of producing complex selective surface topography with high resolution [112]. Moreover, laser treatment is a rapid and ultraclean nanofabrication technique that has precise, targeted, and guided surface roughening that can be performed under controlled conditions for the selective changes in implants [66]. Chang *et al.* used 3D laser-printed porous Ti grade-5 and reported that porous dental implant had the active new bone formation and good osteointegration. Also, its biomechanical parameters are significantly higher than the commercially controlled samples [113].

3 Surface nanotopography

Recent advances in implant development have led to nanoscale topographies. Nanotopography is a characteristic of a surface that implies a specific physiobiological interaction between the nanopatterns and the environment. At the nanoscale, better interaction with the cell membrane has been reported [114]. Generally, numerous nanopatterns have been developed for bone regeneration applications (Figure 15). Therefore, biomimetic nanotopographies with mechano-bactericidal activity attracted a lot of attention as they can rupture the cell membrane through physical forces (Figure 16). This group is categorized into two subclasses: (i) nanopillars and (ii) nanoblades and their derivations. The first consists of nanopillars, nanospikes, nanotubes, nanocones, nanospears, nanoneedles, nanowires, and spinules. The latter includes nanoblades and nanocolumns [19,115].

The efficacy of bactericidal activity of nanopillars is dependent on several parameters but only four key geometric parameters including spacing, base diameter, tip diameter, and height are considered for the measurements (Figure 17) [116]. However, obtaining the optimum results requires considering the finite size and shape of bacteria plus the geometry of the nanopattern on the degree of bacterial membrane stretching using parameters such as bacterial stretching modulus, bending modulus, adhesion energy of the cell membrane, as well as radius, height, and spacing of the nanopillars [117].

Normally, nanopatterns are biocompatible yet decreasing in parameters like the tip diameter can reversely affect the osteogenic cells [118]. Therefore, utilization of nanotopographies with no bactericidal potential may be a sensible option as they are still able to chemically interact with bacteria and eliminate them. Of this group, nanopillars, nanotubes, nanofibers, nanogrooves, nanopits, and nanorods demonstrated higher cellular affinity [20,119,120].

3.1 Nanopillars

Nanopillars can be fabricated on the Ti surface by the AO technique with different states in arrangement [123,124]. The mechano-bactericidal activity of this nanotopography was first found from surfaces in nature [34]. This activity occurs by scratching the adsorbed cell wall and rupturing it by putting stress beyond its elastic limit [117,122,125]. Biologically, changes in the height of nanopillars lead to different responses from the cytoskeletal organization and cell morphology. The bactericidal mechanism of nanopillar and its derivations can be augmented by the deflection of elastic nanopatterns that induce additional lateral stress on the bacterial cell wall (Figure 18) [126]. In this case, both carbon nanotubes (CNTs) and high-aspect-ratio silicon nanowires displayed notable promotion in their mechano-bactericidal activity caused by their potential to deflect regarding bacterial attachment.

As shown in Figure 17(d), the amount of lateral tip deflection (δ) caused by the generated forces from bacterial adsorption (P) is controlled by the length (L) of the nanopillars, as well as the attaching position of the bacteria to the cell membrane. Therefore, to obtain equal energy as longer nanopillars, shorter and low-aspect-ratio nanopillars should deflect less. Mcnamara *et al.* evaluated the cell organization of cytoskeleton cells on different nanopillars' heights (8, 15, 55, 100 nm pillars) spread to polygonal shapes and observed that cytoskeleton cells were highly organized on 8 and 15 nm pillars, while by a gradual increase in the height, less organization were seen [127,128]. Moreover, planar control can significantly affect the focal adhesions and most of the larger focal adhesion per cell, but it can reversely affect the total number of adhesions per cell [127,128]. Similarly, variation in nanopillars' height could not affect the osteogenic differentiation but it could enhance its bactericidal activity as it was higher and sharper [123,129]. Also, differences in their shapes can significantly affect osteogenic cell differentiation [130].

3.1.1 Nanospikes

Nanospikes are a derivation of nanopillars with a longer length, sharper tips, and high aspect ratio. Physical parameters of nanospikes were 20–80 nm in diameter and 500 nm in height, which by considering their sharpness, they can also restrict cellular activities. Therefore, Ivanova *et al.* fabricated the only *in vivo* biocompatible and mechano-bactericidal nanospikes by using black silicon [118]. Nanospikes are able to induce severe stress on the cell membrane

Table 1: A summary of nanofabrication techniques and their advantages for dental implants [101]

Mechanical methods			
Technique	**Surface morphology**	**Advantages**	**Disadvantages**
Machining	0.3–1 μm R_a with 10 nm oxide layer	• Enhanced cell adhesion and osteointegration	• Fabricating imperfect surfaces that prolong the healing process
Grinding	Less than 1 μm R_a	• Improved osteointegration, hydrophilicity, density, and viscosity	• May cause several damages to the surface • Difficult operation for dental implants
Polishing	~ 350 nm R_a	• Improved osteointegration and surface quality • The potential to use different chemicals within the slurry	• Performing multiple steps
SB	0.3–3 μm R_a	• Enhanced osteointegration • Controllable surface roughness	• Particles remain on the surface
SP	25–80 nm grains	• Increased cell adhesion, differentiation, and viability	• Superficial grain refinement
		• Higher surface quality	• Limited particle size for dental application
Attrition	Less than 100 nm grains	• Higher surface quality • Deeper grain refinement	• Not applicable for dental implant • Increased hydrophobicity at smaller scales

Chemical methods		
Technique	**Surface morphology**	**Advantages**
AE	0.3–1 μm R_a with 10 nm oxide layer	• Increase anchorage of fibrin and osteogenic cells • Potential of fabricating nanotopography
HPT	Less than 10 nm inner oxide layer Up to 40 nm outer porous layer	• Improved biocompatibility • Ability to form apatite
AT	~1 μm layer of sodium titanate (Na_2TiO_3) gel	• Improved cell differentiation • Ability to form apatite
Sol–gel	Less than 10 μm of a thin layer of ceramic	• Wide selectivity of biomaterials • Ability to deposit complex compounds • Easy processes • Highly bioactive surface
Electrochemical treatment	~ 10 nm–10 μm layer of uniform TiO_2	• Enhanced bioactivity and corrosion resistance • Potential of fabricating nanotopographies
CVD	~1 μm layer of TiC, TiN, TiCN, diamond-like carbon, and diamond NPs	• Enhanced biocompatibility • Significantly high surface quality
SAMs	—	• Highly improved biogenic and/or biocidal activities

Physical methods		
Technique	**Surface morphology**	**Advantages**
PS	Less than 100 nm layer of metallic, ceramic, or polymer compounds	• Improved surface quality and biocompatibility • Wide selectivity of biomaterials
SD	Less than 1 μm layer of TiC, TiN, TiCN, and amorphous carbon	• Enhanced biocompatibility • Significantly high surface quality
IBAD		• Enhanced biocompatibility

(*Continued*)

Table 1: *Continued*

Mechanical methods			
Technique	**Surface morphology**	**Advantages**	**Disadvantages**
	~10 nm of a modified layer with/ without TiN or TiO_2	• Significantly high surface quality	
Lithography	~60 nm layer of ultrafine nanotopography	• Potential of fabricating specific nanotopographies • Enhanced bioactivity • Improved bone-implant contact	
Laser treatment	—	• Ability to fabricate multiphase composition at micro- and nanoscale • Improved cell adhesion and overall biogenic activities	

that has high efficacy against both Gram-positive and Gram-negative bacteria, even highly resilient *Bacillus subtilis* (*B. subtilis*) endospores were annihilated [132]. Black silicon nanospikes are not able to interact with the biological environment and if the surface sustains unharmed after sterilization, it has the potential for mechano-bactericidal applications.

3.1.2 Nanotubes

Nanotube arrays, also known as nanodarts, on the Ti surface have been achieved by numerous methods. In this nanotopography, physical parameters including the tube diameter, the thickness of the nanotube layer, and the crystalline structure can influence the cellular responses [133–135]. Nanotube arrays are of attractive topographies due to their effectiveness to promote osteointegration [136,137]. Moreover, nanotube arrays of Ta on the Ti surface significantly increase the cell morphology and proliferation, and osteogenic differentiation of stem cells [138,139]. Gulati *et al.* evaluated the influence of dual topography composed of microscale spherical particles and vertically aligned TiO_2 nanotubes *via* 3D printers. This topography could obtain good enhancement in osteogenic gene expression [140].

Generally, when bacteria are adsorbed onto the surface of CNTs, it leads to tip deflection and retraction, which subsequently disturbs the physical membrane of the bacteria and results in cell death [141]. The bactericidal effectiveness of CNTs is different, *e.g.*, short CNTs with an aspect ratio of 100 have higher efficiency than longer CNTs with an aspect ratio of 3,000 (Figure 19). This effect is attributed to the larger storage of elastic energy by short CNTs that can spontaneously pierce the membrane [142]. The mechano-bactericidal of CNTs was discovered when Elimelech *et al.* observed significant damage to the cell membrane of *Escherichia coli* (*E. coli*) as it directly contacts single-walled CNTs (SWCNTs) [143]. SWCNTs with diameters between 1 and 5 nm have less effect on the direct piercing of a phospholipid bilayer and the free energy costs are regarded as the minimum energy for creating a pore in the bilayer [142]. However, hydrophobic SWCNTs demonstrated greater interaction with phospholipid tails and subsequently entrapped the CNT in the bilayer core in parallel orientation [144]. It should be noted that increasing the tension on the membrane facilitates the translocation of nano-objects through the membrane. Moreover, highly hydrophobic CNTs, as well as graphene, are able to create unstable pores in the membrane by rotation of lipid tails to carbon surface and constant extraction of lipids [145].

3.1.3 Nanoblades

Graphene sheets, also known as nanoblades, with 10–15 nm edges, are of the second category of mechano-bactericidal nanotopographies that are 2D sheet-like nanomaterials consisting of a single layer of carbon atoms. In most nanoblades, it is essential to be perpendicularly oriented, but in nanosheets, the orientation of 37° demonstrated sufficient bactericidal activity [146–148]. The general antibacterial activity of graphene has been achieved through both physical and chemical states [149–152]. The physical interaction of graphene is shared with its derivations, namely graphene family nanomaterials (GFNs), which due to possessing certain parameters, their bactericidal activities can be predicted [153]. The addition of graphene nanosheets in chemical suspensions (Figure 20) provides sufficient antibacterial activity to rupture both Gram-negative and Gram-positive bacteria by creating pores in their cell membrane and stimulating the alteration of osmotic pressure that resulted in cell death [147].

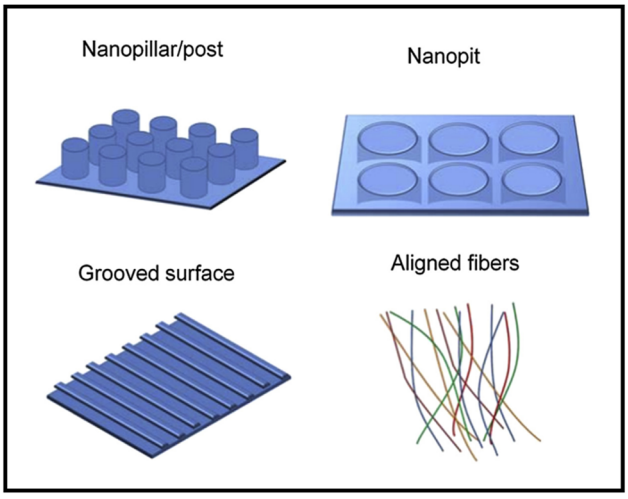

Figure 15: Schematic illustration of some nanopatterns [121]. Copyright 2016, Elsevier™.

Akhavan *et al.* evaluated the antibacterial activity of graphene oxide nanowalls (GONWs) on *E. coli* and *S. aureus* as Gram-negative and Gram-positive bacteria, respectively. They observed GONWs have stronger antibacterial activities against *S. aureus* by colony-forming unit (CFU) enumeration and quantification of cytoplasmic RNA leakage [153]. Similarly, Liu *et al.* confirmed that the bactericidal effect of GFNs against Gram-positive bacteria like *E. coli* was attributed to their sharp edges that can induce sufficient stress on the cell membrane (Figure 21) [154]. The mechanical disruption of GFNs is bonded to the degree of lipophilicity as the higher lipophilic one is able to facilitate the extraction of lipids from the cell membrane [155,156]. However, the progress of extermination of bacteria consists of complex processes including extraction of the lipids, formation of pores, alternation of osmotic pressure, and ultimately, cell death.

3.1.4 Nanofibers

Of the nanotopographies with biological activity, nanofibers are a great choice for bone tissue engineering scaffolds. Nanofibers possess notable properties including high surface-to-volume ratio, well-retained topography, facile control of components, and the capacity to mimic the native ECM that can affect adhesion, proliferation, and differentiation of stem cells [158–160]. Xu *et al.* fabricated a scaffold made of polylactic acid (PLA) and chitosan by the electrospinning technique. To generate a core–shell and island-like structure, they mixed electrospinning with automatic phase separation and crystallization. By culturing preosteoblast cells (MC3T3-E1), they

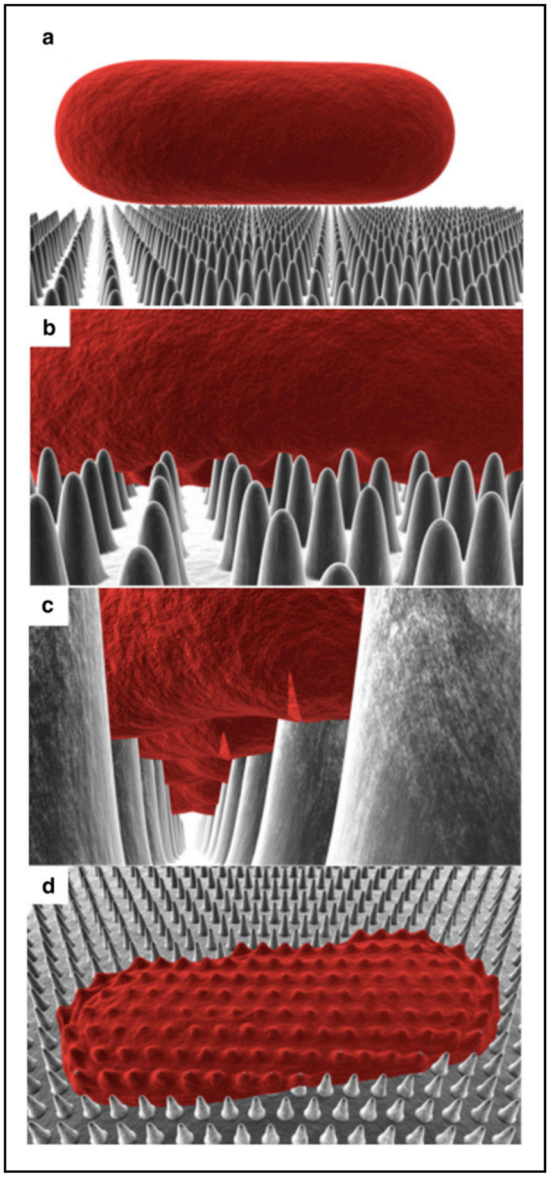

Figure 16: Schematic illustration of the mechano-bactericidal function of the surface. (a) Contacts of a bacteria cell with the wing nanopillar surface. (b) Adsorption of the membrane to the surface protrusions leads to stretching of the cell membrane. (c) Gradual progress of adsorption leads to broad stretching at the contact regions and ultimately (d) cell death [122]. Copyright 2013, Elsevier™.

observed a balanced hydrophilic and hydrophobic surface that successfully enhanced mineralization and cell growth, as well as alkaline phosphatase (ALP) activity of MC3T3-E1 cells [161]. The utilization of simple techniques like electrospinning provided a remarkable potential for some bioactive materials or NPs to incorporate into the nanofibrous structured scaffold [162–164]. Yao *et al.* assessed the biological responses of gelatin nanofibrous scaffold with locally immobilized deferoxamine (DFO). It reduced the cytotoxicity of human umbilical vein endothelial cells (HUVECs)

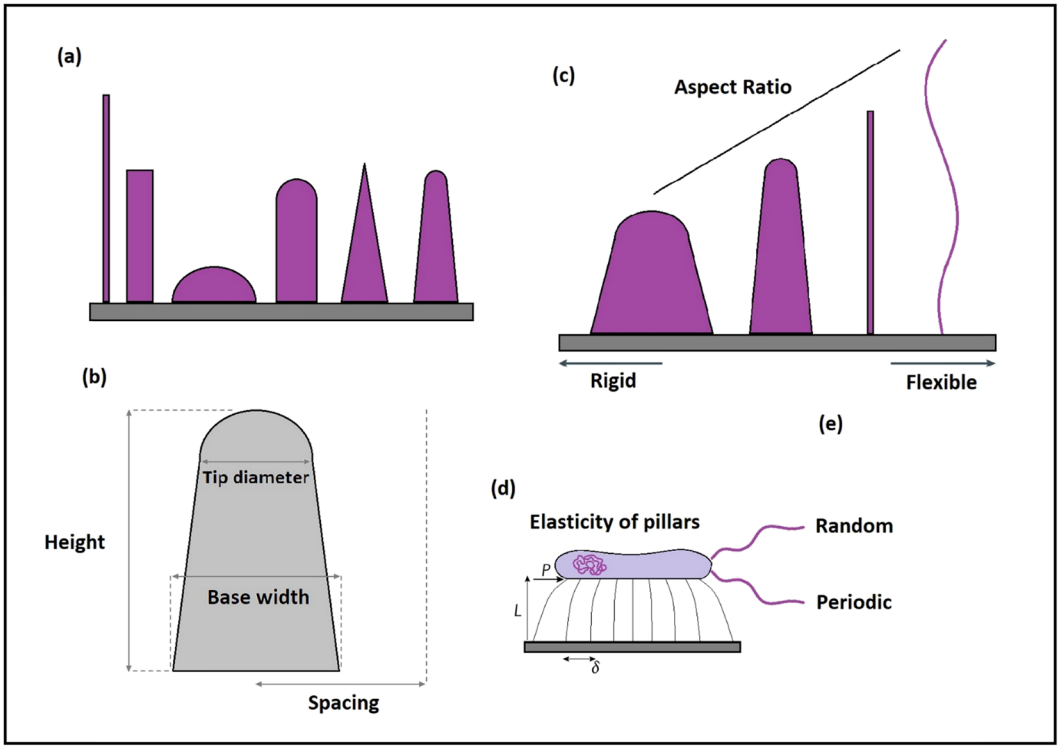

Figure 17: Schematic illustration of the physical parameters affecting the mechano-bactericidal activity of nanopillars and their derivations. (a) Examples of different nanopatterns with varied biocide levels. (b) The geometric characteristics are simplified based on the spacing, base diameter, tip diameter, and height. (c) Increasing the aspect ratio changes the rigid nanopillar to a flexible one, and subsequently, is accompanied by different cellular and antibacterial responses. (d) According to the aforementioned parameters, the strength of each individual nanopattern to impose physical forces on the cell membrane is related to the geometries. (e) Fabrication of nanopatterns can be either in random or periodic arrays. Therefore, the optimized mechano-bactericidal function demands significant attention to the geometric parameters and cautious fabrication.

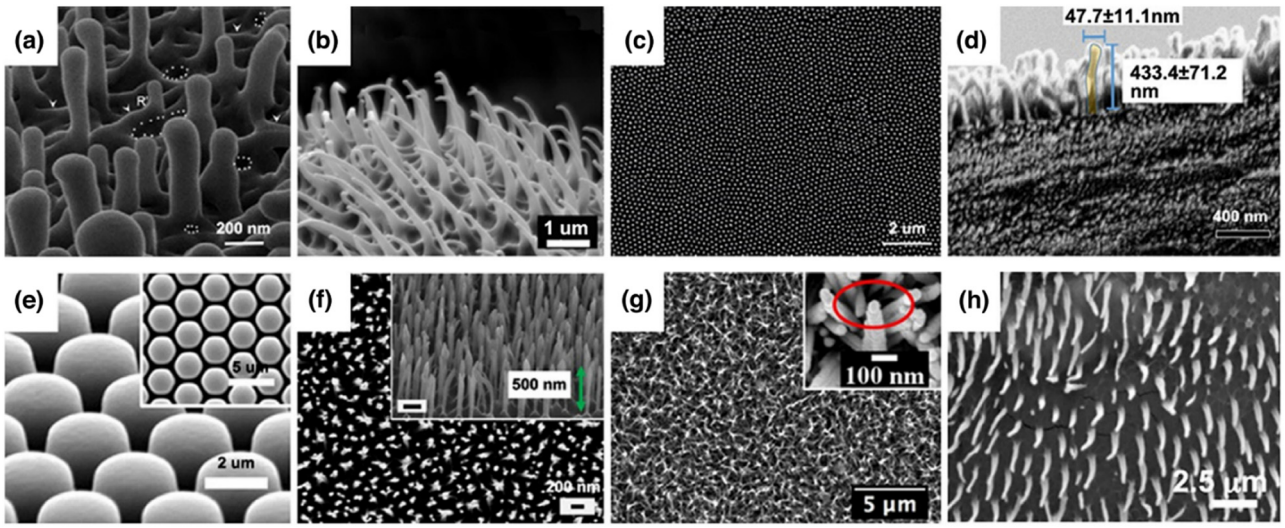

Figure 18: SEM images of some (a–d) natural bactericidal nanotopography and (e–h) synthetic bactericidal nanotopography [131]. Copyright 2021, Elsevier™.

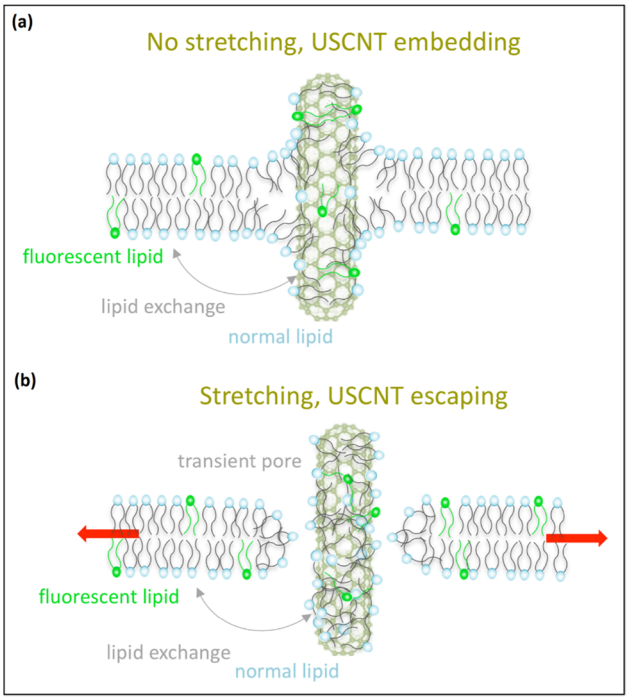

Figure 19: Suggested penetration mechanism of hydrophobic ultrashort CNT (USCNT) by rupturing the lipid bilayer of the cell wall. (a) Dioleoylphosphatidyl-choline (DOPC)-capped USCNT interacts with the bacterial cell membrane by exchanging lipids. (b) USCNT becomes wrapped by lipids that results in dysfunctioning the membrane *via* the formation of pores. To obtain a general perspective of the process, some normal lipids of the bilayer were substituted by fluorescent lipids that can be detected by fluorescence microscopes [145]. Copyright 2018, ACS Publications.

and human mesenchymal stem cells (MSCs). Also, it has significantly promoted vascular endothelial growth factor (VEGF) expression in human MSCs and BMP-2 expression in HUVECs [165].

3.1.5 Nanogrooves

Despite no bactericidal activity, nanogrooves are still an interesting option for their potential to promote the migration and proliferation of osteoblast cells [166]. An investigation on cellular affinity on micro- and nanogrooved surfaces displayed a significant reduction of up to 40% of cell-repelling capacity on microgrooved than nanogrooved surfaces [167]. Klymov *et al.* compared the smooth and grooved CaP-coated surface by culturing osteoblast-like MC3TC cells. They found that not only did nanogrooved surfaces promote the differentiation and mineralization processes but they also organized the morphological deposition of minerals [168].

3.1.6 Nanopits

Nanopits can be generated by PVD techniques with controlled nanopore size. Herein, a few pieces of research have been done to understand the physiobiological function of this nanopattern. Lavenus *et al.* evaluated the presence of human MSCs on the Ti surface with varied nanopore diameters. They observed that human MSCs exhibited a more branched cell morphology on nanopores with 30 nm pore size [169]. Similarly, Dalby *et al.* investigated the influence of spatial arrangement of nanopits on osteogenic differentiation on the poly(methylmethacrylate) (PMMA) surface and cultured osteoprogenitor and MSCs on nanopits with diameter, depth, and center–center spacing of 120, 100, and 300 nm, respectively, as well as with the spatial arrangement of the square array, hexagonal array, disordered square arrays with 20 and 50 nm displacement from their square position (20-DSA and 50-DSA), and randomly positioned. Within the 21st day,

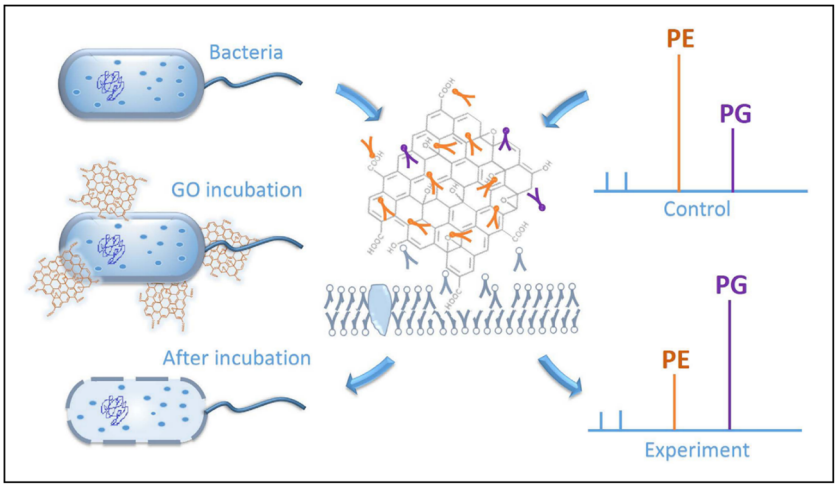

Figure 20: Schematic illustration of the antibacterial activity of graphene oxide (GO)-based on mass spectrometry [157]. Copyright 2016, Scientific Reports.

observation demonstrated a significant increase in levels of osteopontin (OPN) and osteocalcin (OCN) on 50-DSA surfaces compared to other surfaces. With the same result for MSCs, it was spotted that MSCs have a greater affinity to DSA surfaces than other surfaces [124].

4 Multifunctional coatings

Modifying implants with NPs is a promising procedure to reduce the risk of failure. Implants, depending on the patient's general condition, may need to be treated with different NPs to guarantee their success (Figure 22). Herein, we classified these NPs according to their nature as (i) metallic-based, (ii) ceramic-based, (iii) polymer-based, (iv) carbon-based, (v) protein-based, and (vi) drug-based coatings (Table 2). In the following sections, the subclasses and their biological applications in modifying the endosseous implant body are explained.

4.1 Metallic-based coatings

4.1.1 Tantalum (Ta^{5+})

Tantalum (Ta) as both implant material and surface coating obtained considerable attention. Ta is a biocompatible metal with high corrosion resistance and favorable elastic modulus [32]. Ta is able to promote bone ingrowth and osteoconductivity, which are notable parameters as the secondary stability of implants [170]. Alves *et al.* deposited Ta-derived coatings on the Ti surface. They observed higher Ca:P ratio formation on the surface, which was attributed to the high oxygen content of the coating that increases the affinity for apatite adhesion [171]. Zhang *et al.* coated tantalum nitride (TaN) on the Ti surface. Results displayed higher antibacterial and corrosion resistance than individual Ti or TiN coatings [172]. Similarly, Zhang *et al.* coated Ta on the Ti surface to assess its biological activities. Ta-treated Ti could effectively kill *Fusobacterium nucleatum* (*F. nucleatum*) and *Porphyromonas gingivalis* (*P. gingivalis*) microbes. Also, it promoted osteointegration by activating the secretion of bone-forming proteins [173].

4.1.2 Titanium (Ti^{4+})

Coating titania (TiO_2) NPs have various applications in medicine. Titania possesses unique photocatalytic properties by being exposed to visible or UV light irradiation [174]. TiO_2 NPs possess excellent biogenic and biocide properties. The antibacterial mechanism of TiO_2 is attributed to the formation of hydroxyl radicals by a photocatalytic reaction in an aqueous environment that targets the peptidoglycan cell membrane and interacts with polyunsaturated

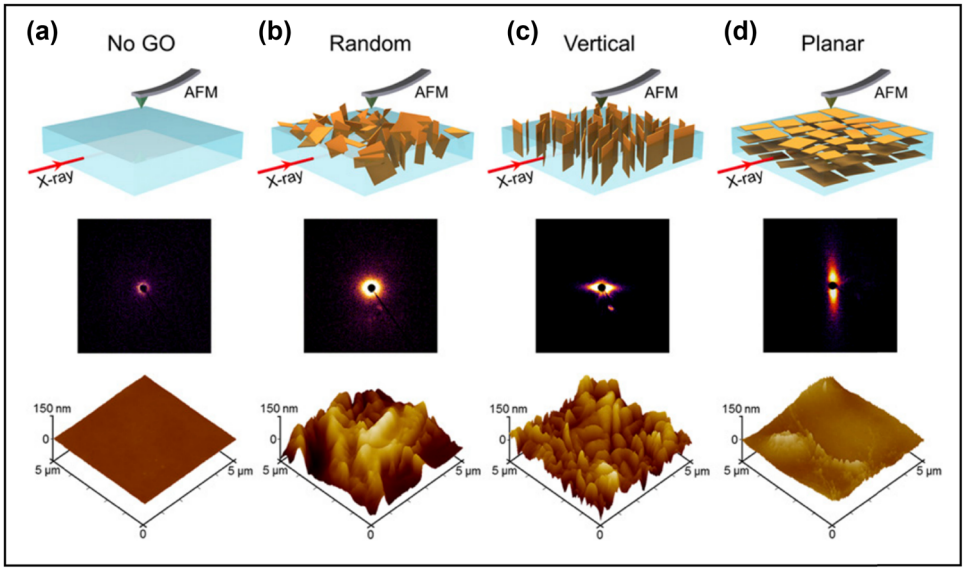

Figure 21: Schematic illustrations, small angle X-ray scattering (SAXS), and atomic force microscopy (AFM) characterization of GO composite to define its orientation in bulk and on the surface of specimens, respectively. According to the 3D illustration, the X-ray beam is located parallel to the film plane, and the AFM probe is placed above the surface. (a) Composite without GO nanosheets displayed minor scattering intensity in the 2D SAXS pattern and smooth surface in the 3D AFM image. (b) Composite with randomly oriented GO nanosheets displayed a notable increase to a broad, isotropic halo in the 2D SAXS pattern, and a sharp increase in roughness in the 3D AFM image. (c) Composite with vertically GO nanosheets displayed anisotropic equatorial scattering in the 2D SAXS pattern, and vertical alignment in the 3D AFM image. (d) Composite with planar GO nanosheets displayed anisotropicmeridional scattering in the 2D SAXS pattern and a smoother surface in the 3D AFM image [148]. Copyright 2017, PNAS.

phospholipids, ultimately damaging the DNA and resulting in cell death [175]. Chidambaranathan *et al.* compared the antifungal activity of TiO_2, ZrO_2, and Al_2O_3 NPs coated on the Ti surface. After 24, 72 h, and 1-week time intervals, TiO_2 demonstrated significant antibacterial activity against *Candida albicans* (*C. albicans*) bacteria than the other NPs [176].

On the other hand, the utilization of titania NPs can improve osteogenic activities like increasing the level of osteoblast cells on the surface, which leads to higher bone generation [177–179]. However, introducing TiO_2 nanotubes attracted considerable attention. Primarily, TiO_2 nanotubes were fabricated to increase the biogenic activity and enhance the osteointegration, but, as a biocide agent, they possess antimicrobial function by being accompanied by other antibiotics compounds like vancomycin, gentamicin, silica-gentamicin, gentamicin sulfate, BMP-2, and heparinized-Ti to eliminate Gram-positive bacteria like *S. aureus* [180–186].

4.1.3 Silicon (Si^{4+})

In nanotechnology, silicon (Si) mainly as silica (SiO_2) NPs obtained a unique position. The utilization of these NPs enhances osteogenic differentiation of MSCs by increasing the osteoblasts' adhesive response that consequently leads to higher osteointegration [187]. Moreover, SiO_2 NPs depending on their size display different levels of hydrophilicity that can be exploited in drug-releasing applications [188]. Also, their products from degradation generate silicic acid [$Si(OH)_4$], which is a supporting compound to generate connective tissues [185]. Csík *et al.* coated the CP-Ti surface with calcium silicate (Ca_2O_4Si) (CaSi) NPs by electrospray deposition (ESD) followed by thermal treatment at 750°C to examine its properties. They observed that CaSi NPs could effectively reduce the *E. coli* and *S. aureus* bacteria and promote human MSC activity [189]. Massa *et al.* assessed the antibacterial activity of SiO_2 and the Ag nanocomposite (NSC/AgNPs) coated on Ti grade-5. They reported that not only did NSC/AgNPs kill the Gram-negative bacteria, *Aggregatibacter actinomycetemcomitans* (*A. actinomycetemcomitans*), but it also reduced the biofilm formation up to 70%, compared to the control group [190]. Catauro *et al.* developed the silica/quercetin hybrid as an antioxidant drug to scavenge the reactive oxygen species (ROS) and reactive nitrogen species (RNS) for dental implant applications. Quercetin is able to maintain the conditions of the general tissues against osteoporosis, pulmonary, and cardiovascular diseases, a particular spectrum of cancer, and premature aging. The results showed that quercetin successfully restricted the dehydrogenases' activity [191].

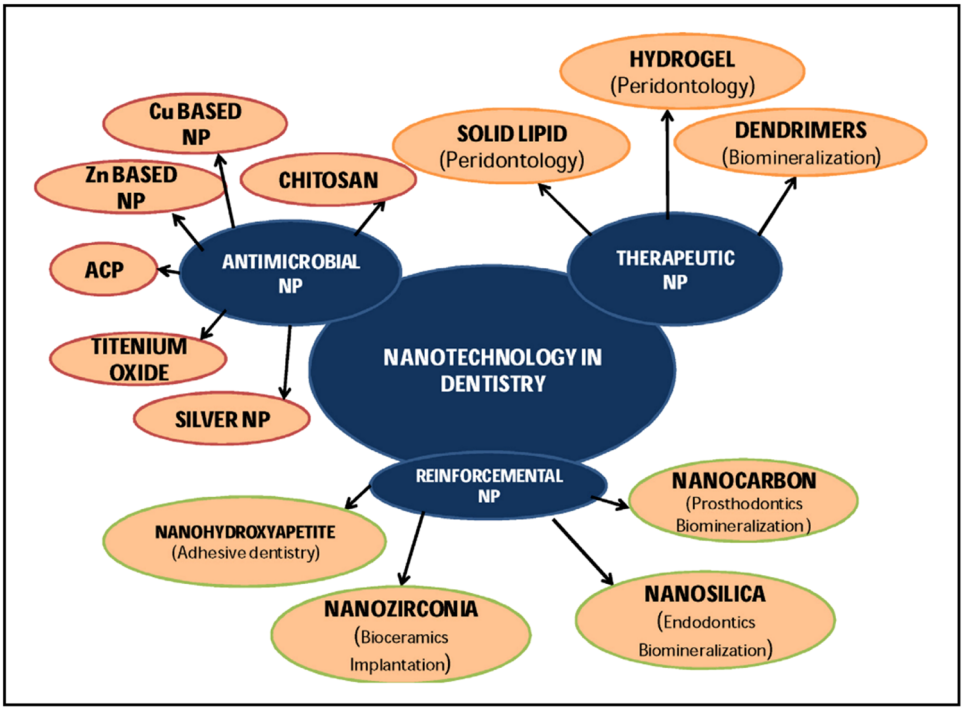

Figure 22: Applications of nanoparticle coating in dentistry [22]. Copyright 2018, Elsevier™.

4.1.4 Cerium (Ce^{4+})

Ceria (CeO_2) is another NP with strong anti-inflammatory and antibacterial activities. CeO_2 NPs possess superoxide dismutase (SOD) and catalase (CAT) enzymatic activities, as well as ROS-scavenging [26]. Li *et al.* evaluated the biological responses of CeO_2 NPs coated on the Ti surface. The results showed that CeO_2 NPs have no cytotoxicity to MC3T3-E1 cells and they can improve cell adhesion; also CeO_2 coating maintained intracellular antioxidant defense system from H_2O_2-treated osteoblasts [192]. Qi *et al.* evaluated the incorporation of CeO_2 and calcium silicate (Ca_2O_4Si). This composite displayed sufficient biocompatibility and antimicrobial activity against *Enterococcus faecalis* (*E. faecalis*) [193]. Ceria with varied nanopatterns exhibited different levels of antibacterial activity. Li *et al.* compared the biocide activity of ceria NPs with different nanotopographies. They fabricated three nanopatterns including nanorod, nanocube, and nano-octahedron to select the one with less presence of *Streptococcus sanguinis* (*S. sanguinis*) bacteria. From *in vitro* and *in vivo* tests, they concluded that nano-octahedron had stronger anti-inflammatory and antibacterial activities [194].

4.1.5 Gold (Au^{3+})

In terms of medical application, gold (Au) NPs have been frequently used due to their notable mechanical, chemical, and optical properties. Despite the high price of gold that may be restrictive, still, its utilization is inevitable. In dentistry, Au NPs demonstrated both biogenic and antibacterial activities but within the range of 40–50 nm, they are toxic. Therefore, their applications have been limited to 20–40 nm, which has been found to be the optimum cellular affinity [195]. Au NPs possess antibacterial, antifungal, and anticancer functions [196,197]. The antifungal effects of Au NPs are highly dependent on their geometry [198]. Technically, the antifungal mechanism of Au NPs is based on the prevention of the H+-ATPase action or transmembrane H+ efflux action of Candida bacteria [30]. In general, the bactericidal effects of Au NPs are weaker than Ag on both Gram-positive and Gram-negative bacteria [199–201]. The antibacterial mechanism of Au NPs is based on the prevention of ribosome subunit for t-RNA binding or changing the membrane potential and obstructs the ATP synthase, which disturbs both the biological system and results in cell death. Also, the interaction of Au NPs is free of ROS, which implies less toxicity on mammalian cells [202].

Regiel-futyra *et al.* coated chitosan-based Au composite NPs on Ti implant. This innovative composite displayed remarkable antibacterial function against antibiotic-resistant strains of *Pseudomonas aeruginosa* (*P. aeruginosa*) and *S. aureus* without any sign of cytotoxicity [203]. Wang *et al.* evaluated the modification of Au NPs with thiol or amine groups to decorate different densities of phenylboronic acid to fabricate Gram-selective antibacterial agents. They observed that modified Au NPs with amine- or thiol-tethered phenylboronic acids can effectively interact with lipopolysaccharide (LPS) and lipoteichoic acid (LTA), as Gram-positive and Gram-negative compounds, respectively. Also, tunable ratios of thiol- and amine-tethered phenylboronic acids lead to different antibacterial activity [204]. Heo *et al.* assessed the effects of Au NPs on osteoblast differentiation. From *in vitro* and *in vivo* tests, they observed an increase in mRNA expression of osteogenic differentiation-specific genes and good bone formation on the Ti surface, respectively [205].

4.1.6 Iron (Fe^{3+})

Iron oxide (Fe_xO_x) has proven its capability as a dental coating. Primarily, magnetite (Fe_3O_4) and maghemite (Fe_2O_3, y-Fe_2O_3) are the two most popular forms of iron oxide NPs without further cytotoxicity [206]. Most Fe_xO_x-derived NPs in biomedicine possess superparamagnetic properties [207]. For example, Fe_2O_3-superparamagnetic can improve osteoblast functions and help to eliminate the formed biofilms [208]. Generally, iron oxide NPs are able to interact with exopolymers that are generated by bacteria and are difficult to be eradicated by many antibiotics and immune cells as they are impenetrable [209].

Thukkaram *et al.* evaluated the efficacy of varying concentrations of iron oxide NPs against biofilm formation on different biomaterials. The optimal effectiveness was obtained at a concentration of 0.15 mg/mL against *S. aureus*, *E. coli*, and *P. aeruginosa* bacteria [210]. In addition to biocide activity, iron oxide NPs possess magnetic properties that displayed higher stability and safety than other commonly used NPs. The cytotoxicity and inflammatory responses of these NPs are highly dependent on concentration rather than size, which could be exploited for designing new drug carriers [211].

4.1.7 Copper (Cu^{2+})

Copper oxide (Cu_xO_x) NPs have unique physical, chemical, and biological properties that expand their medical applications. Similar to Ag, CuO-derived NPs displayed excellent antibacterial activity. However, the utilization of such metallic ions was restricted as their adverse effects were induced by

remaining residues [212]. In addition to being antibacterial, Cu_xO_x NPs possess antifungal, antibiofilm, and antimicrobial activities [21]. The antibacterial mechanism of these NPs is based on passing through nano-mimic pores on the bacteria cell membrane and disturbing their biological activity by damaging the vital enzymes. This progress is highly dependent on the size, stability, and the concentration of NPs in the medium [213].

Likewise, antimicrobial activity is the result of the generation of ROS, which increases the oxidative stress of the cells [214]. Rosenbaum *et al.* coated CuO-derived NPs on the TiO_2 surface and have not found a sign of *S. aureus* and *E. coli* bacteria [215,216]. Liu *et al.* included copper in the Ti alloy composition and observed significant activity against *Streptococcus mutans* (*S. mutans*) and *P. gingivalis* [217]. Khan *et al.* evaluated the inhibitory effect of Cu_xO_x NPs within a size of 40 nm to prevent biofilm formation. *In vitro* results revealed that a concentration of 50 mg/mL can successfully prevent the development of oral bacteria and their polysaccharides [218].

4.1.8 Zinc (Zn^{2+})

Recently, zinc oxide (ZnO) NPs have become an attractive candidate as a biologically active ion that promote osteointegration and restrict the adhesion of bacteria [219,220]. The general bactericidal mechanism of ZnO NPs consists of a combination of (i) generation of H_2O_2 and (ii) formation of electrostatic interaction that accumulates ZnO NPs on the bacteria cell membrane, (iii) generation of ROS that leads to the release of Zn^{2+} ions, and ultimately, dysfunctioning the cell membrane [213]. This progress is applicable against both Gram-positive and Gram-negative bacteria [213,221]. Hu *et al.* coated ZnO NPs on the TiO_2 surface and restricted the growth of *S. aureus* and *E. coli* bacteria [222]. Similarly, Luo *et al.* fabricated ZnO@ZnS nanorod-array and optimized the release rate of Zn^{2+} ions that demonstrated higher bactericidal activity against *S. aureus* and *E. coli* bacteria [223]. Tabrez Khan *et al.* assessed the inhibitory function of ZnO NPs against biofilm-forming bacteria and colonizers. They observed that ZnO is able to provide significant bactericidal activity on different surfaces [218].

4.1.9 Magnesium (Mg^{2+})

Magnesium (Mg) is an attractive metal that can be fully adsorbed without acute toxicity. Physically, Mg possesses similar parameters to the human bone but, chemically, it has a limited range of applications that is mainly the result of its high rate of degradation. This high interaction of Mg^{2+} ion is attributed to the chloride ion (Cl^-) available in ECM that forms the $MgCl_2$ compound [224]. In general, the presence of Mg^{2+} ion promotes proliferation and differentiation of osteoblast cells [225]. Also, magnesium oxide (MgO) possesses good bactericidal activity with the mechanism of disturbing the bacteria cell membrane, which leads to leakage of intracellular contents and ultimately cell death [226,227]. To control the release rate of Mg^{2+} ions, simply compounding it with other materials cannot increase its corrosion resistance. For example, magnesium phosphates (MgPs) demonstrated higher *in vivo* adsorption than the calcium phosphate (CaP) compounds [228]. Kishen *et al.* compared the antimicrobial activity of MgO, sodium hypochlorite (NaOCl), and chitosan NPs. They concluded that both MgO and chitosan NPs have comparable or superior bactericidal activity than NaOCl against *E. faecalis* bacteria [229].

4.1.10 Silver (Ag^+)

Of the most practical antimicrobial coatings, AgNPs have been taking the lead. In retrospect, the high release of Ag^+ ions from the implant surface would disturb the normal biological activities, but AgNPs at low doses displayed high biocompatibility and antibacterial activity with no sign of cytotoxicity, genotoxicity as well as side-effects [177,230]. The utilization of Ag^+ ions was in the form of silver nitrate ($AgNO_3$), silver sulfadiazine ($C_{10}H_9AgN_4O_2S$), silver chloride (AgCl), and pure metal that could exterminate a wide spectrum of both Gram-positive and Gram-negative bacteria. However, AgNPs demonstrated higher antimicrobial efficacy than the aforementioned forms [231]. Ag at the nanoscale can facilitate the formation of holes onto the bacteria cell membrane and result in cell death [232]. This mechanism is attributed to the interaction of AgNPs with disulfide or sulfhydryl groups of enzymes [233]. In recent research works, the fabrication of Ag-based composite NPs has been widely seen. Choi *et al.* fabricated PDA and AgNPs on the Ti surface. They observed lower colonization of *S. mutans* and *P. gingivalis* microbes with a coating of these NPs than uncoated Ti [234,235]. Gunputh *et al.* coated AgNPs on the TiO_2 nanotube surface with and without a top coating of HAp NPs to evaluate its biocide activity against *S. aureus* microbe. *In vitro* results revealed that AgNPs could effectively reduce the presence of the microbe. Also, the addition of HAp did not improve the biocidal function but it could diminish the release rate of Ag^+ ions [236].

4.1.11 Selenium (Se^{2-})

Selenium (Se) NPs are unique elements with high biocidal potential against bacteria, viruses, and cancer cells. Se^{2-} ions are a vital element in biological processes that control the elimination of ROS and modulation of a specific enzyme that lacks its increased susceptibility to viral infections [237,238]. Nanoscale Se exhibits a reduced risk of toxicity than its other forms like selenomethionine (SeMet) [239]. Therefore, the utilization of SeNPs as chemopreventive and chemotherapeutic coatings with both antibacterial and antiviral activity became attractive [240–243]. Moreover, SeNPs have proven to possess high bactericidal activity against *S. aureus* and *Staphylococcus epidermidis* (*S. epidermidis*) bacteria, which are the main cause of implant failure [244,245]. Srivastava *et al.* examined different concentrations of SeNPs to eliminate various bacteria. They found that at concentrations of 100, 100, 100, and 250 μg/mL, these NPs can kill 99% of *Pseudomonas aeruginosa* (*P. aeruginosa*), *S. aureus*, *Streptococcus pyogenes* (*S. pyogenes*), and *E. coli*, respectively [246].

4.2 Ceramic-based coatings

4.2.1 Bioinert ceramics

4.2.1.1 Zirconium (Zr^{4+})

The utilization of zirconia (ZrO_2) NPs in dentistry has been expanding since these NPs displayed great potential in improving the physicochemical properties of different compounds. Zirconia is a bioinert ceramic with low toxicity. Also, it cannot dissolve in water, which causes less adhesion of bacteria [247]. Zirconia-based NPs demonstrated antimicrobial activity against some microorganisms like *E. faecalis* [248]. In terms of biogenicity, ZrO_2 NPs promote the attachment and proliferation of osteoblast and fibroblast cells and release nontoxic ions [249–252]. However, compared to Ti, ZrO_2 NPs are at disadvantage to promote cell viability [253]. Huang *et al.* coated ZrO_2 NPs on the Ti implant *via* the PS technique. After 2 weeks, the *in vivo* test showed a higher level of osteoblast cells that was attributed to the theory that adhesion of osteoblast cells can be promoted by higher free-energy surface [136,254].

4.2.2 Bioactive ceramics

4.2.2.1 Bioactive glass

Bioactive glasses (BGs) mainly refer to the mixture of silica, calcium oxide (CaO), sodium oxide (Na_2O), and phosphorous pentoxide (P_2O_5) as silicate-based compounds [255,256]. BGs compared to other bioglasses (*e.g.*, borate-based glass or phosphate-based glass), or ceramic glasses, have a higher potential to merge with the host tissue [257–259]. Moreover, manifold elements can be doped with BGs to modify their properties, for example, utilization of Na^+, Mg^{2+}, Al^{3+}, Ti^{4+}, or Ta^{5+} ions can reduce or increase the solubility as well as Ag^+, strontium (Sr^{2+}), or Zn^{2+} for modifying bactericidal activity, cellular viability, or anti-inflammatory responses of BGs, respectively [257,260,261]. Kalantari *et al.* evaluated the synthesis and osteogenic applications of monticellite for bone tissue engineering and compared its biological activity with HAp. They concluded that monticellite has a higher bone formation than HAp and it also provides minor antibacterial activity due to the presence of Si^{4+} ions in its components [262–267].

4.2.3 Biodegradable ceramics

Biodegradable ceramics refer to calcium-derived compounds (CDCs), mainly calcium phosphate (CaP)-based materials including α/β-TCP, tetracalcium phosphate (TTCP) [$Ca_4(PO_4)_2O$], and hydroxyapatite (HAp) [$Ca_{10}(PO_4)_6(OH)_2$], which have above 1.5 Ca:P ratio [21,268]. These CDCs by containing similar components as natural bone demonstrated remarkable cellular affinity that subsequently promotes the osteogenic cells anchorage and higher osteoconductivity and osteointegration [269,270]. Schouten *et al.* compared the *in vivo* biological activity of the Ti surface with and without the utilization of CaP coatings. The results showed that the presence of the CaP compound on the implant site increased the bone healing process and led to higher osteointegration [271]. However, the controversial parameter of these CDCs is their low solubility. Okuda *et al.* evaluated the adsorption of rod-shaped particles of HAp in the rabbit femur. They observed that 24 weeks after implantation, 80% of HAp remained and after 72 weeks, although most of the HAp was resorbed, still the presence of HAp around the implantation site could be detected [272]. Therefore, synthesizing the biphasic CDCs with different combining ratios may be an optimal solution to control their degradation rates [273].

Despite the broad uses of CDCs, still, the challenges of fabricating an ideal compound for bone restorative applications remain. Hence, the utilization of multifunctionalized compounds tends to be a reasonable answer to fulfill the demands for this purpose. Immobilizing growth factors or peptides as a guiding cell behavior have been conducted, yet their fast denaturation is their main drawback [274–278]. Bisphosphonates (BPs), such as alendronate and zoledronate, are other molecules that have been widely used as medicine to treat bone metabolic disorders. BPs are used to prevent osteoclastogenesis, a feature that helps to cure osteoporosis or Paget's disease [279]. Other interesting molecules that contribute to several transduction pathways are glycosaminoglycans (GAGs). The family of GAGs including hyaluronic acid (HA), heparin, heparan, chondroitin, and keratin sulfates, are ubiquitous molecules that exist in the stem cells niche and ECM, and they have a high affinity for growth factors and proteins [280–287]. GAGs' family displayed a significant impact on regenerative progress in various cell lineages like the immune system, fibroblast, endothelial, and skeletal cells [280,288,289]. Recent studies have led to the utilization of PDA, a catechol-containing biomimetic molecule. PDA demonstrated a notable impact on bone mineralization *via* concentrating Ca^{2+} ions at the interface. Yong *et al.* deposited PDA-assisted HAp on porous Ti scaffold. *In vitro* tests revealed that such coating can promote proliferation, attachment, and bioactivity by inducing ALP expression in MC3T3-E1 cells [290]. However, assimilating to osteogenic cells, CDCs also allow bacteria to colonize and increase the risk of failure. To overcome this problem, CDCs are usually accompanied by an antibacterial agent to acquire a biocidal function [291,292].

In addition to CaP-based materials, there are CaP-based salts like calcium sulfate ($CaSO_4$) and calcium carbonate ($CaCO_3$) that have been extensively used in clinical applications. Ohgushi *et al.* examined the bone-forming responses of Ti surface coated with $CaCO_3$. They concluded that $CaCO_3$ demonstrated considerable potential in bone restorative applications, which can be compared with similar compounds like HAp [293].

4.3 Polymer-based coatings

4.3.1 Chitosan

Chitosan is a natural polymer with vast applications in medicine. Chitosan is a cationic polysaccharide that is derived from the deacetylation of chitin [294]. Chitosan possesses remarkable properties consisting of antimicrobial, antiviral, antifungal, antitumor, immunoadjuvant, anti-thrombogenic, and anti-cholesteremic [295]. The antibacterial mechanism of chitosan NPs is attributed to the principle of electrostatic interaction and result in the dysfunctioning cell membrane, increase in permeability, and ultimately cell death [296]. A combination of chitosan with other materials can overcome different bacteria growth. Divakar *et al.* fabricated Ag-conjugated chitosan NPs for promoting bioactivity of Ti surfaces. The results demonstrated that NPs successfully restricted the growth, adhesion, and biofilm formation of *S.mutans* and *P.gingivalis* bacteria [297,298]. Palla-Rubio *et al.* coated hybrid silica-chitosan NPs on Ti implants and reported that 5–10% concentration of chitosan is suitable for obtaining sufficient bactericidal efficacy [299].

4.3.2 Peptides

Peptides coating on the implant surface is a recent procedure to increase bioactivity. Antimicrobial peptides (AMPs) with tailored heads are able to be physically adsorbed or chemically bonded to the surface. This coating mechanism is based on the production of AMPs from the host's proteins and reusing them affords low toxicity and bacterial resistance [300]. These peptides cover a broad spectrum of pathogens, including both Gram-negative and Gram-positive bacteria [301]. Herein, a wide range of AMP families has proven their antimicrobial activity that consists of lactoferrin 1–11 (LF1–11), alpha-defensins (ADs), beta-defensins (BDs), histatin, adrenomedullin, cathelicidins, GL13K, Pac-525, KSL, and LL-37 [302–308]. Godoy-Gallardo *et al.* examined the biofunction of hLF1–11 on the Ti surface. *In vitro* results demonstrated a satisfactory reduction in adherence and biofilm formation of *S. sanguinis* and *Lactobacillus salivarius* (*L. salivarius*) bacteria in the early stage [309,310].

4.4 Carbon-based coatings

Recently, carbon-based coatings (CBCs) have shown remarkable applications in dentistry. These materials with strong C–C bonds demonstrated excellent physical properties such as notable hardness, high thermal conductivity, and optical transparency for the surface. In this term, nanocrystalline diamond (NCD), graphene and its family, and carbon nanotubes are the most frequently used CBCs on endosseous implant bodies. Coating the implant surface with NCD provides a smooth surface with significant corrosion resistance, which is a favorable surface for preventing bacterial

colonization [21]. Moreover, these NPs are capable of antioxidant and anticarcinogenic properties [311].

Graphene and GFNs consist of a single layer form of carbon atoms and have a high surface area. Graphene with its honeycomb lattice shape covers the surface of implants and possesses impermeability. This ability can effectively reduce the corrosion rate and biofilm of dental implants [312,313]. Such physiobiological activities can be shared with GFNs like GO and graphene nanoplatelets. In addition to graphene, CNTs provide notable physiochemical characteristics in terms of biocide, biogenic, and drug carrier functions. The hollow cylindrical shape of CNTs is an appropriate surface for osteoblast cells' anchorage while it can also rupture the bacteria cell membrane. Metzler *et al.* evaluated the osteointegration of NCD on Ti grade-5 implant. After 5 months, the *in vivo* results showed sufficient osteointegration [314]. Rago *et al.* investigated the antibacterial mechanism of graphene nanoplatelets against microorganisms. They found that the strong mechanical bonds between the layers of the graphene nanoplatelet lead to trapping bacteria cells and ultimately result in cell death [315]. Hu *et al.* evaluated the bactericidal efficacy of GO against certain bacteria. They observed that GO could significantly reduce the level of *S. mutans* bacteria [316]. However, a few documents regarding CBCs restrict their potential as an independent coating.

4.5 Protein-based coatings

4.5.1 Extracellular matrix proteins

Deposition of ECM proteins on the implant surface is a promising approach to facilitate the adhesion of osteogenic proteins. In general, the immobilization of ECM proteins leads to the promotion of bone healing and osteointegration. Hence, several proteins and biomolecules exist in the ECM and demonstrate biological activities in bone restorative applications that consist of collagens, osteopontin, pectin, cytokine, laminin, elastin, hyaluronan, insulin, fibrinogen, glycans, proteoglycans, poly(amino-acids), sialoprotein, fatty acids, sugars, *etc.* [317]. Among them, collagens attracted considerable attention as they have the potential to improve the attachment, proliferation, and differentiation of osteoblast and human MSCs [318]. Saadatmand *et al.* evaluated the collagen-chondroitin sulfate (CCS) and collagen-sulfated hyaluronan (CSH) coatings on a screw-type Ti implant in a minipig model. From *in vivo* results, they found that the bone formation in both coatings was greater than the uncoated control following 8 weeks [319].

4.5.2 Growth factors

Vascular endothelial growth factor (VEGF) and bone morphogenetic proteins (BMPs) are used in the coating. The first has the signaling function that involves vasculogenesis and angiogenesis. The latter is a family of growth factors, especially in the formation of bone and cartilage. This family can improve the regulation of osteogenic cells and the differentiation of MSCs [320]. Moreover, recombinant human BMPs (rhBMPs) like rhBMP-2 and rhBMP-7 have been used for therapeutic applications [321]. Guang *et al.* evaluated the biological activities of VEGF on primary rat osteoblast cells. They observed that VEGF can increase the activity of ALP, gene and protein expression of vasculogenesis, and proliferation of osteoblast cells [322]. Faßbender *et al.* modified the release rate of BMP-2 by optimizing the thickness of gentamicin-loaded poly(D,L-lactide-acid) (PDLLA). They concluded that sustained release was achieved after initial healing with a notable increase in the stiffness and ratio of bone volume to total volume at day 42, and also, higher mineralization was achieved after the 42nd day until the 84th day [323]. Al-Jarsha *et al.* fabricated BMP7-loaded poly(ethyl-acrylate) (PEA) on Ti surface. The results revealed that a low concentration of BMP-7 is able to optimize osteointegration *via* establishing a specific delivery system [324].

4.6 Drug-based coatings

Drug-based coatings are of the most practical procedures to combat high infections with multifactorial, complex, and hard-to-manage characteristics. Antibiotic drugs displayed higher efficacy against a broad spectrum of both Gram-positive and Gram-negative bacteria. Coating drugs on the implant surface usually occurs *via* indirect ways like using drug carriers with different biophysiochemical characteristics and release mechanisms (Figure 23). Herein, the frequently used antibiotic includes amoxicillin, doxycycline (DOX), tetracycline, polydopamine (PDA), cefotaxime, quercitrin, chlorhexidine (CHX), gentamycin, norfloxacin, and vancomycin.

Bottino *et al.* examined the biocidal activity of new antibiotic, tetracycline-containing fibers, for dental applications. Not only did they restrict the biofilm formation and progression of peri-implantitis, but also they reduced the colonization of bacteria including *P. gingivalis*, *F. nucleatum*,

Table 2: A summary of the aforementioned multifunctional coatings and their biogenic mechanisms

Category	Subcategory	Biogenic and/or biocidal activities					Further advantages
		Angiogenesis	Osteoinduction	Osteoconduction	Osteogenesis	Antibacterial	
Metal	Tantalum (Ta^{5+})			×		×	
	Titanium (Ti^{4+})				×	×	
	Silicon (Si^{4+})	×			×	×	
	Cerium (Ce^{4+})		×			×	Anti-inflammatory
	Gold (Au^{3+})				×	×	Antifungal and anticancer
	Iron (Fe^{3+})					×	Antibiofilm
	Copper (Cu^{2+})	×			×	×	Antifungal, antibiofilm, and antimicrobial
	Zinc (Zn^{2+})				×	×	Antibiofilm
	Magnesium (Mg^{2+})	×			×	×	
	Silver (Ag^{+})					×	Antimicrobial
	Selenium (Se^{2-})					×	Viruses and cancer cells
	Strontium (Sr^{2+})				×		Osteoclastogenesis
	Cobalt (Co^{2+})	×					
Ceramic	Zirconium (Zr^{4+})				×	×	
	Bioactive glass	×		×	×	×	
	CaP-Based materials			×	×		
Polymer	Chitosan					×	Antimicrobial, antiviral, antifungal, antitumor, immunoadjuvant, anti-thrombogenic, and anti-cholesteremic
	Peptides					×	Antimicrobial
Carbon	Carbon family					×	Antibacterial, antimicrobial, antioxidant, and anticarcinogenic
Protein	ECM proteins	×			×	×	
	Growth factors	×			×		
Drug	Organic drugs			×	×		

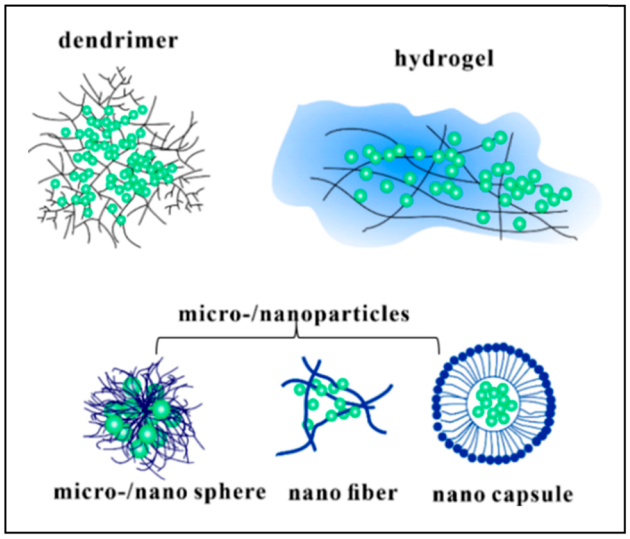

Figure 23: Schematic illustration of different carrier-based drug-releasing biomaterials [23]. Copyright 2020, MDPI.

Prevotella intermedia (*P. intermedia*), and *A. actinomycetemcomitans* at different concentrations [325,326]. Gomez-Florit *et al.* evaluated the anti-inflammatory effect and soft tissue regeneration of quercitrin coated on the Ti surface. For these tests, they used human gingival fibroblasts and interleukin-1-beta (IL-1β) to mimic the situations. The results revealed that quercitrin can increase the attachment of fibroblasts cells and also reduce the level of matrix metalloproteinase-1 (MMP-1), which led to increasing mRNA, and also pro-inflammatory prostaglandin-E_2 (PGE_2) under both inflammatory and basal conditions [327]. Researchers coated vancomycin-loaded silica films on the Ti surface by the sol–gel technique. The results showed a reduction in the release rate of vancomycin and adherence of *S. aureus* bacteria [70,328,329]. Ding *et al.* coated DOX-treated HAp on the Ti surface and from *in vivo tests* they observed that DOX could reduce the progression of peri-implantitis [330]. Also, by adjusting the environment pH, the release rate of DOX-loaded poly(lactide-*co*-glycolic-acid) (PLGA) can be controlled [331]. Wood *et al.* evaluated the inhibitory function of CHX coated on TiO_2 surface against *Streptococcus gordonii* (*S. gordonii*) bacteria. CHX demonstrated a successful reduction of *S. gordonii* but it had a high release rate and could only sustain for a short period [230]. Kazek *et al.* loaded amoxicillin in PLGA for evaluating its antibacterial activity on the Ti surface. Such coatings revealed successful inhibitory activity against *S. aureus* and *S. epidermidis* in the first few hours [332]. Rojas-Montoya *et al.* controlled the release rate of norfloxacin by changing the phases of CaP compounds in the synthesis process. They fabricated a rod-like nanostructure with fast desorption within the first 8 h and gradually reduced it until 32 h [333]. Lucke *et al.* fabricated PDLLA to reduce bone and soft-tissue infection. They concluded that 10% gentamicin-loaded PDLLA can significantly reduce the level of *S. aureus* bacteria in rat models [334]. He *et al.* assessed the effectiveness of cefotaxime sodium immobilized on the PDA-coated Ti surface. The results showed that this coating restricted the growth and adhesion of both *E. coli* and *S. mutans* as Gram-negative and Gram-positive bacteria, respectively. The addition of cefotaxime sodium could keep the antibacterial function for a longer period [96].

5 Drug delivery systems (DDSs)

In recent developments, the use of DDSs in implant coatings has attracted the attention of the scientific community. Drug delivery refers to the approaches in transporting and increasing the concentration of therapeutic compounds to the target tissue. Generally, DDS according to the release mechanism is classified as passive or active targeting. Passive targeting refers to the biophysiochemical properties of the delivery system with no affinity for ligands. However, active targeting is the enhanced version of passive targeting in which the release mechanism is determined by an inside or outside inducer. For evaluating a delivery system, three major factors can influence the drug release kinetics that includes the external environment, payload property, and material matrix. In designing a DDS, it should be taken into account that (i) short-term antibacterial drugs are utilized for immediate acute infection, (ii) long-term antibacterial drugs are utilized for preventing bacteria colonization, and (iii) in both cases, drugs should not include alternation in surface materials [32,335].

As mentioned above, drug release kinetics can be determined by the drug release mechanism. The DDS occurs through four main categories and their subcategories including (i) diffusion-controlled as (a) reservoirs and (b) matrices, (ii) chemically controlled as (a) biodegradation and (b) chemical cleavage, (iii) solvent-controlled, and (iv) pH-sensitive. Also, physiochemical and biological mechanisms like diffusion, osmosis, swelling, portioning, dissolution, targeting, and molecular interaction follow these categories [336]. Herein, the challenge is to design a DDS with the selectivity of a therapeutic drug

to the target site and an optimal release mechanism in the desired manner. For this purpose, soluble polymers, enzymatically degradable, and pH-responsive DDSs displayed a successful controlled release.

5.1 Material matrix

Of major parameters to obtain the optimal drug release is to design a specific drug system using biomaterials. Generally, the modification of the implant surface occurs *via* biochemical approaches including physisorption, covalent bonding, or carrier systems [337]. Physisorption refers to the direct coating and adsorption of therapeutic drugs by controlling the surface topography. Covalent binding refers to the immobilization of therapeutic drugs on the implant surface *via* the utilization of spacers like hydroxyl (–OH) or amine (–NH) groups. Covalent bonding is a suitable approach for coating cell-adhesive proteins including osteopontin, collagen, vitronectin, or fibronectin. Carrier systems refer to the utilization of biomaterials mainly ceramic-based and polymer-based materials for entrapping therapeutic drugs and releasing them over a controlled period. The release of therapeutic drugs in the adjacent environment of an implant using carrier systems occurs *via* degradation, diffusion, or osmolality mechanisms. Herein, synthetic biodegradable polymers, CaP-based compounds, and bioactive glasses due to their biocompatibility and degradability are the best choices for DDSs [338,339]. Biodegradable polymers are composed of various synthetic and natural polymers with unique characteristics. Polymers depending on their scale provide different advantages and disadvantages. However, it is not possible to use macro- or microsized polymers as DDSs due to their nonbiodegradability or limited cellular uptake. Therefore, restrained applications of large polymers increase the interest in NP-based drug systems. NP-based drug systems as implant coatings are in the form of nanoporous biomaterials, polymeric systems, and hydrogels [340]. The biophysiochemical characteristics of these carriers should be engineered to grant the optimum results for possible therapeutic drugs for bone restorative applications [341].

To design a delivery system, several parameters of drug molecules should be considered. On top of them, solubility is the prior factor as it can influence both material matrix and external environment, and is the main parameter in the release mechanisms of implant coatings. Hence, to obtain the favorable carrier system with a desirable level of hydrophilicity the utilization of copolymerization of different polymers like PLGA, biphasic CaP compounds, and BGs-doped compounds, are highlighted [23].

6 Essential parameters

6.1 Roughness

Surface roughness is one of the key factors in designing an implant. Microroughness was fully explored and confirmed as the better surface for the anchorage of osteoblast cells and primary stability [342,343]. However, most commercial dental implant manufacturers tend to have a smoother surface with a R_a of 0.5–1 µm [33,344–346]. Selecting this range of roughness is attributed to cell preference, which Yang *et al.* observed that human bone-marrow MSCs have optimal differentiation on Hap-coated Ti surfaces with R_a of 0.77–1.09 µm and mean distances between peaks (R_{Sm}) of 53.9–39.3 µm [347]. By the entering of roughness at the nanoscale, implant surfaces have gone through dramatic changes (Figure 24). Nanoroughness can promote protein adsorption, osteoblast cell attachment, and growth factor incorporation [9]. Moreover, gene expression can be influenced by surface roughness, and several parameters such as the production of growth factors, cytokines, and the response of the adjacent skeletal have a significant impact on the success of an implant [348]. Chen *et al.* observed that nanoroughness with R_a of 71.0 ± 11.0 nm can support more induction of osteogenic genes such as osteopontin (OPN), BMP-2, and runt-related transcription factor (RUNX2). Also, nanoroughness with a R_a of 14.3 ± 2.5 nm demonstrated higher expression of other osteogenic genes like collagen type 1 (COL1A1) and osteocalcin (OCN) [349]. Similarly, fibroblast cells adhere more to smooth surfaces. On the contrary, osteoblast cells proliferation and collagen synthesis tend to be higher on moderate roughness but epithelial cells and ECM molecules adsorption have been reported to be greater on rough surfaces [134,350–353]. The enhancement of protein adsorption is mainly affected by increasing the surface area on nanoroughness, which facilitates cell attachment, and subsequently, promotes osteointegration and mechanical bonding [354,355]. Despite all research done on the behavior of cells, there are no general rules for optimum surface roughness and further investigation is required.

6.2 Wettability

Wettability refers to the degree of hydrophilicity or hydrophobicity of the surface that is attributed to the result of surface chemistry [356]. To find the wettability, the CA between the interface of the droplet and the horizontal

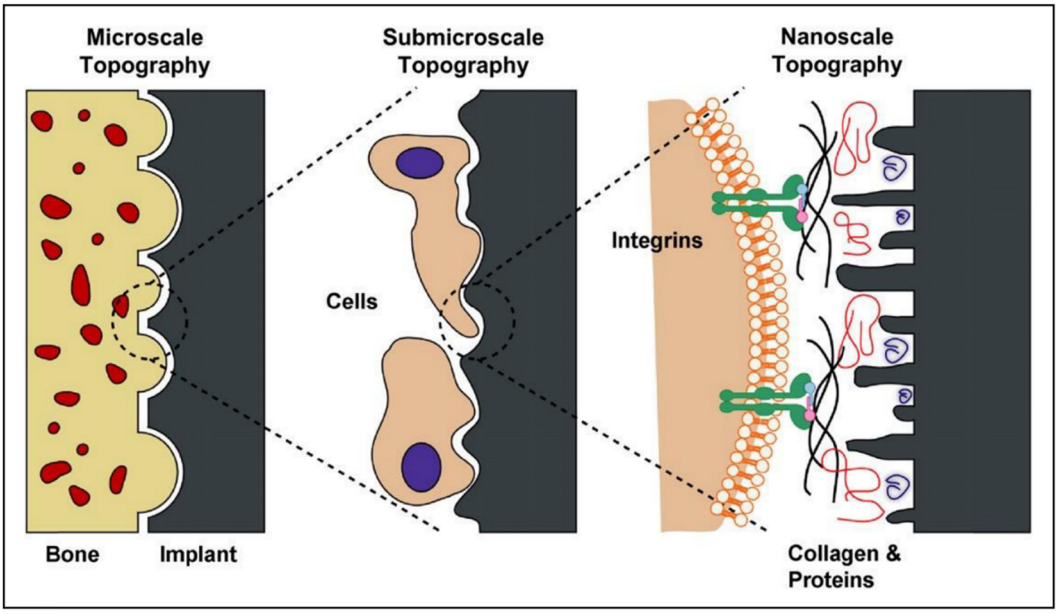

Figure 24: Schematic illustration of the three levels of interactions between the bone and implant. At the macroscale level, the implant supplies acceptable mechanical stability to the bone. At the micro/ submicroscales, the implant is able to directly interact with osteoblasts and MSCs. At the nanoscale, cell membrane receptors, such as integrins, can recognize proteins adsorbed on the surface, which in turn are modulated by the nanostructures on the surface [342]. Copyright 2014, Elsevier™.

surface is measured. When the measured CA is <90°, the outcome surface is hydrophilic and above 90° it is hydrophobic. Hydrophilic surfaces at nanoscale demonstrated better interactions with the biological environment, which indicates biocompatibility as well as high surface energy (Figure 25) [356,357]. D'Elía *et al.* examined the wettability of Hap-coated surfaces with macro-, micro-, and nano-roughness under controlled conditions. They used rat

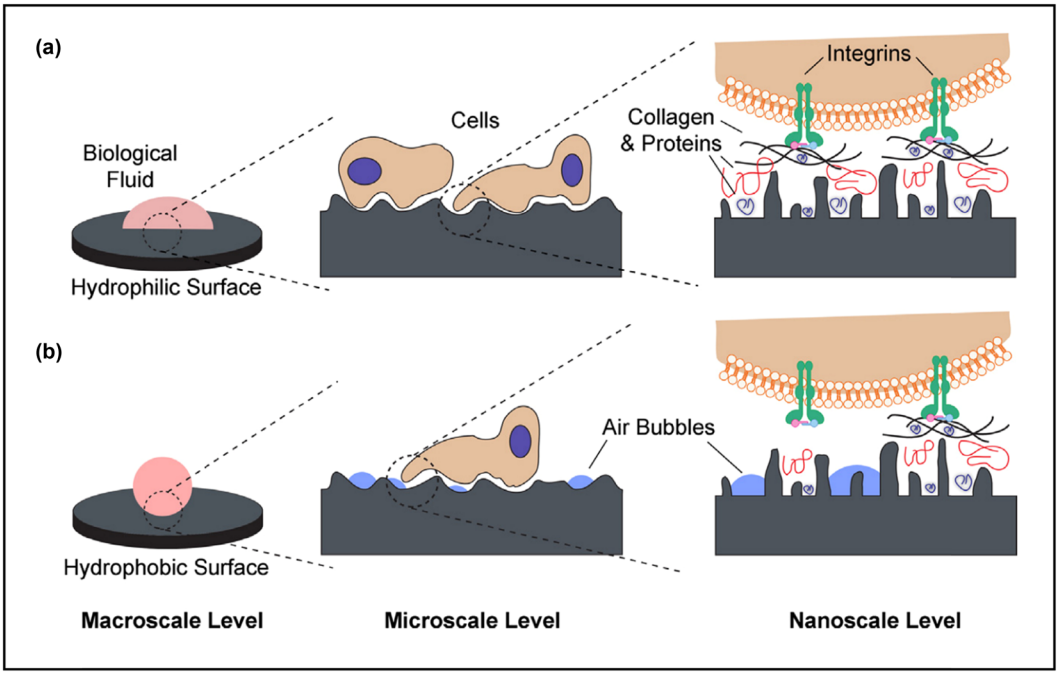

Figure 25: Schematic illustration of possible interactions at three levels of a (a) hydrophilic and (b) hydrophobic surface. (a) Hydrophilic surface allows direct interaction with biological fluids and subsequent cell membrane receptors. (b) Hydrophobic surface is prone to hydrocarbon contamination that results in the entrapment of air bubbles and interference with the biological environment [356]. Copyright 2014, Elsevier™.

osteoblasts and MSCs to test the surfaces and reported different states of physisorbed H_2O molecules on their surface [156]. Likewise, Hotchkiss *et al.* investigated the effect of immune cells on different wettability and micro- and nanoroughness surfaces. After culturing macrophages on a smooth Ti surface, it displayed an increase in the level of interleukins IL-1β, IL-6, and TNF-α, which result in inflammation. However, macrophages on the rough hydrophilic Ti surface increased interleukins IL-4 and IL-10, which activate the anti-inflammatory M2-like state of the macrophage [358]. Thus, there is no standard measurement for wettability to predict cellular behavior and it demands further investigation.

6.3 Charge

Generally, the surface charge indicates the interaction between the implant surface with its environment molecules, which leads to the reduction of bioactivity of the surface. This reduction has a significant impact on wettability, and subsequently, cellular responses that cause fewer bindings with useful ions and proteins [359–361]. By positively charging the surface, protein localization and biological responses can be influenced [362,363]. In terms of surface charge, limited research studies have evaluated its necessities but extended studies investigated the concept of decontamination utilizing techniques such as radio frequency glow-discharge (RFGD), photofunctionalization using ultraviolet A (UV-A), and ultraviolet C (UV-C) [360,364–366]. Decontaminating the implant results in the generation of a superhydrophilic surface but this reduction in CA is unstable and dramatically increases [367]. However, Rupp *et al.* evaluated nanocrystalline anatase coated on the Ti surface *via* the reactive pulse magnetron sputtering (RPMG) technique and fabricated a superhydrophilic surface with CA < 5° in 75 s. They claimed that according to the fast hydrophilization and slow re-hydrophobization, such a surface treatment has adequate potential for clinical applications [368]. Therefore, considering the significant period between production and implantation of an implant, more investigations regarding the sustainability of the surface charge and applicable processes are recommended.

7 Conclusion and outlook

In this review, we organize various aspects of a dental implant from the perspective of nanotechnology. Based on the results, we found that there is no gold standard for modifying an implant because the success rate depends on many parameters such as the patients' general condition. Nevertheless, the outcomes of cutting-edge technology such as nano-topographies, nanoparticles, and nanodelivery systems demonstrated higher biophysiochemical activities that directly affect the success rate of dental implants. Hence, we provide sufficient pieces of information for researchers to give them a better understanding of nanotechnology in dentistry.

In general, implant failure is associated with inadequate osteointegration that may be exacerbated by microbial infection. Therefore, the combination of long-lasting features such as nanotopographies and NPs may be considered as an ideal modification for the next generation of dental implants. Nanotopography has brought the insight that antibacterial activities cannot be limited to chemical interactions, and nanopatterns with specific geometries can also reduce or abolish bacteria. In this case, dominating the fabrication process is the key factor for producing the optimal geometries. However, a few reports on this issue restrict their potential as an independent modification. Thus, the use of manifold NPs with different biocidal and osteogenic functions as well as engineered delivery systems is more highlighted.

Funding information: The authors state no funding involved.

Author contributions: All authors have accepted responsibility for the entire content of this manuscript and approved its submission.

Conflict of interest: The authors state no conflict of interest.

References

[1] Adell R, Lekholm U, Rockler B, Branemark P. A 15-year study of osseointegrated implants in the treatment of the edentulous jaw. Int J Oral Surgery. 1981;10(6):387–416. doi: 10.1016/S0300-9785(81)80077-4.

[2] Adler L, Buhlin K, Jansson L. Survival and complications: a 9 - to 15 - year retrospective follow - up of dental implant therapy. J Oral Rehabilitation. 2020 Jan;47:67–77. doi: 10.1111/joor.12866.

[3] Oh S, Shiau HJ, Sc D, Reynolds MA. Survival of dental implants at sites after implant failure: a systematic review. J Prosthet Dent. 2020 Jan;123:1–7. doi: 10.1016/j.prosdent.2018.11.007.

[4] Güven SŞ, Cabbar DF, Güler N. Local and systemic factors associated with marginal bone loss around dental implants: a retrospective clinical study. Quintessence Int. 2020;51:128–41. doi: 10.3290/j.qi.a42950.

[5] Bazli L, Nargesi khoramabadi H, Chahardehi AM, Arsad H, Malekpouri B, Asgari Jazi M, et al. Factors influencing the failure of dental implants: a systematic review. J Compos Compd. 2020;2:18–25.
[6] Naghib SM, Zare Y, Rhee KY. A facile and simple approach to synthesis and characterization of methacrylated graphene oxide nanostructured polyaniline nanocomposites. Nanotechnol Rev. 2020;9:53–60. doi: 10.1515/ntrev-2020-0005.
[7] Naghib SM, Behzad F, Rahmanian M, Zare Y, Rhee KY. A highly sensitive biosensor based on methacrylated graphene oxide-grafted polyaniline for ascorbic acid determination. Nanotechnol Rev. 2020;9:760–7. doi: 10.1515/ntrev-2020-0061.
[8] Sartipzadeh O, Naghib SM, Shokati F, Rahmanian M, Majidzadeh-A K, Zare Y, et al. Microfluidic-assisted synthesis and modelling of monodispersed magnetic nanocomposites for biomedical applications. Nanotechnol Rev. 2020;9:1397–407. doi: 10.1515/ntrev-2020-0097.
[9] Mendonça G, Mendonça DBS, Araga FJL. Advancing dental implant surface technology – From micron- to nanotopography. Biomaterials. 2008;29:3822–35. doi: 10.1016/j.biomaterials.2008.05.012.
[10] Xia L. Importance of nanostructured surfaces. Amsterdam: Elsevier Ltd; 2021. doi: 10.1016/b978-0-08-102999-2.00002-8.
[11] Rajendran YSKIN. Surface modification methods for titanium and its alloys and their corrosion behavior in biological environment: a review. J Bio- Tribo-Corrosion. 2019. doi: 10.1007/s40735-019-0229-5.
[12] Rasouli R, Barhoum A, Uludag H. A review of nanostructured surfaces and materials for dental implants: surface coating, patterning and functionalization for improved performance. Biomater Sci. 2018;6:1312–38. doi: 10.1039/c8bm00021b.
[13] Fox KE, Tran NL, Nguyen TA, Nguyen TT, Tran PA. Surface modification of medical devices at nanoscale – recent development and translational perspectives. Amsterdam: Elsevier Inc.; 2019. doi: 10.1016/B978-0-12-813477-1.00008-6.
[14] Kurup A, Dhatrak P, Khasnis N. Materials today: proceedings surface modification techniques of titanium and titanium alloys for biomedical dental applications: a review. Mater Today Proc. 2020;39:6. doi: 10.1016/j.matpr.2020.06.163.
[15] Subramani K, Mathew RT, Pachauri P. Titanium surface modification techniques for dental implants-From microscale to nanoscale. Second edn. Amsterdam: Elsevier Inc.; 2018. doi: 10.1016/B978-0-12-812291-4.00006-6.
[16] Cavalu S, Antoniac IV, Mohan A, Bodog F, Doicin C, Mates I, et al. Nanoparticles and nanostructured surface fabrication for innovative cranial and maxillofacial surgery. Mater (Basel). 2020;13:1–23. doi: 10.3390/ma13235391.
[17] Rupp F, Liang L, Geis-Gerstorfer J, Scheideler L, Hüttig F. Surface characteristics of dental implants: a review. Dent Mater. 2018;34:40–57. doi: 10.1016/j.dental.2017.09.007.
[18] Article R. Implant surface microtopography – a review. Asian Pac J Health Sci. 2020;7:48–53. doi: 10.21276/apjhs.2020.7.2.12.
[19] Linklater DP, Baulin VA, Juodkazis S, Crawford RJ, Stoodley P, Ivanova EP. Mechano-bactericidal actions of nanostructured surfaces. Nat Rev Microbiol. 2021;19:8–22. doi: 10.1038/s41579-020-0414-z.
[20] Chen Z, Bachhuka A, Wei F, Wang X, Liu G, Vasilev K, et al. Manipulation of osteoimmunomodulation in bone. Nanoscale. 2017;9:18129–52. doi: 10.1039/c7nr05913b.
[21] Parnia F, Yazdani J, Javaherzadeh V, Maleki Dizaj S. Overview of nanoparticle coating of dental implants for enhanced osseointegration and antimicrobial purposes. J Pharm Pharm Sci. 2017;20:148–60. doi: 10.18433/J3GP6G.
[22] Priyadarsini S, Mukherjee S, Mishra M. Nanoparticles used in dentistry: a review. J Oral Biol Craniofacial Res. 2018;8:58–67. doi: 10.1016/j.jobcr.2017.12.004.
[23] Latif M, Habib SR, Khurshid Z. Customized therapeutic surface coatings for dental implants. Fish Shellfish Immunol. 2020;104:1–37.
[24] Bapat RA, Joshi CP, Bapat P, Chaubal TV, Pandurangappa R, Jnanendrappa N, et al. The use of nanoparticles as biomaterials in dentistry. Drug Discov Today. 2019;24:85–98. doi: 10.1016/j.drudis.2018.08.012.
[25] Hosnedlova B, Kepinska M, Skalickova S, Fernandez C, Ruttkay-Nedecky B, Peng Q, et al. Nano-selenium and its nanomedicine applications: a critical review. Int J Nanomed. 2018;13:2107–28. doi: 10.2147/IJN.S157541.
[26] Dong H, Liu H, Zhou N, Li Q, Yang G, Chen L. Surface modified techniques and emerging functional coating of dental implants. Coating. 2020;10:1–25. doi: 10.3390/coatings10111012.
[27] Das S, Kumar S, Samal SK, Mohanty S, Nayak SK. Review a review on superhydrophobic polymer nanocoatings: recent development, application. Ind Eng Chem Res. 2018;57:2727–45. doi: 10.1021/acs.iecr.7b04887.
[28] Devgan S, Sidhu SS. Evolution of surface modification trends in bone related biomaterials: a review. Mater Chem Phys. 2019;233:68–78. doi: 10.1016/j.matchemphys.2019.05.039.
[29] Raura N, Garg A, Arora A, Roma M. Nanoparticle technology and its implications in endodontics: a review. Biomater Res. 2020;24:1–8. doi: 10.1186/s40824-020-00198-z.
[30] Bapat RA, Chaubal TV, Dharmadhikari S, Abdulla AM, Bapat P, Alexander A, et al. Recent advances of gold nanoparticles as biomaterial in dentistry. Int J Pharm. 2020;586:119596. doi: 10.1016/j.ijpharm.2020.119596.
[31] Koopaie M. Nanoengineered biomaterials for advanced drug delivery, nanoparticulate syst dental drug delivery. Amsterdam: Elsevier Ltd.; 2020. p. 525–59. doi: 10.1016/B978-0-08-102985-5.00022-X.
[32] Mandracci P, Mussano F, Rivolo P, Carossa S. Surface treatments and functional coatings for biocompatibility improvement and bacterial adhesion reduction in dental implantology. Coatings. 2016;6:6. doi: 10.3390/coatings6010007.
[33] Tobin EJ. AC NU SC. Adv Drug Deliv Rev. 2017;112:88–100. doi: 10.1016/j.addr.2017.01.007.
[34] Ivanova EP, Hasan J, Webb HK, Truong VK, Watson GS, Watson JA, et al. natural bactericidal surfaces: mechanical rupture of pseudomonas aeruginosa cells by cicada wings. Small (Weinh an der Bergstrasse, Ger). 2012;8:72–4. doi: 10.1002/smll.201200528.
[35] Wang XX, Hayakawa S, Tsuru K, Osaka A. Bioactive titania gel layers formed by chemical treatment of Ti substrate with a H_2O_2/HCl solution. Biomaterials. 2002;23:1353–7. doi: 10.1016/S0142-9612(01)00254-X.
[36] Esmael SK, Jassim RK, Al-hiloh SA. *In vitro* study for nano hydroxyl apatite and chitosan coated surface after immersion in simulated body fluid. Med -Leg Update. 2020;20:1919–26.
[37] Ballo AM, Omar O, Xia W, Palmquist A. Dental implant surfaces – physicochemical properties, biological performance,

and trends. Implant Dent – A Rapidly Evol Pract. 2011;6:209–27. doi: 10.5772/17512.
[38] Anil S, Anand PS, Alghamdi H, Janse JA. Dental implant surface enhancement and osseointegration. Implant Dent – A Rapidly Evol Pract. 2011;15:80–7. doi: 10.5772/16475.
[39] Salou L, Hoornaert A, Louarn G, Layrolle P. Enhanced osseointegration of titanium implants with nanostructured surfaces: an experimental study in rabbits. Acta Biomater. 2015;11:494–502. doi: 10.1016/j.actbio.2014.10.017.
[40] Alla RK, Ginjupalli K, Upadhya N, Shammas M, Krishna R, Sekhar R. Surface roughness of implants: a review. 2011;25:112–8.
[41] Zhong Z. Advanced polishing, grinding and finishing processes for various manufacturing applications: a review. Mater Manuf Process. 2020;35:1–25. doi: 10.1080/10426914.2020.1772481.
[42] Madarkar R, Agarwal S, Attar P, Ghosh S, Rao P. V, Application of ultrasonic vibration assisted MQL in grinding of Ti – 6Al – 4V. Mater Manuf Process. 2017;33:1–8. doi: 10.1080/10426914.2017.1415451.
[43] Okawa S, Watanabe K. Chemical mechanical polishing of titanium with colloidal silica containing hydrogen peroxide – mirror polishing and surface properties. Dental Mater J. 2009;28:68–74.
[44] Ozdemir Z, Ozdemir A, Basim GB. Application of chemical mechanical polishing process SC. Mater Sci Eng C. 2016;68:383–96. doi: 10.1016/j.msec.2016.06.002.
[45] Lee J, Kim S, Han J, Yeo IL, Yoon H, Lee J. Effects of ultrasonic scaling on the optical properties and surface characteristics of highly translucent CAD/CAM ceramic restorative materials: an *in vitro* study. Ceram Int. 2019;45:14594–601. doi: 10.1016/j.ceramint.2019.04.177.
[46] Shemtov-yona K, Rittel D, Dorogoy A. Mechanical assessment of grit blasting surface treatments of dental implants. J Mech Behav Biomed Mater. 2014;39:375–90. doi: 10.1016/j.jmbbm.2014.07.027.
[47] Le Guéhennec L, Soueidan A, Layrolle P, Amouriq Y. Surface treatments of titanium dental implants for rapid osseointegration. Dent Mater. 2007;23:844–54. doi: 10.1016/j.dental.2006.06.025.
[48] Jemat A, Ghazali MJ, Razali M, Otsuka Y. Surface modifications and their effects on titanium dental implants. Biomed Res Int. 2015;2015:1–11. doi: 10.1155/2015/791725.
[49] Schupbach P, Glauser R, Bauer S. Al_2O_3 particles on titanium dental implant systems following sandblasting and acid-etching process. Int J Biomater. 2019;2019:9–12.
[50] Prof A, Prof A. Surface modification of titanium and titanium alloys: technologies, developments and future interests. doi: 10.1002/adem.201901258.
[51] Ganesh BKC, Sha W, Ramanaiah N, Krishnaiah A. Effect of shotpeening on sliding wear and tensile behavior of titanium implant alloys. J Mater. 2014;56:480–6. doi: 10.1016/j.matdes.2013.11.052.
[52] Unal O, Karaoglanli AC, Varol R, Kobayashi A. Microstructure evolution and mechanical behavior of severe shot peened commercially pure titanium. Vaccum. 2014;110:1–5. doi: 10.1016/j.vacuum.2014.08.004.
[53] Deng Z, Yin B, Li W, Liu J, Yang J, Zheng T, et al. Surface characteristics of and *in vitro* behavior of osteoblast-like cells on titanium with nanotopography prepared by high-energy shot peening. Int J Nanomed. 2014;9:5565–73.
[54] Jelliti S, Richard C, Retraint D, Roland T, Chemkhi M, Demangel C. Effect of surface nanocrystallization on the corrosion behavior of Ti – 6Al – 4V titanium alloy. Surf Coat Technol. 2013;224:82–7. doi: 10.1016/j.surfcoat.2013.02.052.
[55] Jamesh M. Effect of surface mechanical attrition treatment of titanium using alumina balls: surface roughness, contact angle and apatite forming ability. Front Mater Sci. 2013;7:285–94. doi: 10.1007/s11706-013-0208-6.
[56] Jain S, Williamson RS, Janorkar AV, Griggs JA, Roach MD. Osteoblast response to nanostructured and phosphorus-enhanced titanium anodization surfaces. J Biomater Appl. 2019;34:419–30. doi: 10.1177/0885328219852741.
[57] Palmquist A, Omar OM, Esposito M, Lausmaa J, Thomsen P. Titanium oral implants: surface characteristics, interface biology and clinical outcome. J R Soc Interface. 2010;7 Suppl 5:7–27. doi: 10.1098/rsif.2010.0118.focus.
[58] Nicolas-Silvente AI, Velasco-Ortega E, Ortiz-Garcia I, Monsalve-Guil L, Gil J, Jimenez-Guerra A. Influence of the titanium implant surface treatment on the surface roughness and chemical composition. Mater (Basel). 2020;13:13. doi: 10.3390/ma13020314.
[59] Orsini G, Assenza B, Scarano A, Piattelli M, Piattelli A. Surface analysis of machined versus sandblasted and acid-etched titanium implants. Int J Oral Maxillofac Implant. 2000;15:779–84.
[60] Variola F, Zalzal SF, Leduc A, Barbeau J, Nanci A. Oxidative nanopatterning of titanium generates mesoporous surfaces with antimicrobial properties. Int J Nanomed. 2014;9:2319–25. doi: 10.2147/IJN.S61333.
[61] Lamolle F, Monjo M, Rubert M, Haugen HJ, Lyngstadaas SP, Ellingsen JE. The effect of hydrofluoric acid treatment of titanium surface on nanostructural and chemical changes and the growth of MC3T3-E1 cells. Biomaterials. 2009;30:736–42. doi: 10.1016/j.biomaterials.2008.10.052.
[62] Khodaei M, Amini K, Valanezhad A, Watanabe I. Surface treatment of titanium dental implant with H2O2 solution. Int J Min Metall Mater. 2020;27:1281–6. doi: 10.1007/s12613-020-2016-1.
[63] Pan J, Liao H, Leygraf C, Thierry D, Li J. Variation of oxide films on titanium induced by osteoblast-like cell culture and the influence of an H_2O_2 pretreatment. J Biomed Mater Res. 1998;40:244–56. doi: 10.1002/(SICI)1097-4636(199805)40:2<244:AID-JBM9>3.0.CO;2-L.
[64] Khodaei M, Kelishadi HS. US CR. Surf Coat Technol. 2018. doi: 10.1016/j.surfcoat.2018.08.037.
[65] Zhou J, Chang C, Zhang R, Zhang L. Hydrogels prepared from unsubstituted cellulose in NaOH/urea aqueous solution. Macromol Biosci. 2007;7:804–9. doi: 10.1002/mabi.200700007.
[66] Pachauri P, Bathala LR, Sangur R. Techniques for dental implant nanosurface modifications. J Adv Prosthodont. 2014;6:498–504. doi: 10.4047/jap.2014.6.6.498.
[67] Pattanayak DK, Yamaguchi S, Matsushita T, Nakamura T, Kokubo T. Apatite-forming ability of titanium in terms of pH of the exposed solution. J R Soc Interface. 2012;9:2145–55. doi: 10.1098/rsif.2012.0107.

[68] Wang W, Luo CJ, Huang J, Edirisinghe M. PEEK surface modification by fast ambient-temperature sulfonation for bone implant applications. J R Society Interface. 2019;16:20180955.
[69] Alcázar JCB, Lemos RMJ, Conde MCM, Chisini LA, Salas MMS, Noremberg BS, et al. Progress in Organic Coatings Preparation, characterization, and biocompatibility of di ff erent metal oxide/PEG-based hybrid coating synthesized by sol–gel dip coating method for surface modification of titanium. Prog Org Coat. 2019;130:206–13. doi: 10.1016/j.porgcoat.2019.02.007.
[70] Adams Jr CS, Antoci V, Harrison G, Patal P, Freeman TA, Shapiro IM, et al. Controlled release of vancomycin from thin sol-gel films on implant surfaces successfully controls osteomyelitis. J Orthopaedic Res: Off Publ Orthopaedic Res Soc. 2009;27:701–9. doi: 10.1002/jor.20815.
[71] Peltola T, Pätsi M, Rahiala H, Kangasniemi I, Yli-Urpo A. Calcium phosphate induction by sol-gel-derived titania coatings on titanium substrates *in vitro*. J Biomed Mater Res, 1998. 1998;41:504–10. doi: 10.1002/(SICI)1097-4636(19980905)41:3<504:AID-JBM22>3.0.CO;2-G.
[72] Liu S, Liu J, Tang Y. Surface modification techniques of titanium and its alloys to functionally optimize their biomedical properties: thematic review. Front Bioeng Biotechnol. 2020;8:1–19. doi: 10.3389/fbioe.2020.603072.
[73] Hsu HC, Hsu SK, Wu SC, Hung YH, Ho WF. Surface modification of nanotubular anodized Ti–7.5Mo alloy using NaOH treatment for biomedical application. Thin Solid Films. 2020;710:138273. doi: 10.1016/j.tsf.2020.138273.
[74] Qiao X, Yang J, Shang Y, Deng S, Yao S, Wang Z, et al. Magnesium-doped nanostructured titanium surface modulates macrophage-mediated inflammatory response for ameliorative osseointegration. Int J Nanomed. 2020;15:7185–98. doi: 10.2147/IJN.S239550.
[75] Indira K, Ningshen S, Mudali UK, Rajendran N. Effect of anodization parameters on the structural morphology of titanium in fluoride containing electrolytes. Mater Charact. 2012;71:58–65. doi: 10.1016/j.matchar.2012.06.005.
[76] Fialho L, Carvalho S. Surface engineering of nanostructured Ta surface with incorporation of osteoconductive elements by anodization. Appl Surf Sci. 2019;495:143573. doi: 10.1016/j.apsusc.2019.143573.
[77] Ismail S, Mamat S, Azam MA. Effect of voltage on Tio_2 nanotubes formation in ethylene glycol solution. J Teknologi. 2017;79:2–5. doi: 10.11113/jt.v79.11294.
[78] Rameshbabu N, Ravisankar B, Saikiran A, Parfenov EV, Valiev RZ. Surface modification of CP-Ti metallic implant material by plasma electrolytic oxidation. IOP Conf Ser Mater Sci Eng. 2019;672:672. doi: 10.1088/1757-899X/672/1/012012.
[79] Dehnavi V, Binns WJ, Noël JJ, Shoesmith DW, Luan BL. Growth behaviour of low-energy plasma electrolytic oxidation coatings on a magnesium alloy. J Magnes Alloy. 2018;6:229–37. doi: 10.1016/j.jma.2018.05.008.
[80] Sedelnikova MB, Komarova EG, Sharkeev YP, Ugodchikova AV, Tolkacheva TV, Rau JV, et al. Modification of titanium surface via Ag-, Sr- and Si-containing micro-arc calcium phosphate coating. Bioact Mater. 2019;4:224–35. doi: 10.1016/j.bioactmat.2019.07.001.
[81] Narayanan R, Kim SY, Kwon TY, Kim KH. Nanocrystalline hydroxyapatite coatings from ultrasonated electrolyte: preparation, characterization, and osteoblast responses. J Biomed Mater Res – Part A. 2008;87:1053–60. doi: 10.1002/jbm.a.31852.
[82] Nie X, Leyland A, Matthews A. Deposition of layered bioceramic hydroxyapatite/TiO_2 coatings on titanium alloys using a hybrid technique of micro-arc oxidation and electrophoresis. Surf Coat Technol. 2000;125:407–14. doi: 10.1016/S0257-8972(99)00612-X.
[83] Hashim MS, Khaleel RS. The bioactivities of prepared Ti, Zn, TiO_2, ZnO and Al_2O nanoparticles by rapid breakdown anodization technique. Surf Interfaces. 2020;20:100640. doi: 10.1016/j.surfin.2020.100640.
[84] Khanaki A, Abdizadeh H, Golobostanfard MR. Electrophoretic deposition of CuIn1-xGaxSe2 thin films using solvothermal synthesized nanoparticles for solar cell application. J Phys Chem C. 2015;119:23250–8. doi: 10.1021/acs.jpcc.5b07300.
[85] Kania DR. Biocompatibility of chemical-vapour- deposited diamond. Biomaterials. 1995;16:483–8.
[86] Catledge SA, Fries MD, Vohra YK, Lacefield WR, Lemons JE, Woodard S, et al. Nanostructured ceramics for biomedical implants review. J Nanosci Nanotechnol. 2002;2:293–312. doi: 10.1166/jnn.2002.116.
[87] Chen M, Li H, Wang X, Qin G, Zhang E. Improvement in antibacterial properties and cytocompatibility of titanium by fluorine and oxygen dual plasma-based surface modification. Appl Surf Sci. 2019;463:261–74. doi: 10.1016/j.apsusc.2018.08.194.
[88] Hofer R, Textor M, Spencer ND. Alkyl phosphate monolayers, self-assembled from aqueous solution onto metal oxide surfaces. Langmuir. 2001;17(13):4014–20.
[89] Hybrid chitosan-β-1,3-glucan matrix of bone scaffold enhances osteoblast adhesion, spreading and proliferation via promotion of serum protein adsorption.pdf, n.d. 2016.
[90] Gawalt ES, Avaltroni MJ, Koch N, Schwartz J. Self-assembly and bonding of alkanephosphonic acids on the native oxide surface of titanium. Langmuir. 2001;17(19):5736–8.
[91] Scotchford CA, Gilmore CP, Cooper E, Leggett GJ, Downes S. Protein adsorption and human osteoblast-like cell attachment and growth on alkylthiol on gold self-assembled monolayers. Hoboken, New Jersey: Wiley Online Library; 2001.
[92] Min SK, Kang HK, Jang DH, Jung SY, Kim OB, Min BM, et al. Titanium surface coating with a laminin-derived functional peptide promotes bone cell adhesion. BioMed Res Int. 2013;2013:1–8.
[93] Kennedy SB, Washburn NR, George Jr CS, Amis EJ. Combinatorial screen of the effect of surface energy on fibronectin-mediated osteoblast adhesion, spreading and proliferation. Biomaterials. 2006;27:3817–24. doi: 10.1016/j.biomaterials.2006.02.044.
[94] Kim SE, Yun Y, Lee JY, Shim J, Park K, Huh J. Co-delivery of platelet-derived growth factor (PDGF- BB) and bone morphogenic protein (BMP-2) coated onto heparinized titanium for improving osteoblast function and osteointegration. Hoboken, New Jersey: Wiley Online Library; 2013. doi: 10.1002/term.
[95] 238 – Collagen fiber orientation around machined titanium and zirconia dental implant necks- an animal study.pdf, n.d. 2009.

[96] He S, Zhou P, Wang L, Xiong X, Zhang Y, Deng Y, et al. Antibiotic-decorated titanium with enhanced antibacterial activity through adhesive polydopamine for dental/bone implant Antibiotic-decorated titanium with enhanced antibacterial activity through adhesive polydopamine for dental/bone implant. J R Society, Interface. 2014;11:20140169.
[97] Tahriri M, Rasoulianboroujeni M, Bader R, Vashaee D, Tayebi L. 13. Growth factors for oral and maxillofacial regeneration applications. Amsterdam: Elsevier Ltd; 2017. doi: 10.1016/B978-0-08-100961-1.00013-X.
[98] Urface IMS, Huang H. E o f rgd i s, n.d. p. 73–9.
[99] Liu X, Chu PK, Ding C. Surface nano-functionalization of biomaterials. Mater Sci Eng R. 2010;70:275–302. doi: 10.1016/j.mser.2010.06.013.
[100] Pre-proof J, Page C. ur l P of. Surf Coat Technol. 2019;382:125161. doi: 10.1016/j.surfcoat.2019.125161.
[101] Liu X, Chu PK, Ding C. Surface modification of titanium, titanium alloys, and related materials for biomedical applications. Mater Sci Eng R Rep. 2005;47:49–121. doi: 10.1016/j.mser.2004.11.001.
[102] Huang X, Wang Y, Tang B, Zhao L, Chu K. Ac ce pt cr t. Appl Surf Sci. 2015;355:32–44. doi: 10.1016/j.apsusc.2015.07.064.
[103] Safavi MS, Walsh FC, Surmeneva MA, Surmenev RA, Allafi JK. Electrodeposited hydroxyapatite - based biocoatings: recent progress and future challenges. Coatings. 2021;11:110.
[104] Ul-Hamid A. The effect of deposition conditions on the properties of Zr-carbide, Zr-nitride and Zr-carbonitride coatings – a review. Mater Adv. 2020;1:988–1011. doi: 10.1039/d0ma00232a.
[105] Rautray TR, Narayanan R, Kim K. Ion implantation of titanium based biomaterials. Prog Mater Sci. 2011;56:1137–77. doi: 10.1016/j.pmatsci.2011.03.002.
[106] Miralami R, Haider H, Sharp JG, Namavar F, Hartman CW, Garvin KL, et al. Surface nano-modification by ion beam – assisted deposition alters the expression of osteogenic genes in osteoblasts. Eng Med. 2019;233:921–30. doi: 10.1177/0954411919858018.
[107] Mas-moruno C, Su B, Dalby MJ. Multifunctional coatings and nanotopographies: toward cell instructive and antibacterial implants. Adv Healthc Mater. 2018;8(1):1801103. doi: 10.1002/adhm.201801103.
[108] Biswas A, Bayer IS, Biris AS, Wang T, Dervishi E, Faupel F. Advances in top – down and bottom – up surface nanofabrication: techniques, applications & future prospects. Adv Colloid Interface Sci. 2012;170:2–27. doi: 10.1016/j.cis.2011.11.001.
[109] Cumming DRS, Thoms S, Beaumont SP, Weaver JMR. Fabrication of 3 nm wires using 100 keV electron beam lithography and poly (methyl methacrylate) resist and poly (methyl methacrylate) resist. Hospital pediatrics. 1996;322:18–21. doi: 10.1063/1.116073.
[110] Vieu C, Carcenac F, Pepin A, Chen Y, Mejias M, Lebib A, et al. Electron beam lithography: resolution limits and applications. Appl Surf Sci. 2000;164:111–7.
[111] Yilbas BS, Al-Sharafi A, Ali H. Self-cleaning of surfaces and water droplet mobility. Amsterdam: Elsevier; 2019. p. 45–98. doi: 10.1016/b978-0-12-814776-4.00003-3.
[112] Aly HM. Lett Editor. 2016;7658:236–8.
[113] Chang C, Tsai P, Chen S, Kuo MY, Sun J, Chang JZ. ScienceDirect 3D laser-printed porous Ti_6Al_4V dental implants for compromised bone support. J Formos Med Assoc. 2019;119:420–9. doi: 10.1016/j.jfma.2019.07.023.
[114] Gittens RA, McLachlan T, Olivares-Navarrete R, Cai Y, Berner S, Tannenbaum R, et al. The effects of combined micron-/submicron-scale surface roughness and nanoscale features on cell proliferation and differentiation. Biomaterials. 2011;32:3395–403.
[115] Lin N, Berton P, Moraes C, Rogers RD, Tufenkji N. Nanodarts, nanoblades, and nanospikes: mechano-bactericidal nanostructures and where to find them. Adv Colloid Interface Sci. 2018;252:55–68. doi: 10.1016/j.cis.2017.12.007.
[116] Kelleher SM, Habimana O, Lawler J, O' Reilly B, Daniels S, Casey E, et al. Cicada wing surface topography: an investigation into the bactericidal properties of nanostructural features. ACS Appl Mater & interfaces. 2015;8:14966–74. doi: 10.1021/acsami.5b08309.
[117] Chem P, Phys C. Bactericidal mechanism of nanopatterned surfaces. Phys Chem Chem Phys. 2015;18:1311–6. doi: 10.1039/C5CP05646B.
[118] Pham VT, Truong VK, Orlowska A, Ghanaati S, Barbeck M, Booms P, et al. "Race for the surface": eukaryotic cells can win. ACS Appl Mater Interfaces. 2016;8:22025–31. doi: 10.1021/acsami.6b06415.
[119] Wang Q, Huang Y, Qian Z. Nanostructured surface modification to bone implants for bone regeneration. J Biomed Nanotechnol. 2018;14:628–48. doi: 10.1166/jbn.2018.2516.
[120] Kim HN, Jiao A, Hwang NS, Kim MS, Kang DH, Kim DH, et al. Nanotopography-guided tissue engineering and regenerative medicine. Adv Drug Deliv Rev. 2012;65:536–58. doi: 10.1016/j.addr.2012.07.014.
[121] Kalaskar DM, Alshomer F. *In situ* tissue regeneration, micro-nanotopographical cues guiding biomater host response. Amsterdam: Elsevier Inc; 2016. p. 137–63. doi: 10.1016/B978-0-12-802225-2.00008-8.
[122] Pogodin S, Hasan J, Baulin VA, Webb HK, Truong VK, Phong Nguyen TH, et al. Biophysical model of bacterial cell interactions with nanopatterned cicada wing surfaces. Biophys J. 2013;104:835–40. doi: 10.1016/j.bpj.2012.12.046.
[123] Sjo T, Dalby MJ, Hart A, Tare R, Oreffo ROC, Su B. Fabrication of pillar-like titania nanostructures on titanium and their interactions with human skeletal stem cells. Acta Biomater. 2009;5:1433–41. doi: 10.1016/j.actbio.2009.01.007.
[124] Dalby MJ, Gadegaard N, Tare R, Andar A, Riehle MO, Herzyk P, et al. The control of human mesenchymal cell differentiation using nanoscale symmetry and disorder. Nat Mater. 2007;6:997–1003. doi: 10.1038/nmat2013.
[125] Xue F, Liu J, Guo L, Zhang L, Li Q. Theoretical study on the bactericidal nature of nanopatterned surfaces. J Theor Biol. 2015;385:1–7. doi: 10.1016/j.jtbi.2015.08.011.
[126] Ivanova EP, Linklater DP, Werner M, Baulin VA, Xu X, Vrancken N, et al. The multi-faceted mechano-bactericidal mechanism of nanostructured surfaces. Proc Natl Acad Sci U S A. 2020;117:12598–605. doi: 10.1073/pnas.1916680117.
[127] Sjöström T, Mcnamara LE, Meek RMD, Dalby MJ, Su B. 2D and 3D nanopatterning of titanium for enhancing osteoinduction of stem cells at implant surfaces. Adv Healthc Mater. 2013;2:1–9. doi: 10.1002/adhm.201200353.

[128] Mcnamara LE, Sjöström T, Burgess KE, Kim JJ, Liu E, Gordonov S, et al. Skeletal stem cell physiology on functionally distinct titania nanotopographies. Biomaterials. 2011;32:32–10. doi: 10.1016/j.biomaterials.2011.06.063.
[129] Kantawong F, Burgess KE, Jayawardena K, Hart A, Burchmore RJ, Gadegaard N, et al. Whole proteome analysis of osteoprogenitor differentiation induced by disordered nanotopography and mediated by ERK signalling. Biomaterials. 2009;30:4723–31. doi: 10.1016/j.biomaterials.2009.05.040.
[130] Guvendik S, Trabzon L, Ramazanoglu M. The effect of Si nano-columns in 2-D and 3-D on cellular behaviour: nanotopography-induced CaP deposition from differentiating mesenchymal stem cells. J Nanosci Nanotechnol. 2011;11:8896–902. doi: 10.1166/jnn.2011.3449.
[131] Zhou C, Koshani R, O'Brien B, Ronholm J, Cao X, Wang Y. Bio-inspired mechano-bactericidal nanostructures: a promising strategy for eliminating surface foodborne bacteria. Curr Opin Food Sci. 2021;39:110–9. doi: 10.1016/j.cofs.2020.12.021.
[132] Ivanova EP, Hasan J, Webb HK, Gervinskas G, Juodkazis S, Truong VK, et al. Bactericidal activity of black silicon. Nat Commun. 2013;4:1–7. doi: 10.1038/ncomms3838.
[133] Park J, Bauer S, Schlegel KA, Neukam FW, Von Der MK, Schmuki P. TiO_2 nanotube surfaces: 15 nm – an optimal length scale of surface topography for cell adhesion and differentiation. Small (Weinh an der Bergstrasse, Ger). 2009;5:666–71. doi: 10.1002/smll.200801476.
[134] 350 – Nanosize and vitality – TiO_2 nanotube diameter directs cell fate.pdf. 2007.
[135] Minagar S, Wang J, Berndt CC, Ivanova EP, Wen C. Cell response of anodized nanotubes on titanium and titanium alloys. J Biomed Mater Res Part A. 2013;101(9):2726–39. doi: 10.1002/jbm.a.34575.
[136] Press D. Adhesion of osteoblasts to a nanorough titanium implant surface. Int J Nanomed. 2011;6:1801.
[137] Feller L, Jadwat Y, Khammissa RAG, Meyerov R, Schechter I, Lemmer J. Cellular responses evoked by different surface characteristics of intraosseous titanium implants. BioMed Res Int. 2015;2015:1–8.
[138] Deng Y, Peng S. Boron nitride nanotubes reinforce tricalcium phosphate scaffolds and promote the osteogenic differentiation of mesenchymal stem cells. J Biomed Nanotechnol. 2016;12:934–47. doi: 10.1166/jbn.2016.2224.
[139] Kulkarni M, Mazare A, Gongadze E, Perutkova Š, Kralj-igli V. Titanium nanostructures for biomedical applications. Nanotechnology. 2015 Feb 13;26:062002. doi: 10.1088/0957-4484/26/6/062002.
[140] Gulati K, Prideaux M, Kogawa M, Lima-marques L, Atkins GJ, Findlay DM, et al. Anodized 3D – printed titanium implants with dual micro- and nano-scale topography promote interaction with human osteoblasts and osteocyte-like cells. Hoboken, New Jersey: Wiley Online Library; 2016. doi: 10.1002/term.
[141] Linklater DP, De Volder M, Baulin VA, Werner M, Jessl S, Golozar M, et al. High aspect ratio nanostructures kill bacteria via storage and release of mechanical energy. ACS Nano. 2018;12:6657–67. doi: 10.1021/acsnano.8b01665.
[142] Skandani AA, Zeineldin R. Effect of chirality and length on the penetrability of single-walled carbon nanotubes into lipid bilayer cell membranes. Langmuir ACS J Surf colloids. 2012;28:7872–9.
[143] Kang S, Pinault M, Pfefferle LD, Elimelech M, Engineering C. Single-walled carbon nanotubes exhibit strong antimicrobial activity. Langmuir : ACS J Surf colloids. 2007;23:8670–3.
[144] Werner M, Sommer J, Baulin VA. Homo-polymers with balanced hydrophobicity translocate through lipid bilayers and enhance local solvent permeability. Soft Matter. 2012;8:11714. doi: 10.1039/c2sm26008e.
[145] Guo Y, Werner M, Seemann R, Baulin VA, Fleury J. Tension-induced translocation of ultra-short carbon nanotube through a phospholipid bilayer. ACS Nano. 2018;12:12042–9. doi: 10.1021/acsnano.8b04657.
[146] Pandit S, Gaska K, Mokkapati VRSS, Celauro E, Derouiche A, Forsberg S, et al. Precontrolled alignment of graphite nanoplatelets in polymeric composites prevents bacterial attachment. Small (Weinh an der Bergstrasse, Ger). 2020;1904756:1–11. doi: 10.1002/smll.201904756.
[147] Pham VTH, Truong VK, Quinn MDJ, Notley SM, Guo Y. Graphene induces formation of pores killing spherical and rod-shaped bacteria. Washington, D.C.: ACS Publications; 2015. p. 1–33.
[148] Lu X, Feng X, Werber JR, Chu C, Zucker I, Kim JH, et al. Enhanced antibacterial activity through the controlled alignment of graphene oxide nanosheets. Proc Natl Acad Sci U S Am. 2017;114:9793. doi: 10.1073/pnas.1710996114.
[149] Wang X, Lyu C, Wu S, Ben Y, Li X, Ge Z, et al. Electrophoresis deposited mesoporous graphitic carbon nitride surfaces with efficient bactericidal properties. ACS Appl bio Mater. 2020;3:2255–62. doi: 10.1021/acsabm.0c00061.
[150] B J.M.C. Ctbf D.O.I. Mater Chem B. 2019;7:4424–31. doi: 10.1039/C9TB00102F.
[151] Bhadra CM, Truong VK, Pham VTH, Kobaisi MAl, Seniutinas G, Wang JY, et al. Antibacterial titanium nano- patterned arrays inspired by dragonfly wings. Nat Publ Gr.; p. 1–12. doi: 10.1038/srep16817.
[152] Reed JH, Gonsalves AE, Román JK, Oh J, Cha H, Dana CE, et al. Ultra-scalable multifunctional nanoengineered copper and aluminum for anti-adhesion and bactericidal applications Ultra-scalable multifunctional nanoengineered copper and aluminum for anti- adhesion and bactericidal applications. ACS Appl Bio Mater. 2019;2:2726–37. doi: 10.1021/acsabm.8b00765.
[153] Akhavan O, Ghaderi E. Toxicity of graphene and graphene oxide nanowalls against bacteria. ACS Nano. 2010;4:5731–6.
[154] Liu S, Zeng TH, Hofmann M, Burcombe E, Wei J, Jiang R. Antibacterial activity of graphite, graphite oxide, graphene oxide, and reduced graphene oxide: membrane and oxidative stress. ACS Nano. 2011;5:6971–80.
[155] Tan KH, Sattari S, Beyranvand S, Faghani A, Ludwig K, Schwibbert K, et al. Biological and environmental phenomena at the interface thermoresponsive amphiphilic functionalization of thermally reduced graphene oxide to study graphene/bacteria hydrophobic interactions. Langmuir: ACS J Surf colloids. 2019;35:4736–46. doi: 10.1021/acs.langmuir.8b03660.
[156] Manuscript A. Cell interaction with graphene microsheets: near-orthogonal cutting versus parallel attachment. Nanoscale. 2015;7:5457–67. doi: 10.1039/C4NR06170E.

[157] Zhang N, Hou J, Chen S, Xiong C, Liu H, Jin Y. Rapidly probing antibacterial activity of graphene oxide by mass spectrometry-based metabolite fingerprinting. New York City: Nat Publ Gr.; 2016. p. 1–10. doi: 10.1038/srep28045.
[158] Liu SP, Lin CH, Lin SJ, Fu RH, Huang YC, Chen SY, et al. Electrospun polyacrylonitrile-based nanofibers maintain embryonic stem cell stemness *via* TGF-beta signaling. J Biomed Nanotechnol. 2016;12:732–42. doi: 10.1166/jbn.2016.2201.
[159] Zhang C, Yuan H, Liu H, Chen X, Lu P. Well-aligned chitosan-based ultrafine fibers committed teno-lineage differentiation of human induced pluripotent stem cells for Achilles tendon regeneration. Biomaterials. 2015;53:716–30. doi: 10.1016/j.biomaterials.2015.02.051.
[160] Wang S, Hu F, Li J, Zhang S, Shen M, Huang M, et al. PT state key laboratory for modification of chemical fibers and polymer materials. Coll of Elsevier Inc. 2016;14:2505–20. doi: 10.1016/j.nano.2016.12.024.
[161] Xu T, Yang H, Yang D, Yu Z. Polylactic acid nanofibers scaffold decorated with chitosan island-like topography for bone tissue engineering. Sci Rep. 2017;7:4794.
[162] Lee YM, Yun HM, Lee HY, Lim HC, Lee HH, Kim HW, et al. Xerogel interfaced nanofibers stimulate bone regeneration through the activation of integrin and bone morphogenetic protein pathways. J Biomed Nanotechnol. 2017;13:180–91. doi: 10.1166/jbn.2017.2329.
[163] Thrivikraman G, Lee PS, Hess R, Haenchen V, Basu B, Scharnweber D. Interplay of substrate conductivity, cellular microenvironment, and pulsatile electrical stimulation toward osteogenesis of human mesenchymal stem cells *in vitro*. ACS Appl Mater Interfaces. 2015;7:23015–28. doi: 10.1021/acsami.5b06390.
[164] Polycaprolactone C, Leszczak V, Baskett DA, Popat KC. Endothelial cell growth and differentiation on. J Biomed Nanotechnol. 2021;11:1080–92. doi: 10.1166/jbn.2015.2021.
[165] Yao Q, Liu Y, Tao J, Baumgarten KM, Sun H. Promote endogenous bone regeneration Hypoxia-mimicking nanofibrous scaffolds promote endogenous bone regeneration. Washington, D.C.: The University of South Dakota; 2016. doi: 10.1021/acsami.6b10538.
[166] Matsuura Y, Hirano T, Sakai K. Friction torque reduction by ultrasonic vibration and its application to electromagnetically spinning viscometer. Jpn J Appl Phys. 2014;53(7S):07KC12.
[167] Klymov A, Bronkhorst EM, Jansen JA, Walboomers XF. Bone marrow-derived mesenchymal cells feature selective migration behavior on submicro- and nano-dimensional multi-patterned substrates. Acta Biomater. 2015;16:117–25. doi: 10.1016/j.actbio.2015.01.016.
[168] Klymov A, Song J, Cai X, Leeuwenburgh S, Jansen JA, Walboomers XF. Increased acellular and cellular surface mineralization induced by nanogrooves in combination with a calcium-phosphate coating. Acta Biomater. 2016;31:368–77. doi: 10.1016/j.actbio.2015.11.061.
[169] Lavenus S, Berreur M, Trichet V, Pilet P, Louarn G, Layrolle P. Adhesion and osteogenic differentiation of human mesenchymal. Eur Cell & Mater. 2011;22:84–96.
[170] Liu Y, Bao C, Wismeijer D, Wu G. The physicochemical/biological properties of porous tantalum and the potential surface modification techniques to improve its clinical application in dental implantology. Mater Sci Eng C. 2015;49:323–9. doi: 10.1016/j.msec.2015.01.007.
[171] Alves CFA, Cavaleiro A, Carvalho S. Bioactivity response of $Ta_{1-x}O_x$ coatings deposited by reactive DC magnetron sputtering. Mater Sci Eng C. 2015;58:110–8. doi: 10.1016/j.msec.2015.08.017.
[172] Zhang Y, Zheng Y, Li Y, Wang L, Bai Y, Zhao Q. Tantalum nitride-decorated titanium with enhanced resistance to microbiologically induced corrosion and mechanical property for dental application. PLoS One. 2015;10:1–22. doi: 10.1371/journal.pone.0130774.
[173] Zhang XM, Li Y, Gu YX, Zhang CN, Lai HC, Shi JY. Ta-coated titanium surface with superior bacteriostasis and osseointegration. Int J Nanomed. 2019;14:8693–706. doi: 10.2147/IJN.S218640.
[174] Wu XF, Song HY, Yoon JM, Yu YT, Chen YF. Synthesis of core-shell Au@TiO_2 nanopartides with truncated wedge-shaped morphology and their photocatalytic properties. Langmuir. 2009;25:6438–47. doi: 10.1021/la900035a.
[175] Besinis A, De Peralta T, Handy RD. The antibacterial effects of silver, titanium dioxide and silica dioxide nanoparticles compared to the dental disinfectant chlorhexidine on Streptococcus mutans using a suite of bioassays. Nanotoxicology. 2014;8:1–16. doi: 10.3109/17435390.2012.742935.
[176] Chidambaranathan AS, Mohandoss K, Balasubramaniam MK. Comparative evaluation of antifungal effect of titanium, zirconium and aluminium nanoparticles coated titanium plates against C. albicans. J Clin Diagn Res. 2016;10:ZC56-9. doi: 10.7860/JCDR/2016/15473.7114.
[177] Zhang P, Zhang Z, Li W. Antibacterial TiO_2 coating incorporating silver nanoparticles by microarc oxidation and ion implantation. J Nanomater. 2013;124:2013–7. doi: 10.1155/2013/542878.
[178] Zhang L, Pornpattananangkul D, Hu C-M, Huang C-M. Development of nanoparticles for antimicrobial drug delivery. Curr Med Chem. 2010;17:585–94. doi: 10.2174/092986710790416290.
[179] Zhao L, Chu PK, Zhang Y, Wu Z. Antibacterial coatings on titanium implants. J Biomed Mater Res – Part B Appl Biomater. 2009;91:470–80. doi: 10.1002/jbm.b.31463.
[180] Raphel J, Holodniy M, Goodman SB, Heilshorn SC. Multifunctional coatings to simultaneously promote osseointegration and prevent infection of orthopaedic implants. Vol. 84, Amsterdam: Elsevier Ltd; 2016. doi: 10.1016/j.biomaterials.2016.01.016.
[181] Hickok NJ, Shapiro IM. Immobilized antibiotics to prevent orthopaedic implant infections. Adv Drug Deliv Rev. 2012;64:1165–76. doi: 10.1016/j.addr.2012.03.015.
[182] Lee DW, Yun YP, Park K, Kim SE. Gentamicin and bone morphogenic protein-2 (BMP-2)-delivering heparinized-titanium implant with enhanced antibacterial activity and osteointegration. Bone. 2012;50:974–82. doi: 10.1016/j.bone.2012.01.007.
[183] Almeida MAN, Servulo EFC, de FPF. Bacterial colonization of metallic surfaces on industrial cooling systems. International Corrosion Congress Front Corrosion Science Technology, 15th; 2002. p. 594/1–/5.
[184] Mydin RBSMN, Hazan R, FaridWajidi MF, Sreekantan S. Titanium dioxide nanotube arrays for biomedical implant

materials and nanomedicine applications. Titanium dioxide – material for a sustainable environment. London, UK: IntechOpen; 2018. doi: 10.5772/intechopen.73060.
[185] Wang J, Wu G, Liu X, Sun G, Li D, Wei H. A decomposable silica-based antibacterial coating for percutaneous titanium implant. Int J Nanomed. 2017;12:371–9. doi: 10.2147/IJN.S123622.
[186] Yang Y, Ao HY, Yang SB, Wang YG, Lin WT, Yu ZF, et al. *In vivo* evaluation of the anti-infection potential of gentamicin-loaded nanotubes on titania implants. Int J Nanomed. 2016;11:2223–34. doi: 10.2147/IJN.S102752.
[187] Inzunza D, Covarrubias C, Von Marttens A, Leighton Y, Carvajal JC, Valenzuela F, et al. Synthesis of nanostructured porous silica coatings on titanium and their cell adhesive and osteogenic differentiation properties. J Biomed Mater Res Part A. 2013;102:1–12. doi: 10.1002/jbm.a.34673.
[188] Kim I, Joachim E, Choi H, Kevin KK. Toxicity of silica nanoparticles depends on size, dose, and cell type. Nanomed Nanotechnol, Biol Med. 2015;11:1–10. doi: 10.1016/j.nano.2015.03.004.
[189] Csík A, Heged C. Electrosprayed calcium silicate nanoparticle-coated titanium implant with improved antibacterial activity and osteogenesis. Colloids Surf B: Biointerfaces. 2021;202:202. doi: 10.1016/j.colsurfb.2021.111699.
[190] Massa MA, Covarrubias C, Bittner M, Fuentevilla IA, Capetillo P, Von Marttens A, et al. Synthesis of new antibacterial composite coating for titanium based on highly ordered nanoporous silica and silver nanoparticles. Mater Sci Eng C. 2014;45:146–53. doi: 10.1016/j.msec.2014.08.057.
[191] Catauro M, Papale F, Bollino F. Silica/quercetin sol–gel hybrids as antioxidant dental implant materials. Sci Technol Adv Mater. 2015 Jun;035001:035001. doi: 10.1088/1468-6996/16/3/035001.
[192] Li K, Xie Y, You M, Huang L, Zheng X. Plasma sprayed cerium oxide coating inhibits H_2O_2-induced oxidative stress and supports cell viability. J Mater Sci Mater Med. 2016;27:1–10. doi: 10.1007/s10856-016-5710-9.
[193] Qi S, Wu J, Xu Y, Zhang Y, Wang R, Li K, et al. Chemical stability and antimicrobial activity of plasma-sprayed cerium oxide-incorporated calcium silicate coating in dental implants. Implant Dent. 2019;28:564–70. doi: 10.1097/ID.0000000000000937.
[194] Li X, Qi M, Sun X, Weir MD, Tay FR, Oates TW, et al. Surface treatments on titanium implants *via* nanostructured ceria for antibacterial and anti-inflammatory capabilities. Acta Biomater. 2019;94:627–43. doi: 10.1016/j.actbio.2019.06.023.
[195] Gold and Silver Nanoparticles in Sensing and Imaging-Sensitivity of Plasmon Response to Size, Shape, and Metal Composition.pdf, n.d. 2006.
[196] Kesharwani P, Choudhury H, Meher JG, Pandey M, Gorain B. Dendrimer-entrapped gold nanoparticles as promising nanocarriers for anticancer therapeutics and imaging. Prog Mater Sci. 2019;103:484–508. doi: 10.1016/j.pmatsci.2019.03.003.
[197] Zaki M, Akhter S, Rahman Z, Akhter S, Anwar M, Pradesh H. Nanometric gold in cancer nanotechnology: current status and future prospect. J Pharm pharmacology. 2013;65:634–51. doi: 10.1111/jphp.12017.
[198] Wani IA, Ahmad T. Size and shape dependant antifungal activity of gold nanoparticles: a case study of Candida. Colloids Surf B Biointerfaces. 2013;101:162–70. doi: 10.1016/j.colsurfb.2012.06.005.
[199] Nautiyal CS. Biocatalytic and antimicrobial activities of gold nanoparticles synthesized by Trichoderma sp. Bioresour Technol. 2014;166:235–42. doi: 10.1016/j.biortech.2014.04.085.
[200] Tp SD, Zhang Y, Yu H. Antibacterial activity and cytotoxicity of Gold(I) and (III) ions and gold. Biochem Pharmacol: Open Access. 2015;4:4. doi: 10.4172/2167-0501.1000199.
[201] Padmos JD, Langman M, Macdonald K, Comeau P, Yang Z, Filiaggi M, et al. Correlating the atomic structure of bimetallic silver – gold nanoparticles to their antibacterial and cytotoxic activities. J Phys Chem C. 2015;119:7472–82. doi: 10.1021/acs.jpcc.5b00145.
[202] Cui Y, Zhao Y, Tian Y, Zhang W, Lü X, Jiang X. The molecular mechanism of action of bactericidal gold nanoparticles on Escherichia coli q. Biomaterials. 2012;33:2327–33. doi: 10.1016/j.biomaterials.2011.11.057.
[203] Regiel-Futyra A, Kus-Liśkiewicz M, Sebastian V, Irusta S, Arruebo M, Stochel G, et al. Development of noncytotoxic chitosan-gold nanocomposites as efficient antibacterial materials. ACS Appl Mater Interfaces. 2015;7:1087–99. doi: 10.1021/am508094e.
[204] Wang L, Li S, Yin J, Yang J, Li Q, Zheng W, et al. The density of surface coating can contribute to different antibacterial activities of gold nanoparticles. Nano Lett. 2020;20:5036–42. doi: 10.1021/acs.nanolett.0c01196.
[205] Heo DN, Ko WK, Lee HR, Lee SJ, Lee D, Um SH, et al. Titanium dental implants surface-immobilized with gold nanoparticles as osteoinductive agents for rapid osseointegration. J Colloid Interface Sci. 2016;469:129–37. doi: 10.1016/j.jcis.2016.02.022.
[206] Laurent S, Forge D, Port M, Roch A, Robic C, Vander Elst L, et al. Magnetic iron oxide nanoparticles: synthesis, stabilization, vectorization, physicochemical characterizations and biological applications. Chem Rev. 2008;108:2064–110. doi: 10.1021/cr068445e.
[207] Motte L. What are the current advances regarding iron oxide nanoparticles for nanomedicine? J Bioanal Biomed. 2012;4:e110. doi: 10.4172/1948-593X.1000e110.
[208] Taylor EN, Webster TJ. The use of superparamagnetic nanoparticles for prosthetic biofilm prevention. Int J Nanomed. 2009;4:145–52. doi: 10.2147/ijn.s5976.
[209] Sathyanarayanan MB, Balachandranath R, Genji Srinivasulu Y, Kannaiyan SK, Subbiahdoss G. The effect of gold and iron-oxide nanoparticles on biofilm-forming pathogens. ISRN Microbiol. 2013;2013:1–5. doi: 10.1155/2013/272086.
[210] Thukkaram M, Sitaram S, Kannaiyan SK, Subbiahdoss G. Antibacterial efficacy of iron-oxide nanoparticles against biofilms on different biomaterial surfaces. Int J Biomater. 2014;2014:2014. doi: 10.1155/2014/716080.
[211] Injumpa W, Ritprajak P, Insin N. Size-dependent cytotoxicity and inflammatory responses of PEGylated silica-iron oxide nanocomposite size series. J Magn Magn Mater. 2017;427:60–6. doi: 10.1016/j.jmmm.2016.11.015.

[212] Ruparelia JP, Chatterjee AK, Duttagupta SP, Mukherji S. Strain specificity in antimicrobial activity of silver and copper nanoparticles. Acta Biomater. 2008;4:707–16. doi: 10.1016/j.actbio.2007.11.006.
[213] Maleki Dizaj S, Barzegar-Jalali M, Zarrintan MH, Adibkia K, Lotfipour F. Calcium carbonate nanoparticles as cancer drug delivery system. Expert Opin Drug Deliv. 2015;12:1649–60. doi: 10.1517/17425247.2015.1049530.
[214] Akhavan O, Ghaderi E. Cu and CuO nanoparticles immobilized by silica thin films as antibacterial materials and photocatalysts. Surf Coat Technol. 2010;205:219–23. doi: 10.1016/j.surfcoat.2010.06.036.
[215] Wang X, Dong H, Liu J, Qin G, Chen D, Zhang E. *In vivo* antibacterial property of Ti-Cu sintered alloy implant. Mater Sci Eng C. 2019;100:38–47. doi: 10.1016/j.msec.2019.02.084.
[216] Rosenbaum J, Versace DL, Abbad-Andallousi S, Pires R, Azevedo C, Cénédese P, et al. Antibacterial properties of nanostructured Cu-TiO_2 surfaces for dental implants. Biomater Sci. 2017;5:455–62. doi: 10.1039/c6bm00868b.
[217] Liu R, Memarzadeh K, Chang B, Zhang Y, Ma Z, Allaker RP, et al. Antibacterial effect of copper-bearing titanium alloy (Ti-Cu) against Streptococcus mutans and Porphyromonas gingivalis. Sci Rep. 2016;6:1–10. doi: 10.1038/srep29985.
[218] Tabrez Khan S, Ahamed M, Al-Khedhairy A, Musarrat J. Biocidal effect of copper and zinc oxide nanoparticles on human oral microbiome and biofilm formation. Mater Lett. 2013;97:67–70. doi: 10.1016/j.matlet.2013.01.085.
[219] Shen X, Hu Y, Xu G, Chen W, Xu K, Ran Q, et al. Regulation of the biological functions of osteoblasts and bone formation by Zn-incorporated coating on microrough titanium. ACS Appl Mater Interfaces. 2014;6:16426–40. doi: 10.1021/am5049338.
[220] Chou AHK, LeGeros RZ, Chen Z, Li Y. Antibacterial effect of zinc phosphate mineralized guided bone regeneration membranes. Implant Dent. 2007;16:89–100. doi: 10.1097/ID.0b013e318031224a.
[221] Mehdipour M, Taghavi Zenouz A, Bahramian A, Yazdani J, Pouralibaba F, Sadr K. Comparison of the effect of mouthwashes with and without zinc and fluocinolone on the healing process of erosive oral lichen planus. J Dent Res Dent Clin Dent Prospect. 2010;4:25–8. doi: 10.5681/joddd.2010.007.
[222] Hu H, Zhang W, Qiao Y, Jiang X, Liu X, Ding C. Antibacterial activity and increased bone marrow stem cell functions of Zn-incorporated TiO_2 coatings on titanium. Acta Biomater. 2012;8:904–15. doi: 10.1016/j.actbio.2011.09.031.
[223] Luo Q, Cao H, Wang L, Ma X, Liu X. ZnO@ZnS nanorod-array coated titanium: good to fibroblasts but bad to bacteria. J Colloid Interface Sci. 2020;579:50–60. doi: 10.1016/j.jcis.2020.06.055.
[224] Park J, Park M, Seo H, Han HS, Lee JY, Koo D, et al. A new corrosion-inhibiting strategy for biodegradable magnesium: reduced nicotinamide adenine dinucleotide (NADH). Sci Rep. 2018;8:1–10. doi: 10.1038/s41598-018-36240-3.
[225] Nabiyouni M, Ren Y, Bhaduri SB. Magnesium substitution in the structure of orthopedic nanoparticles: a comparison between amorphous magnesium phosphates, calcium magnesium phosphates, and hydroxyapatites. Mater Sci Eng C. 2015;52:11–7. doi: 10.1016/j.msec.2015.03.032.
[226] Yamamoto O, Ohira T, Alvarez K, Fukuda M. Antibacterial characteristics of $CaCO_3$-MgO composites. Mater Sci Eng B Solid-State Mater Adv Technol. 2010;173:208–12. doi: 10.1016/j.mseb.2009.12.007.
[227] Jin T, He Y. Antibacterial activities of magnesium oxide (MgO) nanoparticles against foodborne pathogens. J Nanopart Res. 2011;13:6877–85. doi: 10.1007/s11051-011-0595-5.
[228] Ewald A, Kreczy D, Brückner T, Gbureck U, Bengel M, Hoess A, et al. Development and bone regeneration capacity of premixed magnesium phosphate cement pastes. Mater (Basel). 2019;12:12. doi: 10.3390/ma12132119.
[229] Kishen A, Shi Z, Shrestha A, Neoh KG. An investigation on the antibacterial and antibiofilm efficacy of cationic nanoparticulates for root canal disinfection. J Endod. 2008;34:1515–20. doi: 10.1016/j.joen.2008.08.035.
[230] Wood NJ, Jenkinson HF, Davis SA, Mann S, O'Sullivan DJ, Barbour ME. Chlorhexidine hexametaphosphate nanoparticles as a novel antimicrobial coating for dental implants. J Mater Sci Mater Med. 2015;26:26. doi: 10.1007/s10856-015-5532-1.
[231] Hamouda IM. Current perspectives of nanoparticles in medical and dental biomaterials. J Biomed Res. 2012;26:143–51. doi: 10.7555/JBR.26.20120027.
[232] Zhao IS, Mei ML. The antibacterial mechanism of silver nanoparticles and its application in dentistry. Int J Nanomed. 2020;15:2555–62.
[233] Maleki Dizaj S. Preparation and study of vitamin A palmitate microemulsion drug delivery system and investigation of co-surfactant effect. J Nanostruct Chem. 2013;3:3. doi: 10.1186/2193-8865-3-59.
[234] Li M, Liu Q, Jia Z, Xu X, Shi Y, Cheng Y, et al. Polydopamine-induced nanocomposite Ag/CaP coatings on the surface of titania nanotubes for antibacterial and osteointegration functions. J Mater Chem B. 2015;3:8796–805. doi: 10.1039/c5tb01597a.
[235] Choi S, Jang Y, Jang J, Lee S, Lee M. Enhanced antibacterial activity of titanium by surface modification with polydopamine and silver for dental implant application. J Appl Biomater Funct Mater. 2019;17:2280800019847067. doi: 10.1177/2280800019847067.
[236] Gunputh UF, Le H, Lawton K, Besinis A, Tredwin C, Handy RD. Antibacterial properties of silver nanoparticles grown in situ and anchored to titanium dioxide nanotubes on titanium implant against Staphylococcus aureus. Nanotoxicology. 2020;14:97–110. doi: 10.1080/17435390.2019.1665727.
[237] Li Y, Lin Z, Zhao M, Xu T, Wang C, Xia H, et al. Multifunctional selenium nanoparticles as carriers of HSP70 siRNAto induce apoptosis of HepG2 cells. Int J Nanomed. 2016;11:3065–76. doi: 10.2147/IJN.S109822.
[238] Li Y, Li X, Zheng W, Fan C, Zhang Y, Chen T. Functionalized selenium nanoparticles with nephroprotective activity, the important roles of ROS-mediated signaling pathways. J Mater Chem B. 2013;1:6365–72. doi: 10.1039/c3tb21168a.
[239] Wang H, Zhang J, Yu H. Elemental selenium at nano size possesses lower toxicity without compromising the fundamental effect on selenoenzymes: comparison with selenomethionine in mice. Free Radic Biol Med. 2007;42:1524–33. doi: 10.1016/j.freeradbiomed.2007.02.013.

[240] Hiraoka K, Komiya S, Hamada T, Zenmyo M, Inoue A. Osteosarcoma cell apoptosis induced by selenium. J Orthop Res. 2001;19:809–14. doi: 10.1016/S0736-0266(00)00079-6.
[241] Tran PA, Sarin L, Hurt RH, Webster TJ. Titanium surfaces with adherent selenium nanoclusters as a novel anticancer orthopedic material. J Biomed Mater Res – Part A. 2010;93:1417–28. doi: 10.1002/jbm.a.32631.
[242] Wei W, Abnet CC, Qiao Y, Dawsey SM, Dong Z, Sun X, et al. Prospective study of serum selenium concentrations and esophageal and gastric cardia cancer, heart disease, stroke, and total death. Am J Clin Nutr. 2018;79(1):80–5.
[243] Perla V, Webster TJ. Better osteoblast adhesion on nano-particulate selenium – A promising orthopedic implant material. J Biomed Mater Res – Part A. 2005;75:356–64. doi: 10.1002/jbm.a.30423.
[244] Stevanović M, Filipović N, Djurdjević J, Lukić M, Milenković M, Boccaccini A. 45S5Bioglass®-based scaffolds coated with selenium nanoparticles or with poly(lactide-co-glycolide)/ selenium particles: processing, evaluation and antibacterial activity. Colloids Surf B Biointerfaces. 2015;132:208–15. doi: 10.1016/j.colsurfb.2015.05.024.
[245] Webster TJ. Ijn-6-1553.Pdf. 2011.
[246] Srivastava N, Mukhopadhyay M. Green synthesis and structural characterization of selenium nanoparticles and assessment of their antimicrobial property. Bioprocess Biosyst Eng. 2015;38:38. doi: 10.1007/s00449-015-1413-8.
[247] Dion I, Bordenave L, Lefebvre F, Bareille R, Baquey C, Monties JR, et al. Physico-chemistry and cytotoxicity of ceramics – Part II Cytotoxicity of ceramics. J Mater Sci Mater Med. 1994;5:18–24. doi: 10.1007/BF00121148.
[248] Guerreiro-Tanomaru JM, Trindade-Junior A, Costa BC, Da Silva GF, Drullis Cifali L, Basso Bernardi MI, et al. Effect of zirconium oxide and zinc oxide nanoparticles on physico-chemical properties and antibiofilm activity of a calcium silicate-based material. Sci World J. 2014;2014:975213. doi: 10.1155/2014/975213.
[249] Marunick M, Gordon S. Prosthodontic treatment during active osteonecrosis related to radiation and bisphosphonate therapy: a clinical report. J Prosthet Dent. 2006;96:7–12. doi: 10.1016/j.prosdent.2006.05.008.
[250] Größner-Schreiber B, Herzog M, Hedderich J, Dück A, Hannig M, Griepentrog M. Focal adhesion contact formation by fibroblasts cultured on surface-modified dental implants: an *in vitro* study. Clin Oral Implant Res. 2006;17:736–45. doi: 10.1111/j.1600-0501.2006.01277.x.
[251] Depprich R, Zipprich H, Ommerborn M, Naujoks C, Wiesmann HP, Kiattavorncharoen S, et al. Osseointegration of zirconia implants compared with titanium: an *in vivo* study. Head Face Med. 2008;4:1–8. doi: 10.1186/1746-160X-4-30.
[252] Degidi M, Artese L, Scarano A, Perrotti V, Gehrke P, Piattelli A. Inflammatory infiltrate, microvessel density, nitric oxide synthase expression, vascular endothelial growth factor expression, and proliferative activity in peri-implant soft tissues around titanium and zirconium oxide healing caps. J Periodontol. 2006;77:73–80. doi: 10.1902/ jop.2006.77.1.73.
[253] Bächle M, Butz F, Hübner U, Bakalinis E, Kohal RJ. Behavior of CAL72 osteoblast-like cells cultured on zirconia ceramics with different surface topographies. Clin Oral Implant Res. 2007;18:53–9. doi: 10.1111/j.1600-0501.2006.01292.x.
[254] Huang Z, Wang Z, Li C, Yin K, Hao D, Lan J. Application of implants: study in implants plasma-sprayed zirconia coating in dental. J Oral Implantol. 2018;44:102–8. doi: 10.1563/ aaid-joi-D-17-00020.
[255] Gou Z, Chang J. Synthesis and *in vitro* bioactivity of dicalcium silicate powders. J European Ceramic Soc. 2004;24:93–9. doi: 10.1016/S0955-2219(03)00320-0.
[256] Zhao W, Chang J. Sol–gel synthesis and *in vitro* bioactivity of tricalcium silicate powders. Mater Lett. 2004;58:2350–3. doi: 10.1016/j.matlet.2004.02.045.
[257] Hoppe A, Güldal NS, Boccaccini AR. A review of the biological response to ionic dissolution products from bioactive glasses and glass-ceramics. Biomaterials. 2011;32:2757–74. doi: 10.1016/j.biomaterials.2011.01.004.
[258] Askari E, Rasouli M, Darghiasi SF, Naghib SM, Zare Y, Rhee KY. Reduced graphene oxide-grafted bovine serum albumin/bredigite nanocomposites with high mechanical properties and excellent osteogenic bioactivity for bone tissue engineering. Bio-Design Manuf. 2021;4:243–57. doi: 10.1007/s42242-020-00113-4.
[259] Naghib SM, Pedram A, Ansari M, Moztarzadeh F. Development and characterization of 316 L stainless steel coated by melt-derived and sol-gel derived 45S5 bioglass for orthopedic applications. Ceram – Silikaty. 2012;56:89–93.
[260] Jones JR. Review of bioactive glass: from Hench to hybrids. Acta Biomater. 2013;9:4457–86. doi: 10.1016/ j.actbio.2012.08.023.
[261] Gross UM. The anchoring of glass ceramics of different solubility in the femur of the rat. J of Biomed Mater Res. 2000;14:607–18.
[262] Kalantari E, Morteza S, Reza NM, Mozafari M. Green solvent-based sol–gel synthesis of monticellite nanoparticles: a rapid and ef fi cient approach. J Sol–Gel Sci Technol. 2017;84:87–95. doi: 10.1007/s10971-017-4461-5.
[263] Kalantari E, Naghib SM. PT SC. Mater Sci Eng C. 2018;98:1087–96. doi: 10.1016/j.msec.2018.12.140.
[264] Nanostructured monticellite for tissue engineering applications – Part II- Molecular and biological characteristics.pdf, n.d. 2018.
[265] Kalantari E, Morteza S, Naimi-jamal MR, Esmaeili R. ScienceDirect nanostructured monticellite: an emerging player in tissue engineering. Mater Today Proc. 2018;5:15744–53. doi: 10.1016/j.matpr.2018.04.187.
[266] Kalantari E, Naghib SM, Iravani NJ, Esmaeili R, Naimi-jamal MR, Mozafari M. Biocomposites based on hydroxyapatite matrix reinforced with nanostructured monticellite ($CaMgSiO_4$) for biomedical application: synthesis, characterization, and biological studies. PT, Mater Sci Eng C. 2019;105:109912. doi: 10.1016/j.msec.2019.109912.
[267] Kalantari E, Naghib SM, Reza M, Aliahmadi A, Jafarbeik N, Mozafari M. Author' s accepted manuscript. Ceram Int. 2018;44:12731–38. doi: 10.1016/j.ceramint.2018.04.076.
[268] Dorozhkin SV. Calcium orthophosphates in nature. Biol Med. 2009;2:399–498. doi: 10.3390/ma2020399.
[269] Lin X, de Groot K, Wang D, Hu Q, Wismeijer D, Liu Y. A review paper on biomimetic calcium phosphate coatings. Open Biomed Eng J. 2015;9:56–64. doi: 10.2174/ 1874120701509010056.

[270] Jing W, Zhang M, Jin L, Zhao J, Gao Q, Ren M, et al. Assessment of osteoinduction using a porous hydroxyapatite coating prepared by micro-arc oxidation on a new titanium alloy. Int J Surg. 2015;24:51–6. doi: 10.1016/j.ijsu.2015.08.030.

[271] Schouten C, Meijer GJ, Van Den Beucken JJ, Leeuwenburgh SC, De Jonge LT, Wolke JG, et al. *In vivo* bone response and mechanical evaluation of electrosprayed CaP nanoparticle coatings using the iliac crest of goats as an implantation model. Acta Biomater. 2010;6:2227–36. doi: 10.1016/j.actbio.2009.11.030.

[272] Okuda T, Ioku K, Yonezawa I, Minagi H, Gonda Y, Kawachi G, et al. The slow resorption with replacement by bone of a hydrothermally synthesized pure calcium-deficient hydroxyapatite. Biomaterials. 2008;29:2719–28. doi: 10.1016/j.biomaterials.2008.03.028.

[273] Daculsi G. Transformation of biphasic calcium phosphate ceramics *in vivo*: ultrastructural and physicochemical characterization. J Biomed Mater Res. 1989;23:883–94.

[274] Mas-Moruno C. Surface functionalization of biomaterials for bone tissue regeneration and repair. Amsterdam: Elsevier Ltd; 2018. doi: 10.1016/B978-0-08-100803-4.00003-6.

[275] Verron E, Bouler JM, Guicheux J. Controlling the biological function of calcium phosphate bone substitutes with drugs. Acta Biomater. 2012;8:3541–51. doi: 10.1016/j.actbio.2012.06.022.

[276] Balasundaram G, Sato M, Webster TJ. Using hydroxyapatite nanoparticles and decreased crystallinity to promote osteoblast adhesion similar to functionalizing with RGD. Biomaterials. 2020;27:2798–805. doi: 10.1016/j.biomaterials.2005.12.008.

[277] Schumacher M, Reither L, Thomas J, Kampschulte M, Gbureck U, Lode A, et al. Bioactive glass composites for controlled growth factor delivery. Biomater Sci. 2017;5:578–88. doi: 10.1039/c6bm00903d.

[278] 200 – Enhanced osteoinduction by controlled release of bone morphogenetic protein-2 from biodegradable sponge composed of gelatin and β-tricalcium phosphate.pdf, n.d. 2005.

[279] Bigi A, Boanini E. Functionalized biomimetic calcium phosphates for bone tissue repair. J Appl Biomater Funct Mater. 2017;15:313–25. doi: 10.5301/jabfm.5000367.

[280] Wang Z, Flax LA, Kemp MM, Linhardt RJ, Baron MJ. Host and pathogen glycosaminoglycan-binding proteins modulate antimicrobial peptide responses in Drosophila melanogaster. Infect Immun. 2011;79:606–16. doi: 10.1128/IAI.00254-10.

[281] Salbach J, Kliemt S, Rauner M, Rachner TD, Goettsch C, Kalkhof S, et al. The effect of the degree of sulfation of glycosaminoglycans on osteoclast function and signaling pathways. Biomaterials. 2012;33:8418–29. doi: 10.1016/j.biomaterials.2012.08.028.

[282] David G, Bernfield M. The emerging rotes of cett surface heparan sutfate proteogtycans. Amsterdam: Elsevier; 1992.

[283] Salbach-Hirsch J, Ziegler N, Thiele S, Moeller S, Schnabelrauch M, Hintze V, et al. Sulfated glycosaminoglycans support osteoblast functions and concurrently suppress osteoclasts. Cell Biochem. 2014;1111:1101–11. doi: 10.1002/jcb.24750.

[284] Rudd TR, Skidmore MA, Guerrini M, Hricovini M, Powell AK, Siligardi G, et al. The conformation and structure of GAGs: recent progress and perspectives. Curr Opin Struct Biol. 2010;20:567–74. doi: 10.1016/j.sbi.2010.08.004.

[285] Korn P, Schulz MC, Hintze V, Range U, Mai R, Eckelt U, et al. Sulfated glycosaminoglycans exploit the conformational plasticity of bone morphogenetic protein-2 (BMP-2) and alter the interaction profile with its receptor. J Biomed Mater Res Part A. 2014;102:2–44.

[286] 216 – Sulfated hyaluronan and chondroitin sulfate derivatives interact differently with human transforming growth factor-β1 (TGF-β1).pdf, n.d. 2011.

[287] Hempel U, Preissler C, Vogel S, Möller S, Hintze V, Becher J, et al. Artificial extracellular matrices with oversulfated glycosaminoglycan derivatives promote the differentiation of osteoblast-precursor cells and premature osteoblasts. BioMed Res Int. 2014;2014:938368.

[288] Baud'huin M, Ruiz-velasco C, Jego G, Charrier C, Gasiunas N, Gallagher J, et al. Glycosaminoglycans inhibit the adherence and the spreading of osteoclasts and their precursors: role in osteoclastogenesis and bone resorption. Eur J Cell Biol. 2011;90:49–57. doi: 10.1016/j.ejcb.2010.08.001.

[289] Irie A, Takami M, Kubo H, Sekino-suzuki N, Kasahara K, Sanai Y. Heparin enhances osteoclastic bone resorption by inhibiting osteoprotegerin activity. Bone. 2007;41:165–74. doi: 10.1016/j.bone.2007.04.190.

[290] Li Y, Yang W, Li X, Zhang X, Wang C, Meng X, et al. Improving osteointegration and osteogenesis of three-dimensional porous Ti6Al4V scaffolds by polydopamine-assisted biomimetic hydroxyapatite coating. ACS Appl Mater Interfaces. 2015;7:5715–24. doi: 10.1021/acsami.5b00331.

[291] Saran N, Zhang R, Turcotte RE. Osteogenic protein-1 delivered by hydroxyapatite-coated implants improves bone ingrowth in extracortical bone bridging. Clin Orthop Relat Res. 2011;469:1470–8. doi: 10.1007/s11999-010-1573-4.

[292] He J, Huang T, Gan L, Zhou Z, Jiang B, Wu Y, et al. Collagen-infiltrated porous hydroxyapatite coating and its osteogenic properties: *in vitro* and *in vivo* study. J Biomed Mater Res – Part A. 2012;100 A:1706–15. doi: 10.1002/jbm.a.34121.

[293] Ohgushi H, Okumura M, Yoshikawa T, Inoue K, Senpuku N, Tamai S, et al. Bone formation processin porous calcium carbonate and hydroxyapatite. J Biomed Mater Res. 1992;26:885–95. doi: 10.1002/jbm.820260705.

[294] Xu A, Zhou L, Deng Y, Chen X, Xiong X, Deng F, et al. A carboxymethyl chitosan and peptide-decorated polyether-etherketone ternary biocomposite with enhanced antibacterial activity and osseointegration as orthopedic/dental implants. J Mater Chem B. 2016;4:1878–90. doi: 10.1039/c5tb02782a.

[295] Younes I, Rinaudo M. Chitin and chitosan preparation from marine sources. Structure, properties and applications. Mar Drugs. 2015;13:1133–74. doi: 10.3390/md13031133.

[296] Shrestha A, Zhilong S, Gee NK, Kishen A. Nanoparticulates for antibiofilm treatment and effect of aging on its antibacterial activity. J Endod. 2010;36:1030–5. doi: 10.1016/j.joen.2010.02.008.

[297] Li W, Yang Y, Zhang H, Xu Z, Zhao L, Wang J, et al. Improvements on biological and antimicrobial properties of titanium modified by AgNPs-loaded chitosan-heparin polyelectrolyte multilayers. J Mater Sci Mater Med. 2019;30:30. doi: 10.1007/s10856-019-6250-x.

[298] Divakar DD, Jastaniyah NT, Altamimi HG, Alnakhli YO, Muzaheed, Alkheraif AA, et al. Enhanced antimicrobial activity of naturally derived bioactive molecule chitosan conjugated silver nanoparticle against dental implant pathogens. Int J Biol Macromol. 2018;108:790–7. doi: 10.1016/j.ijbiomac.2017.10.166.

[299] Palla-Rubio B, Araújo-Gomes N, Fernández-Gutiérrez M, Rojo L, Suay J, Gurruchaga M, et al. Synthesis and characterization of silica-chitosan hybrid materials as antibacterial coatings for titanium implants. Carbohydr Polym. 2019;203:331–41. doi: 10.1016/j.carbpol.2018.09.064.

[300] Townsend L, Williams RL, Anuforom O, Berwick MR, Halstead F, Hughes E, et al. Antimicrobial peptide coatings for hydroxyapatite: electrostatic and covalent attachment of antimicrobial peptides to surfaces. J R Soc Interface. 2017;14:14. doi: 10.1098/rsif.2016.0657.

[301] Gao Q, Feng T, Huang D, Liu P, Lin P, Wu Y, et al. Antibacterial and hydroxyapatite-forming coating for biomedical implants based on polypeptide-functionalized titania nanospikes. Biomater Sci. 2020;8:278–89. doi: 10.1039/c9bm01396b.

[302] He Y, Zhang Y, Shen X, Tao B, Liu J, Yuan Z, et al. The fabrication and *in vitro* properties of antibacterial polydopamine-LL-37-POPC coatings on micro-arc oxidized titanium. Colloids Surf B Biointerfaces. 2018;170:54–63. doi: 10.1016/j.colsurfb.2018.05.070.

[303] Warnke PH, Voss E, Russo PA, Stephens S, Kleine M, Terheyden H, et al. Antimicrobial peptide coating of dental implants: biocompatibility assessment of recombinant human beta defensin-2 for human cells. Int J Oral Maxillofac Implant. 2013;28:982–8. doi: 10.11607/jomi.2594.

[304] Li JY, Wang XJ, Wang LN, Ying XX, Ren X, Liu HY, et al. High *in vitro* antibacterial activity of Pac-525 against Porphyromonas gingivalis biofilms cultured on titanium. Biomed Res Int. 2015;2015:2015. doi: 10.1155/2015/909870.

[305] Gorr SU, Abdolhosseini M, Shelar A, Sotsky J. Dual host-defence functions of SPLUNC2/PSP and synthetic peptides derived from the protein. Biochem Soc Trans. 2011;39:1028–32. doi: 10.1042/BST0391028.

[306] Chen X, Hirt H, Li Y, Gorr SU, Aparicio C. Antimicrobial GL13K peptide coatings killed and ruptured the wall of streptococcus gordonii and prevented formation and growth of biofilms. PLoS One. 2014;9:9. doi: 10.1371/journal.pone.0111579.

[307] Holmberg KV, Abdolhosseini M, Li Y, Chen X, Gorr SU, Aparicio C. Bio-inspired stable antimicrobial peptide coatings for dental applications. Acta Biomater. 2013;9:8224–31. doi: 10.1016/j.actbio.2013.06.017.

[308] Khurshid Z, Naseem M, Sheikh Z, Najeeb S, Shahab S, Zafar MS. Oral antimicrobial peptides: types and role in the oral cavity. Saudi Pharm J. 2016;24:515–24. doi: 10.1016/j.jsps.2015.02.015.

[309] Godoy-Gallardo M, Mas-Moruno C, Yu K, Manero JM, Gil FJ, Kizhakkedathu JN, et al. Antibacterial properties of hLf1-11 peptide onto titanium surfaces: a comparison study between silanization and surface initiated polymerization. Biomacromolecules. 2015;16:483–96. doi: 10.1021/bm501528x.

[310] Godoy-Gallardo M, Mas-Moruno C, Fernández-Calderón MC, Pérez-Giraldo C, Manero JM, Albericio F, et al. Covalent immobilization of hLf1-11 peptide on a titanium surface reduces bacterial adhesion and biofilm formation. Acta Biomater. 2014;10:3522–34. doi: 10.1016/j.actbio.2014.03.026.

[311] Leoncini E, Ricciardi W, Cadoni G, Arzani D, Petrelli L, Paludetti G, et al. Adult height and head and neck cancer: a pooled analysis within the INHANCE consortium. Head Neck. 2014;36:1391–48. doi: 10.1002/HED.

[312] Mejías Carpio IE, Santos CM, Wei X, Rodrigues DF. Toxicity of a polymer-graphene oxide composite against bacterial planktonic cells, biofilms, and mammalian cells. Nanoscale. 2012;4:4746–56. doi: 10.1039/c2nr30774j.

[313] Malhotra R, Han YM, Morin JLP, Luong-Van EK, Chew RJJ, Castro Neto AH, et al. Inhibiting corrosion of biomedical-grade Ti-6Al-4V alloys with graphene nanocoating. J Dent Res. 2020;99:285–92. doi: 10.1177/0022034519897003.

[314] Metzler P, Von Wilmowsky C, Stadlinger B, Zemann W, Schlegel KA, Rosiwal S, et al. Nano-crystalline diamond-coated titanium dental implants – A histomorphometric study in adult domestic pigs. J Cranio-Maxillofacial Surg. 2013;41:532–8. doi: 10.1016/j.jcms.2012.11.020.

[315] Rago I, Bregnocchi A, Zanni E, D'Aloia AG, De Angelis F, Bossu M, et al. Antimicrobial activity of graphene nanoplatelets against Streptococcus mutans. IEEE-NANO 2015 – 15th International Conference on Nanotechnology; 2015, p. 9–12. doi: 10.1109/NANO.2015.7388945.

[316] Hu W, Peng C, Lv M, Li X, Zhang Y, Chen N, et al. Protein corona-mediated mitigation of cytotoxicity of graphene oxide. ACS Nano. 2011;5:3693–700. doi: 10.1021/nn200021j.

[317] Terheyden H, Lang NP, Bierbaum S, Stadlinger B. Osseointegration – communication of cells. Clin Oral Implant Res. 2012;23:1127–35. doi: 10.1111/j.1600-0501.2011.02327.x.

[318] Zhang BGX, Myers DE, Wallace GG, Brandt M, Choong PFM. Bioactive coatings for orthopaedic implants-recent trends in development of implant coatings. Int J Mol Sci. 2014;15:11878–921. doi: 10.3390/ijms150711878.

[319] Saadatmand S, Vos JR, Hooning MJ, Oosterwijk JC, Koppert LB, Bock GHDe, et al. This article has been accepted for publication and undergone full peer review but has not been through the copyediting, typesetting, pagination and proof-reading process which may lead to differences between this version and the version of record. Laryngoscope. 2014;102:2–31.

[320] Katagiri T, Watabe T. Bone morphogenetic proteins. Cold Spring Harb Perspect Biol. 2016;8:1–28. doi: 10.1101/cshperspect.a021899.

[321] Kim JE, Kang SS, Choi KH, Shim JS, Jeong CM, Shin SW, et al. The effect of anodized implants coated with combined rhBMP-2 and recombinant human vascular endothelial growth factors on vertical bone regeneration in the marginal portion of the peri-implant. Oral Surg Oral Med Oral Pathol Oral Radiol. 2013;115:e24–31. doi: 10.1016/j.oooo.2011.10.040.

[322] Guang M, Huang B, Yao Y, Zhang L, Yang B, Gong P. Effects of vascular endothelial growth factor on osteoblasts around dental implants *in vitro* and *in vivo*. J Oral Sci. 2017;59:215–23. doi: 10.2334/josnusd.16-0406.

[323] Faßbender M, Minkwitz S, Strobel C, Schmidmaier G, Wildemann B. Stimulation of bone healing by sustained bone morphogenetic protein 2 (BMP-2) delivery. Int J Mol Sci. 2014;15:8539–52. doi: 10.3390/ijms15058539.

[324] Al-Jarsha M, Moulisová V, Leal-Egaña A, Connell A, Naudi KB, Ayoub AF, et al. Engineered coatings for titanium implants to present ultralow doses of BMP-7. ACS Biomater Sci Eng. 2018;4:1812–9. doi: 10.1021/acsbiomaterials.7b01037.

[325] Bottino MC, Münchow EA, Albuquerque MTP, Kamocki K, Shahi R, Gregory RL, et al. Tetracycline-incorporated polymer nanofibers as a potential dental implant surface modifier. J Biomed Mater Res – Part B Appl Biomater. 2017;105:2085–92. doi: 10.1002/jbm.b.33743.

[326] Shahi RG, Albuquerque MTP, Münchow EA, Blanchard SB, Gregory RL, Bottino MC. Novel bioactive tetracycline-containing electrospun polymer fibers as a potential antibacterial dental implant coating. Odontology. 2017;105:354–63. doi: 10.1007/s10266-016-0268-z.

[327] Gomez-Florit M, Pacha-Olivenza MA, Fernández-Calderón MC, Córdoba A, González-Martín ML, Monjo M, et al. Quercitrin-nanocoated titanium surfaces favour gingival cells against oral bacteria. Sci Rep. 2016;6:1–9. doi: 10.1038/srep22444.

[328] Butler RJ, Marchesi S, Royer T, Davis IS. The effect of a subject-specific amount of lateral wedge on knee. J Orthop Res. Sept., 2007;25:1121–7. doi: 10.1002/jor.

[329] Radin S, Ducheyne P. Controlled release of vancomycin from thin sol-gel films on titanium alloy fracture plate material. Biomaterials. 2007;28:1721–9. doi: 10.1016/j.biomaterials.2006.11.035.

[330] Ding L, Zhang P, Wang X, Kasugai S. A doxycycline-treated hydroxyapatite implant surface attenuates the progression of peri-implantitis: a radiographic and histological study in mice. Clin Implant Dent Relat Res. 2019;21:154–9. doi: 10.1111/cid.12695.

[331] Alécio ABW, Ferreira CF, Babu J, Shokuhfar T, Jo S, Magini R, et al. Doxycycline release of dental implants with nanotube surface, coated with poly lactic-co-glycolic acid for extended pH-controlled drug delivery. J Oral Implantol. 2019;45:267–73. doi: 10.1563/aaid-joi-D-18-00069.

[332] Kazek-k A, Nosol A, Joanna P, Monika Ś, Go M, Brzychczyw M. PLGA-amoxicillin-loaded layer formed on anodized Ti alloy as a hybrid material for dental implant applications. Mater Sci & Eng C. 2019;94:998–1008. doi: 10.1016/j.msec.2018.10.049.

[333] Rojas-Montoya ID, Fosado-Esquivel P, Henao-Holguín LV, Esperanza-Villegas AE, Bernad-Bernad MJ, Gracia-Mora J. Adsorption/desorption studies of norfloxacin on brushite nanoparticles from reverse microemulsions. Adsorption. 2020;26:825–34. doi: 10.1007/s10450-019-00138-x.

[334] Lucke M, Schmidmaier G, Sadoni S, Wildemann B, Schiller R, Haas NP, et al. Gentamicin coating of metallic implants reduces implant-related osteomyelitis in rats. Bone. 2003;32:521–31. doi: 10.1016/S8756-3282(03)00050-4.

[335] de Avila ED, Castro AGB, Tagit O, Krom BP, Löwik D, van Well AA, et al. Anti-bacterial efficacy *via* drug-delivery system from layer-by-layer coating for percutaneous dental implant components. Appl Surf Sci. 2019;488:194–204. doi: 10.1016/j.apsusc.2019.05.154.

[336] Kamaly N, Yameen B, Wu J, Farokhzad OC. Degradable controlled-release polymers and polymeric nanoparticles: mechanisms of controlling drug release. Chem Rev. 2016;116:2602–63. doi: 10.1021/acs.chemrev.5b00346.

[337] Bruschi M, Steinmüller-Nethl D, Goriwoda W, Rasse M. Composition and modifications of dental implant surfaces. J Oral Implant. 2015;2015:1–14. doi: 10.1155/2015/527426.

[338] Askari E, Khoshghadam-Pireyousefan M, Naghib SM, Akbari H, Khosravani B, Zali A, et al. A hybrid approach for in-situ synthesis of bioceramic nanocomposites to adjust the physicochemical and biological characteristics. J Mater Res Technol. 2021;14:464–74. doi: 10.1016/j.jmrt.2021.06.063.

[339] Rahmanian M, seyfoori A, Dehghan MM, Eini L, Naghib SM, Gholami H, et al. Multifunctional gelatin–tricalcium phosphate porous nanocomposite scaffolds for tissue engineering and local drug delivery: *in vitro* and *in vivo* studies. J Taiwan Inst Chem Eng. 2019;101:214–20. doi: 10.1016/j.jtice.2019.04.028.

[340] Mauri E, Rossi F, Sacchetti A. Tunable drug delivery using chemoselective functionalization of hydrogels. Mater Sci Eng C. 2016;61:851–7. doi: 10.1016/j.msec.2016.01.022.

[341] Askari E, Naghib SM, Zahedi A, Seyfoori A, Zare Y, Rhee KY. Local delivery of chemotherapeutic agent in tissue engineering based on gelatin/graphene hydrogel. J Mater Res Technol. 2021;12:412–22. doi: 10.1016/j.jmrt.2021.02.084.

[342] Gittens RA, Olivares-navarrete R, Schwartz Z, Boyan BD. Implant osseointegration and the role of microroughness and nanostructures: lessons for spine implants. ACTA Biomater. 2014;10:3363–71. doi: 10.1016/j.actbio.2014.03.037.

[343] Nelson C, Assis F, Lucia A, Guilherme P. Influence of implant shape, surface morphology, surgical technique and bone quality on the primary stability of dental implants. J Mech Behav Biomed Mater. 2012;16:169–80. doi: 10.1016/j.jmbbm.2012.10.010.

[344] Marinucci L, Balloni S, Becchetti BE, Belcastro S, Guerra M, Calvitti M, et al. Effect of titanium surface roughness on human osteoblast proliferation and gene expression *in vitro*. Int J Oral Maxillofac Implants. 2005;21:719–25.

[345] Gil FJ, Manzanares N, Badet A, Aparicio C, Ginebra M. Biomimetic treatment on dental implants for short-term bone regeneration. Clin oral investigations. 2013;18:59–66. doi: 10.1007/s00784-013-0953-z.

[346] Ronold HJ, Lyngstadaas SP, Ellingsen JE. Analysing the optimal value for titanium implant roughness in bone attachment using a tensile test. Biomaterials. 2003;24:4559–64. doi: 10.1016/S0142-9612(03)00256-4.

[347] Yang W, Han W, He W, Li J, Wang J, Feng H, et al. Surface topography of hydroxyapatite promotes osteogenic differentiation of human bone marrow mesenchymal stem cells. Mater Sci Eng C. 2016;60:45–53. doi: 10.1016/j.msec.2015.11.012.

[348] Boyan BD, Sylvia VL, Liu Y, Sagun R, Cochran DL, Lohmann CH, et al. Surface roughness mediates its e! ects on osteoblasts via protein kinase A and phospholipase A. Biomaterials. 1999;20:2305–10.

[349] Chen H, Huang X, Zhang M, Damanik F, Baker MB, Leferink A, et al. Tailoring surface nanoroughness of electrospun scaffolds for skeletal tissue engineering. Acta Biomater. 2017;59:82–93. doi: 10.1016/j.actbio.2017.07.003.

[350] 349 – Bioactive nanofibers- synergistic effects of nanotopography and chemical signaling on cell guidance.pdf, n.d. 2007.

[351] Lopez BS. Determining optimal surface roughness of TiO_2 blasted titanium implant material for attachment,

proliferation and differentiation of cells derived from human mandibular alveolar bone. Clin Oral Implants Res. 2001;12:515–25.
[352] Cochran DL, Schenk RK, Lussi A, Higginbottom FL, Buser D. Bone response to unloaded and loaded titanium implants with a sandblasted and acid-etched surface: a histometric study in the canine mandible. Jpn Soc Biomater Aust Soc Biomater. 1997;40:1–11.
[353] Wennerberg ANN. The importance of surface roughness for implant. Int. J Mach Tools Manuf. 1998;38:657–62.
[354] Lim JY, Liu X, Vogler EA, Donahue HJ. Systematic variation in osteoblast adhesion and phenotype with substratum surface characteristics. Hoboken, New Jersey: Wiley Online Library; 2003.
[355] Jayaraman M, Meyer U, Martin B, Joos U, Wiesmann H. Influence of titanium surfaces on attachment of osteoblast-like cells *in vitro*. Biomaterials. 2004;25:625–31. doi: 10.1016/S0142-9612(03)00571-4.
[356] Gittens RA, Scheideler L, Rupp F, Hyzy SL, Geis-gerstorfer J, Schwartz Z, et al. A review on the wettability of dental implant surfaces II: biological and clinical aspects. ACTA Biomater. 2014;10:2907–18. doi: 10.1016/j.actbio.2014.03.032.
[357] Elias CN. Factors affecting the success of dental implants. London, UK: IntechOpen; 1990.
[358] Hotchkiss KM, Reddy GB, Hyzy SL, Schwartz Z, Boyan BD, Olivares-navarrete R. Titanium surface characteristics, including topography and wettability, alter macrophage activation. Acta Biomater. 2016;31:425–34. doi: 10.1016/j.actbio.2015.12.003.
[359] Dobrovolskaia MA, Neil SEM. Immunological properties of engineered nanomaterials. Nat Nanotechnol. 2007;2:469–78.
[360] Att W, Hori N, Iwasa F, Yamada M, Ueno T, Ogawa T. The effect of UV-photofunctionalization on the time-related bioactivity of titanium and chromium – cobalt alloys. Biomaterials. 2009;30:4268–76. doi: 10.1016/j.biomaterials.2009.04.048.
[361] Ohgaki M, Kizuki T, Katsura M, Yamashita K. Manipulation of selective cell adhesion and growth by surface charges of electrically polarized hydroxyapatite. J Biomed Mater Res. 2001;57:2–3.
[362] Zheng H, Mortensen LJ, Ravichandran S, Bentley K, Delouise LA, Carolina S. Effect of nanoparticle surface coating on cell toxicity and mitochondria uptake of. J Biomed Nanotechnol. 2017;13:155–66. doi: 10.1166/jbn.2017.2337.
[363] Chen L, Mccrate JM, Lee JC, Li H. The role of surface charge on the uptake and biocompatibility of hydroxyapatite nanoparticles with osteoblast cells. Nanotechnology. 2011 Mar 11;105708:105708. doi: 10.1088/0957-4484/22/10/105708.
[364] Roy M, Pompella A, Kubacki J, Szade J, Roy RA. Photofunctionalization of titanium: an alternative explanation of its chemical- physical mechanism. PLoS One. 2016;11:1–11. doi: 10.1371/journal.pone.0157481.
[365] Li S, Ni J, Liu X, Zhang X, Yin S, Rong M. Surface characteristics and biocompatibility of sandblasted and acid-etched titanium surface modified by ultraviolet irradiation: an *in vitro* study. J Biomed Mater Res Part B, Appl Biomater. 2012;100:1587–98. doi: 10.1002/jbm.b.32727.
[366] Baier E, Cornell F, York N. Investigation of three-surface properties of several metals and their relation to blood compatibility Hoboken, New Jersey: Wiley Online Library; 1972.
[367] Dini C, Nagay BE, Cordeiro JM, Nilson C, Rangel EC. UV-photofunctionalization of a biomimetic coating for dental implants application. Mater Sci Eng C. 2020;110:110657. doi: 10.1016/j.msec.2020.110657.
[368] Rupp F, Haupt M, Klostermann H, Kim HS, Eichler M, Peetsch A, et al. Multifunctional nature of UV-irradiated nanocrystalline anatase thin films for biomedical applications. Acta Biomater. 2010;6:4566–77. doi: 10.1016/j.actbio.2010.06.021.